Scientific Papers

Natural History Museum
The University of Kansas

29 October 1997 Number 4:1–41

# Redescription of the Paleogene *Shelania pascuali* from Patagonia and Its Bearing on the Relationships of Fossil and Recent Pipoid Frogs



By

ANA MARÍA BÁEZ[1] AND LINDA TRUEB[2]

[1]*Departamento de Geología, Facultad de Ciencias Exactas, Universidad de Buenos Aires, Pabellón II, Ciudad Universitaria, 1428 Buenos Aires, Argentina*

[2]*Division of Herpetology, Natural History Museum, and Department of Systematics and Ecology, The University of Kansas, Lawrence, Kansas 66045-2454, USA*

CONTENTS





ISSN No. 1094-0782

ABSTRACT *Shelania pascuali* Casamiquela, 1960, is redescribed on the basis of a series of 30 recently discovered specimens, which range in estimated snout-vent length from 30–100 mm, from the Paleogene of Patagonia. This large pipoid anuran is distinguished by possessing a long, narrow braincase; an hourglass-shaped frontoparietal; a robust antorbital process on the edentate maxilla; long, straight ilia that describe a V-shape in dorsal profile; and a trunk that is long relative to the lengths of the head and limbs. A phylogenetic analysis of 11 fossil and Recent pipoid taxa based on 51 osteological characters resulted in three equally most-parsimonious trees of 84 steps. In each arrangement, rhinophrynids and palaeobatrachids are successive sister groups to a clade composed of *Saltenia, Shelania, Eoxenopoides, "Xenopus" romeri*, xenopodines, and pipines. *"Xenopus" romeri* always clusters as a stem taxon with the xenopodines, as does *Eoxenopoides* with the pipines. The phylogenetic positions of *Shelania* and *Saltenia* remain unresolved. In two of the trees, these taxa are sister to the clade comprising the remaining pipid taxa—either forming a clade or as successive sister taxa; in the other tree, *Shelania* is the sister taxon to [*"Xenopus" romeri* + xenopodines], and *Saltenia* is the sister to [*Eoxenopoides* + pipines]. Whereas the addition of fossil taxa did not affect previous hypotheses of the relationships among extant taxa of pipoid anurans, it did alter and supplement interpretations of character evolution. Moreover, owing to the inclusion of fossil taxa, several characters that previously had not been included in neontological studies were examined.

*Key words: Shelania pascuali, Palaeobatrachus, Eoxenopoides reuningi, Saltenia ibanezi, Xenopus, "Xenopus" romeri, Silurana, Rhinophrynus, Chelomophrynus bayi,* pipoids, South America, Paleogene, phylogeny.

RESUMEN Se redescribe *Shelania pascuali* Casamiquela, 1960, procedente del Paleógeno de Patagonia, sobre la base de una serie de 30 ejemplares recientemente descubiertos, con longitudes corporales estimadas entre 30 y 100 mm. Este anuro pipoideo de gran tamaño se distingue por poseer un neurocraneo largo y angosto; un frontoparietal de bordes laterales cóncavos; un robusto proceso anteorbitario en la maxilla edéntula; largos y rectos iliones que, articulados, forman una "V" en vista dorsal; y un tronco relativamente largo en relación con la longitud de la cabeza y miembros. Un análisis filogenético de 11 taxones de pipoideos fósiles y vivientes, basado en 51 caracteres osteológicos, dio como resultado tres árboles máximamente parsimoniosos de 84 pasos. En todos ellos los rinofrínidos y los palaeobatráquidos son los taxones hermanos sucesivos de un clado compuesto por *Saltenia, Shelania, Eoxenopoides, "Xenopus" romeri,* xenopodinos, y pipinos. *"Xenopus" romeri* siempre se agrupa con los xenopodinos como "stem-taxon," como ocurre con *Eoxenopoides reuningi* con respecto a los pipinos. Las posiciones filogenéticas de *Shelania* y *Saltenia* no quedan resueltas. En dos de los árboles aparecen como taxones hermanos del clado constituído por los restantes taxones de pípidos, ya sea conformando un clado o como taxones hermanos sucesivos; en el árbol restante *Shelania* es el taxón hermano de [*"Xenopus" romeri* + xenopodines], y *Saltenia* lo es de [*Eoxenopoides* + pipines]. Mientras que la inclusión de taxones fósiles no afectó hipótesis previas sobre las relaciones entre los taxones vivientes de anuros pipoideos, alteró y complementó interpretaciones de la evolución de los caracteres. Más aún, debido a la inclusión de taxones fósiles fueron examinados varios caracteres que no habían sido incluídos en estudios neontológicos.

*Palabras claves: Shelania pascuali, Palaeobatrachus, Eoxenopoides reuningi, Saltenia ibanezi, Xenopus, "Xenopus" romeri, Silurana, Rhinophrynus, Chelomophrynus bayi,* pipoideos, América del Sur, Paleógeno, filogenia.

## INTRODUCTION

In recent years, the continuing search for fossil vertebrates, particularly mammals, in the Paleogene of southern South America has led to the discovery of anuran remains. Most of these new finds of frogs have come from Patagonia, and many are associated with lacustrine volcaniclastics. These Patagonian records represent samples of the batrachofaunas of middle latitudes on a relatively isolated continent, under milder climatic conditions than those prevailing at present (Pascual and Ortiz Jaureguizar, 1990; Báez et al., 1991; Pascual et al., 1996). The association of these fossils with volcanic depositional events (which usually cause the episodic disruption of

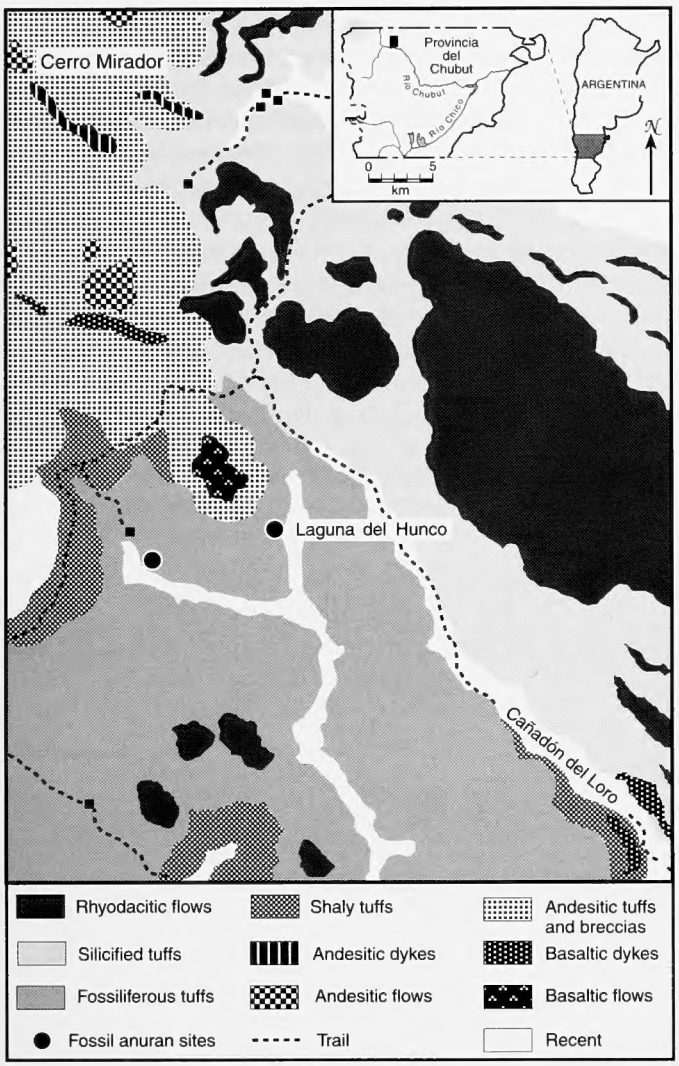


Fig. 1. Geologic map of the Laguna del Hunco region, a western Patagonian locality in northwestern Chubut Province, Argentina, from which *Shelania pascuali* was recovered (adapted from Petersen, 1946). The small black squares represent houses of local residents.

aquatic ecosystems and may result in mass death) may have contributed to the preservation of individual skeletons of varying ontogenetic ages (including larvae), which provide detailed insights into the composition of local populations. Occasionally these records include traces of the outlines of soft tissues (e.g., Báez, 1991). Many of these anuran fossils either are undescribed or only partially described; nonetheless, it is significant that their existence documents the widespread occurrence of pipids and *Caudiverbera*-like leptodactyloids in southern lacustrine environments.

In 1960, Casamiquela reported the presence of frogs from the early Tertiary lacustrine tuffs of Laguna del Hunco in northwestern Patagonia—a locality renown for its abundant and taxonomically diverse fossil flora (Berry, 1925; Fig. 1). Casamiquela (1960; 1961; 1965) described the original sample, as well as additional material, and concluded that the fossils represented a new pipoid genus and species—*Shelania pascuali*. About 20 more specimens were discovered in the same rock unit at a nearby site (Cañadón Peralta Nahueltripay; Fig. 1) nearly 25 years later by a field party led by Dr. José Bonaparte from the Fundación Lillo–Universidad de Tucumán. Subsequent field work by Báez and others at both localities has yielded additional anuran remains. Collectively, this material represents a significant number of specimens on which the following redescription of *Shelania pascuali* is based.

It is important to state clearly the definitions of the names Pipidae, Pipoidea, and Pipamorpha as used in this paper and as defined by Ford and Cannatella (1993). Pipoids are a clade of archaeobatrachian frogs that comprises the common ancestor of the rhinophrynids, the extinct palaeobatrachids, the pipids, and all of its descendants. Pipimorpha is the stem-based pipoid taxon that excludes Rhinophrynidae; Pipidae is restricted to the common ancestor of *Xenopus, Silurana, Pipa, Hymenochirus,* and *Pseudhymenochirus* and all of its (i.e., the common ancestor's) descendants. However, the position of many fossil taxa (including *Shelania*) is ambiguous. Pending resolution of their historical relationships, we consider Pipidae to include those pipoid taxa that are more closely related to the living genera than to Rhinophrynidae and to Palaeobatrachidae. There are three putative genera of pipids—viz., *Thoraciliacus, Cordicephalus,* and *Shomronella* from the Lower Cretaceous of Israel. Because these taxa are poorly known and have been unavailable to us to date, we exclude them from our working definition of Pipidae.

Several new fossil discoveries (e.g., Báez and Calvo, 1989; Evans et al., 1996) indicate that by the middle Cretaceous, when South America and Africa were narrowly separated, pipids occurred on the African and South American continental plates where they exist today. The evolutionary relationships of the living pipid genera have been addressed in recent papers (Trueb and Cannatella, 1986; Cannatella and Trueb, 1988a, b; de Sá and Hillis, 1990; Cannatella and de Sá, 1993), but despite the relatively good fossil record (Estes and Reig, 1973; Báez, 1996), the information provided by the extinct taxa has yet to be effectively incorporated in phylogenetic analyses of pipoids.

In an effort to resolve the phylogenetic relationships of *Shelania,* and to contribute to an understanding of the evolution of pipoid anurans, we have performed a preliminary cladistic analysis using Recent and some selected fossil pipoids as terminal taxa. This research is part of a larger project to reexamine pipoid relationships, but before a comprehensive cladistic analysis can be conducted, other pipid

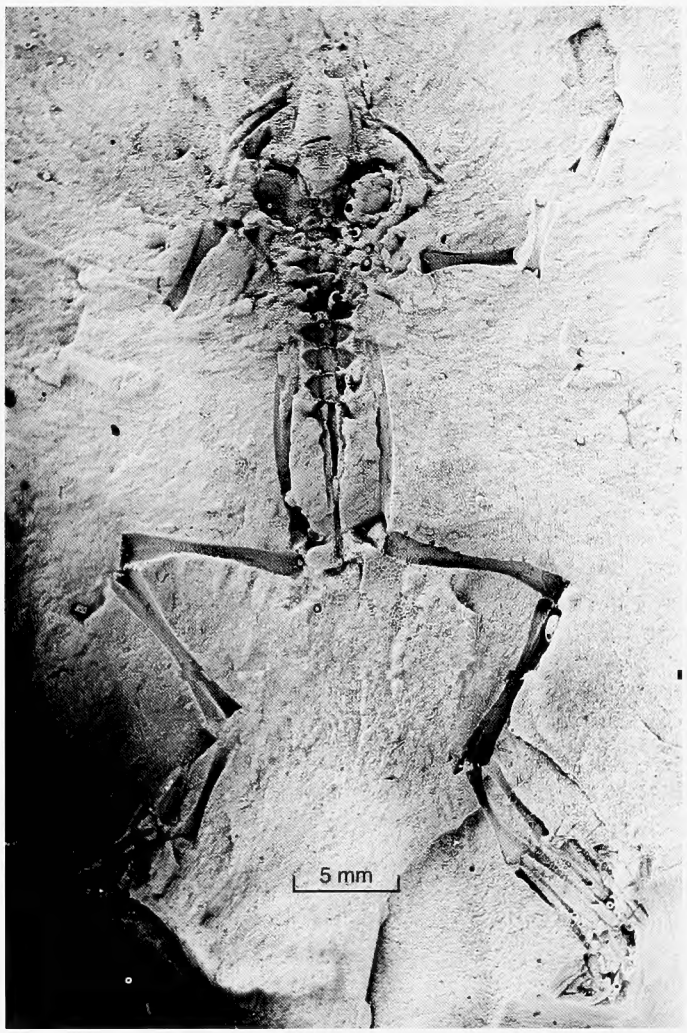


Fig. 2. Photograph of a latex peel of the holotype of *Shelania pascuali* (PVL 2186 dusted with ammonium chloride) representing a ventral view. The relative immaturity of the individual is evidenced by the lack of fusion between the halves of the pelvic girdle and between the tibiale and fibulare. In addition, note the presence of what appears to be the hypochord that terminates anteriorly ventral to the sacrum.

fossils must be described or restudied to enhance our understanding of the evolutionary history of this group of frogs.

## PREVIOUS PALEONTOLOGICAL WORK

In 1960, Casamiquela briefly described a new taxon, *Shelania pascuali* ‡, based on three specimens from Laguna del Hunco (Instituto Lillo Paleontología 2186, holotype; 2187–88), for which he erected Eoxenopodidae (= Eoxenopoididae Casamiquela, 1961). In this family he included not only *Shelania* but also *Eoxenopoides reuningi*‡ Haughton from the Cretaceous of South Africa (Haughton, 1931; Estes, 1977). In his more complete description of *Shelania pascuali*, Casamiquela (1961) emphasized the close relationship of *Shelania* with *Eoxenopoides* and *Xenopus*, and discussed the biogeographic significance of these records.

The arguments used by Casamiquela (1960; 1961) to erect Eoxenopodidae were reviewed critically by Nevo (1968) in his work on pipids from the Lower Cretaceous of Israel. Most of the diagnostic characters of Eoxenopodidae (e.g., absence of quadratojugal, presence of opisthocoelous vertebrae, fused sacrum and urostyle, short scapula) are shared by all pipid anurans. Other "familial" characters reported by Casamiquela (e.g., large otic capsules, narrow coracoids, oval skull shape) are ontogenetically or taxonomically variable in pipids. Thus, Nevo (1968) referred all taxa in the proposed Eoxenopodidae, including *Shelania*, to Pipidae.

*Shelania* was diagnosed as being similar to *Xenopus* and *Eoxenopoides*, but differing from them mainly in the morphology of the frontoparietal and scapula, and in the lack of fusion of the proximal tarsals (Casamiquela, 1960; 1961). Hecht (1963) questioned Casamiquela's (1960; 1961) interpretation of the characters that he used to diagnose *Shelania pascuali*, noting that the three specimens seem to be recently metamorphosed individuals (Fig. 2). Three additional specimens (Museo de La Plata 62-XII-20-1; 62-XII-21-1; 62-XII-22-2) from the same locality subsequently were described and assigned to the same genus and species by Casamiquela (1965). Casamiquela (1965:307) reaffirmed the validity of *Shelania pascuali*, conceding that although some of the examples exhibited juvenile features, "the adult characters were already formed." Based on their examination of the same six specimens, Estes (1975a, b) and Gasparini and Báez (1975) thought that the frogs from Laguna del Hunco should be referred to the genus *Xenopus* as *X. pascuali* (Casamiquela) because of their similarity. This taxonomic similarity was not obvious to Casamiquela because he misidentified (anatomically) some of the bones.

## ACKNOWLEDGMENTS

For the loan of fossil and Recent specimens, we are indebted to Rodolfo Casamiquela (Museo Jorge H. Gerhold, Ing. Jacobacci, Río Negro), Ruben Cuneo (Museo Paleontológico Feruglio, Trelew), J. E. González (Museo Nacional de Ciencias Naturales, Madrid), W. Ronald Heyer (United States National Museum), Jaime Powell (Insituto Miguel Lillo, Tucumán), José Rosado (Museum of Comparative Zoology, Harvard), Roger Smith (South African Museum), and Helga Snekal (Asociación Paleontológica Bariloche, San Carlos de Bariloche). Richard Tinsley (University of Bristol, U.K.) and H. R. Kobel (Université de Genève, Swit-

‡Indicates fossil taxon.

zerland) kindly provided specimens of extant pipids, many of which were prepared as skeletons for comparisons with fossil taxa. Field assistance was provided to Báez by Edgardo Romero, and photographs were made by Mario Rabaglia (Universidad de Buenos Aires). Many thanks are due to individuals who provided technical support in the preparation of specimens examined for this work; among them are past students at The University of Kansas—Gary Ten Eyck, David Cannatella, Linda Ford, and present students Analía Púgener and Anne Maglia. We appreciate the comments of the two latter individuals on earlier drafts of this manuscript. Finally, we are grateful for the remarkable forbearance of our respective families during the long months involved in the preparation of this paper. Financial support for this research was provided by NSF Grant DEB 95-21691 to Linda Trueb and Consejo Nacional de Investigaciones Cientificas y Técnicas de Argentina (CONICET) Grants PID-BID 427/92 and PIA 6081/96 to Ana Báez.

## MATERIALS AND METHODS

### General Methodology

The fossil frogs occur in fine-grained tuffaceous sediments and are preserved mostly as dorsal and ventral impressions of relatively complete skeletons (usually partially articulated); in addition, there are many impressions of isolated bones. Some specimens, especially those from the Cañadón Peralta Nahueltripay, were collected by splitting slabs of rock along laminations; as a result, there are part and counterpart specimens identified as "A" and "B." Pieces of bone were preserved in many specimens, but because the fragmentary nature of these sectioned bones renders them uninformative, they were removed mechanically with fine needles under a stereomicroscope. We prepared high-fidelity silicone rubber molds or peels of the cleaned impressions with the commercial product RTV 524 by Contident (Buenos Aires).

Measurements were taken from the peels with calipers under a zoom stereomicroscope; however, portmortem skeletal disarticulation frequently prevents measurement of whole structural complexes (e.g., vertebral column length) and calculation of indices. Examination of the silicon peels, in addition to actual specimens, was used to determine character states; drawings of specimens were made with the aid of a camera lucida. The description of *Shelania* is based on several specimens, because no single specimen is complete enough to permit a detailed account of the skeleton. A number of different ontogenetic stages are represented by these specimens; thus, a limited analysis of developmental changes is possible.

The dried skeletons used for comparisons were prepared using dermestid beetles; final preparation of dry skeletons was accomplished by hand-picking and bleaching. Skulls of Recent frogs were disarticulated by boiling them in 2% KOH. Alcian-Alizarin specimens were prepared following the methods of Dingerkus and Uhler (1977), and the serial cross sections prepared following the method of Baldauf (1958).

This study includes the specimens originally described by Casamiquela and materials subsequently collected by other individuals. The institutional codes for the specimens examined are, as follow: Asociación Paleontológica Bariloche, San Carlos de Bariloche, Río Negro (BAR); Centro de Investigaciones Científicas, Viedma, Río Negro (CIC); Facultad de Ciencias Exactas y Naturales, Universidad de Buenos Aires, Paleontología (CPBA); Divisão de Geologia e Mineralogia, Departamento Nacional da Produçao Mineral, Rio de Janeiro (DGM); The University of Kansas Natural History Museum, Division of Herpetology (KU); The University of Kansas Natural History Museum, Division of Vertebrate Paleontology (KUVP); Museo de La Plata (MLP); Museo Jorge H. Gerhold, Ing. Jacobacci, Río Negro (MJHG); Museum of Comparative Zoology at Harvard (MCZ); Fundación Miguel Lillo, Tucumán, Vertebrate Paleontology Section (PVL); Museo Paleontológico Egidio Feruglio, Trelew, Chubut (MPEF); South African Museum (SAM); and United States National Museum (USNM).

### Cladistic Methodology

A cladistic analysis was performed to address the phylogenetic placement of *Shelania*. Several anuran high-level taxonomic schemes have been proposed in the last 20 years (e.g., Duellman and Trueb, 1994); the evidential support for currently accepted families was examined most recently by Ford and Cannatella (1993). In the latter study, the monophyletic Pelobatoidea was proposed as the sister group of Pipoids, with both taxa comprising the Mesobatrachia; however, the interrelationships of fossil and extant pelobatoid taxa remain unresolved (Lathrop, 1997). Also, Cannatella (1985) proposed that *Discoglossus* and *Alytes* form a clade that shares a more recent common ancestor with the monophyletic group (Mesobatrachia + Neobatrachia), than with other taxa traditionally included in the Discoglossidae. Based on these hypotheses, we selected *Discoglossus* and *Pelobates* as outgroups to study the relationships of *Shelania* among pipoids.

Apart from the extant pipoid taxa Hymenochirini (*Hymenochirus* and *Pseudhymenochirus*), *Pipa*, *Rhinophrynus*, *Silurana*, and *Xenopus*, we included some fossil pipoids for

which comparisons to *Shelania* might be relevant. Thus, the remaining ingroup taxa are the Holarctic Cretaceous to Pliocene *Palaeobatrachus* (Špinar, 1972; Vergnaud-Grazzini and Hoffstetter, 1972), *Chelomophrynus* from the middle Eocene of Wyoming (Henrici, 1991), *Eoxenopoides* from western South Africa (Haughton, 1931; Estes, 1977), *Saltenia* from the Upper Cretaceous of northwestern Argentina (Reig, 1959; Báez, 1981), and "*Xenopus*" *romeri* from the middle Paleocene of Brazil (Estes, 1975a, b). The age of the *Eoxenopoides*-bearing beds was discussed by Estes (1977), who concluded that an age ranging from the late Eocene through the Oligocene was the most acceptable; however, recent data suggest a Late Cretaceous age for *Eoxenopoides* (Scholtz, 1985; Smith, 1988; van Dijk, 1995).

It should be noted that we consider *Silurana* (containing *S. tropicalis* and *S. epitropicalis*) to be equivalent in rank to *Xenopus*, eschewing the more conservative view that *Silurana* is a subgenus of *Xenopus*. We have done this to test the relationships of this morphologically distinct pipid taxon, the phylogenetic position of which is disputed. In addition, "*Xenopus*" *romeri* is treated as a fossil taxon independent of both *Xenopus* and *Silurana*, because this species has been referred to both of the later genera by different authors (Estes, 1975a, b; Buffetaut and Rage, 1993).

Data for the living and fossil taxa were derived from examination of specimens, as well as from the literature; see Appendix. Some characters from the character matrix of Cannatella and Trueb (1988a, b) were used in this study. Of the original 94 characters used in those analyses, only 19 are used here either because the others are not applicable to the fossil taxa or are extremely homoplastic. A total of 51 characters, binary and multi-state, representing all major structural regions of the skeleton was scored for the 13 taxa. Multi-state characters were treated as non-additive, because of lack of evidence of order of transformation.

A cladistic analysis was performed using PAUP (Phylogenetic Analysis Using Parsimony) software (Version 3.1) of David L. Swofford (1991) on a Macintosh 9500, using the branch-and-bound algorithm. The level of support for each discovered node was measured by calculating Bremer (decay) indices (Bremer, 1988; 1994), and the commands used to calculate these indices using PAUP were obtained with AutoDecay (Version 3.0) software of Eriksson and Wikström (1995). MacClade (Version 3.0) software of Maddison and Maddison (1992) was used to trace character evolution.

### SPECIMENS EXAMINED

In addition to the specimens of *Shelania pascuali* listed below (Redescription), the following specimens were examined for comparative purposes.

RECENT MATERIAL (skeletons, unless designated as histological sections of skull): DISCOGLOSSIDAE: *Discoglossus pictus:* KU 148617. *Discoglossus sardus:* KU 129239. HYLIDAE: *Smilisca baudinii:* KU 89924. PELOBATIDAE: *Pelobates fuscus:* KU 129240; MCZ 1012-3. *Pelobates syriacus:* KU 146856. *Pelobates varaldii:* MCZ 31970. *Scaphiopus couchii:* KU 73385. PIPIDAE: *Hymenochirus boettgeri:* KU 209543 (sections). *Hymenochirus curtipes:* KU 204127, 204131. *Pipa arrabali:* KU 107439 (sections). *Pipa carvalhoi:* CPBA 9, 13, 30; KU 128760 (sections). *Pipa parva:* CPBA 24; KU 115770 (sections); USNM 115775. *Pipa pipa:* CPBA 7. *Pipa snethlageae:* CPBA 20; MCZ 85572. *Silurana epitropicalis:* KU 195660. *Silurana tropicalis:* CPBA 36; KU 195667, 216330 (sections). *Xenopus laevis:* KU 195934, 207853 (sections). *Xenopus largeni:* KU 206863. *Xenopus muelleri:* KU 97203, 196041 (sections), 196043; MCZ 51689. *Xenopus pygmaeus:* KU 206872. *Xenopus vestitus:* KU 206873. *Xenopus wittei:* KU 195673. RHINOPHRYNIDAE: *Rhinophynus dorsalis:* KU 69084, 84885–86, 186799.

FOSSIL MATERIAL: *Eoxenopoides reuningi:* (Casts made by Richard Estes.) REPUBLIC OF SOUTH AFRICA: Namaqualand, near Banke: SAM K–4596, 4597, 4600, 4604, 4609A,B, 4610–11, 4615, 4618B, 4619–20, 4624B, 4627B, 4956, 9938 (type), 9940, 9944–45, 9948, 9965. *Palaeobatrachus diluvianus:* Czech Republic: Bechlejovice, near Bratislava: Oligo-Miocene: KUVP 124939. *Palaeobatrachus novotny:* Czech Republic: Bechlejovice, near Bratislava: Oligo-Miocene: KUVP 124909, 124911. *Palaeobatrachus* sp.: Czech Republic: Bechlejovice, near Bratislava: Oligo-Miocene: KUVP 124971A,B, 124972A, 124975A,B, 124976A,B. *Palaeobatrachus* sp.: (Photograph of cast from National Museum of Prague in Argentina). *Saltenia ibanezi*: (Casts made by Richard Estes and Ana Báez.) ARGENTINA: Provincia de Salta: Quebrada del Río de las Conchas, near Alemanía: Las Curtiembres Formation: CPBA 9726, 9728, 9734; MLP 59-VIII-5; 62-XII-5-77A, 62-XII-5-110. *Xenopus romeri:* BRAZIL: Estado Rio de Janeiro: São José de Itaboraí: DGM 568–73, 575–78.

## STRATIGRAPHIC PROVENANCE AND AGE OF MATERIAL

The first mention of the richly fossiliferous deposits of Laguna del Hunco, a western Patagonian locality in northwestern Chubut Province (Fig. 1), was by Berry (1925), who described plants from pyroclastic rocks that had been collected by Burton Clarke. (See Feruglio, 1949:89.) Subsequently, other authors (Pianitzki, 1936; Frenguelli, 1940;

Petersen, 1946; Feruglio, 1949; Groeber, 1954) discussed the stratigraphy and age of the deposits, and reported new fossil taxa from this locality. In addition to plants, siluriform fishes (Pianitzki, 1936; Dolgopol de Sáez, 1941), crustaceans, and coleopteran, orthopteran, and dipteran insects (Frenguelli, 1940) were discovered. Pipoid frogs (Casamiquela, 1960) and pleurodiran turtles (Archangelsky, 1974; Gasparini and Báez, 1975) were found later.

In his detailed geological study of the middle portion of the Chubut River Valley, Petersen (1946) considered the fossiliferous horizons to be the younger member of his "Serie Riodacítica" or "Serie de la Laguna del Hunco." This sequence is a volcanic-sedimentary complex that rests disconformably on the Late Cretaceous marine beds of the Paso del Sapo Formation, and is disconformably covered by the Eocene volcanic members of the El Mirador Formation (Volkheimer and Lage, 1981; Mazzoni and Aragón, 1985; Mazzoni et al., 1991). In more recent studies, the unit that includes the frog-bearing beds has been referred to either as the Laguna del Hunco Formation (Proserpio, 1978; Aragón and Romero, 1984) or La Huitrera Formation (Volkheimer and Lage, 1981).

For many years, the age of the fossiliferous deposits remained controversial. Initially, the age of the flora was largely based on correlation with other floras, the stratigraphic position and age of which were assumed to be determined more accurately. Berry (1925), who referred to the flora of Laguna del Hunco as "Mirhoja," considered it to be of Miocene age based on comparison with the floras from the Arauco-Concepción area (37° S) in Chile. Berry upheld the Miocene age of the Laguna del Hunco flora in a later work (1938:32), and interpreted that it was about coeval with the flora from the Arauco-Concepción coal measures, as well as with those from Río Pichileufu (41°7' S, 70°50' W) and Río Chalía (49°33' S, 71° W) in Argentina. However, on the basis of paleontological and regional geological arguments not summarized here, Feruglio (1949:310–311) concluded that the floras of Laguna del Hunco and Río Pichileufu, if indeed synchronous, must be older than postulated by Berry. Subsequent studies (Archangelsky, 1974; Arguijo and Romero, 1981) demonstrated that the Arauco-Concepción flora is of Paleocene or Early Eocene age.

A Paleogene age is supported independently by the radiometric dating of volcanic rocks that immediately underlie the fossiliferous beds. Thus, reports on the flora and anurans during the last 15 years accepted a late Paleocene–early Eocene age based on the isotopic dating of a single ignimbrite sample that gave an age of 57 ± 3 Ma (Archangelsky, 1974). However, in the light of recent radiometric work, ignimbrite flows beneath the fossil-bearing succession are about 50 Ma, and El Mirador andesites-basalts above it are recorded to have isotopic ages near 43 Ma (Mazzoni et al., 1991). These data suggest that the frog-bearing unit represents the time span between 47.2 and 43.4 Ma. (Mazzoni et al., 1991) and that it should be considered Lutetian Age following the Cenozoic time scale of Berggren et al. (1995).

The fossil frogs occur within a well-stratified succession composed of thinly bedded to laminated and reworked sandy pyroclastics and shales; these are associated with welded pyroclastic flows and a suite of volcanic rocks. Modern regional studies indicate that the Laguna del Hunco volcanic-sedimentary complex is part of an extended silicic volcanic belt (the 60–42 Ma, Pilcaniyeu Belt; Rapela et al., 1988) linked with the Paleogene subduction along western South America (Rapela et al., 1984; 1988). Field observations suggest deposition within lacustrine bodies confined to morphotectonic depressions related to caldera-style volcanic activity (Aragón and Romero, 1984). Close stratigraphic association with a "mixed" flora featuring subtropical and subantarctic forms (Paleoflora Mixta *fide* Romero, 1978) suggests a humid, but seasonal, climatic regime (Aragón and Romero, 1984).

On the right flank of the Cañadón del Hunco, in the vicinity of the ephemeral Laguna del Hunco (Fig. 1), the upper half of the 300-m-thick lacustrine complex is well exposed. Three main plant-bearing levels were identified in this area, the two lowest of which also yielded fishes (Petersen, 1946). The stratigraphic position of the level yielding the first-described frog specimens was not determined precisely because the frogs were not collected in situ (Casamiquela, 1965). However, Archangelsky (1974) cited the occurrence of frogs in the lowest of the plant-bearing levels identified by Petersen. Isolated specimens also were collected in the upper level by Báez and colleagues. The material found by the Fundación Lillo–Universidad de Tucumán field party, as well as some specimens collected by Báez and others subsequently, originate from exposures of the same stratigraphic unit; these exposures are located relatively close to the original fossiliferous frog site at Laguna del Hunco. These additional specimens were collected from a single bed in a canyon (called Cañadón de Peralta Nahueltripay by Feruglio, 1949:88) that extends west of Cañadón del Hunco and joins the latter on its west side (Fig. 1). Insects and scarce plant remains are associated with the frogs.

## REDESCRIPTION OF *SHELANIA*

AMPHIBIA: ANURA: PIPIDAE

### *Shelania* Casamiquela, 1960

**Type species.**—*Shelania pascuali* Casamiquela, 1960.

**Diagnosis.**—As for *Shelania pascuali*, the only known species.

### *Shelania pascuali* Casamiquela, 1960

*Xenopus pascuali* Estes, 1975a, b; Gasparini and Báez, 1975; Báez, 1976; Báez and Gasparini, 1977; 1979.

**Holotype.**—PVL 2186, incomplete young individual (ca. 35 mm snout-vent length), mostly in ventral view (Fig. 2).

**Type locality.**—Cañadón del Hunco in the vicinity of the Laguna del Hunco (42°20' S, 70° W) middle Chubut Valley, Provincia del Chubut, Argentina.

**Type horizon and age.**—Laguna del Hunco Formation; Early or Middle Eocene.

**Referred specimens.**—ARGENTINA: *Provincia del Chubut:* middle Chubut River Valley: Cañadón del Hunco in the vicinity of the Laguna del Hunco: PVL 2187–88, 3989; MLP 62-XII-21-1, 62-XII-22-1, 62-XII-20-1; CIC 3-3-75/1; MJHG 2-3-72; CPBA 9855–56, 12222, 12224, 12226, 12231–32. Cañadón Peralta Nahueltripay, ca. 2.5 km SSE from the house of Doña Tomasa Cuerda: PVL 3991–98, 3983, 3994, 4002, 4007, 4009–010, 4081–87; CBPA 12211–12, 12219, 12223; MPEF-PV 1150, 1151.

**Emended diagnosis.**—Pipimorph frog (sensu Ford and Cannatella, 1993), attaining a snout-vent length of about 100 mm. Although we acknowledge that a cladistically proper diagnosis should be restricted to only those characters that distinguish *Shelania* from its sister lineage, our purpose is to provide a "working" diagnosis that facilitates comparisons with other fossil taxa, as well as extant anurans. With this caveat in mind, *Shelania pascuali* can be distinguished from all other known fossil and Recent pipids by the following combination of primitive and derived character states. (1) Braincase relatively long and narrow (Figs. 3–5). (2) Frontoparietal constricted at midlength with medially concave lateral margins and longitudinal, parasagittal crests (Figs. 3–5). (3) Azygous, deep nasal lacking a notably long rostral process and not contributing to the anterior margin of the orbit (Fig. 5). (4) Edentate maxilla bearing long antorbital processes that extend to the sphenethmoid medially (Fig. 5). (5) Extensively ossified sphenethmoid with distinct, large frontoparietal fontanelle (Fig. 6B). (6) Anterior ramus of pterygoid located lateral to maxilla and not transversely laminar. (7) Anterior ramus of pterygoid widely expanded in transverse plane and long; subtends orbit and articulates with maxilla at anterolateral corner of orbit (Fig. 5). (8) Ilia long, straight, and describing a distinct V-shape (rather than U-shape) (Fig. 6). (9) Combined length of urostyle + sacrum greater than length of presacral trunk (Fig. 6). (10) Sacral diapophyses moderately and symmetrically dilated with nearly straight, rather than concave, anterior and posterior margins (Fig. 6).

Of the described fossil pipid taxa, *Shelania pascuali* is most likely to be confused with *"Xenopus" romeri*, *Saltenia ibanezi*, and *Eoxenopoides reuningi*. It differs from the latter two taxa in having long, straight ilia and, proportionally, a much longer urostyle. In addition, *Shelania pascuali* differs from *Saltenia ibanezi* and *Eoxenopoides reuningi* in having a narrower braincase and a frontoparietal with medially concave, rather than parallel, lateral margins. Moreover, unlike *Shelania pascuali*, both *Saltenia ibanezi* and *Eoxenopoides reuningi* lack a distinct dorsal skull table defined by parasagittal frontoparietal crests. *Shelania pascuali* differs from *"Xenopus" romeri* in having a narrower braincase, relatively larger scapulae, ilia that are depressed in their anterior halves, and lacking extensive fusion of skull bones.

**Description and variation.**—The estimated snout-vent lengths of the specimens examined range between 30 mm and 100 mm. One specimen (PVL 3991; Fig. 3) consists of more or less complete cranial and postcranial skeletal remains; its snout-vent length is estimated to be about 90 mm. Other specimens (e.g., PVL 3989, CPBA 12222) have measurably longer braincases and isolated bones (e.g., ilia) than does PVL 3991, and are thought to have been at least 100 mm in snout-vent length. Unfortunately, the holotype (Fig. 2) is one of the smallest examples; as discussed below, this specimen is a juvenile (probably a metamorphic or early postmetamorphic individual) that is estimated to have a snout-vent length of about 30 mm.

#### Cranium

*Sphenethmoid:* In its natural position, this anterior bone of the braincase is obscured completely by the frontoparietals and nasal bones (Figs. 4, 5). However, the general configuration of the sphenethmoid can be described from disarticulated specimens (CPBA 12213; 12231; Fig. 6B). The bone is long, extensively ossified, and complete dorsomedially and dorsoventrally. The lateral walls of the sphenethmoid are distinctly flared anterolaterally, and the anterodorsal margin of each half of the bone is concave. This configuration is typical of anurans in which the sphenethmoid forms the posteromedial walls of the olfactory capsule, and those in which the orbitonasal canal is enclosed in bone. The margins of the frontoparietal fon-

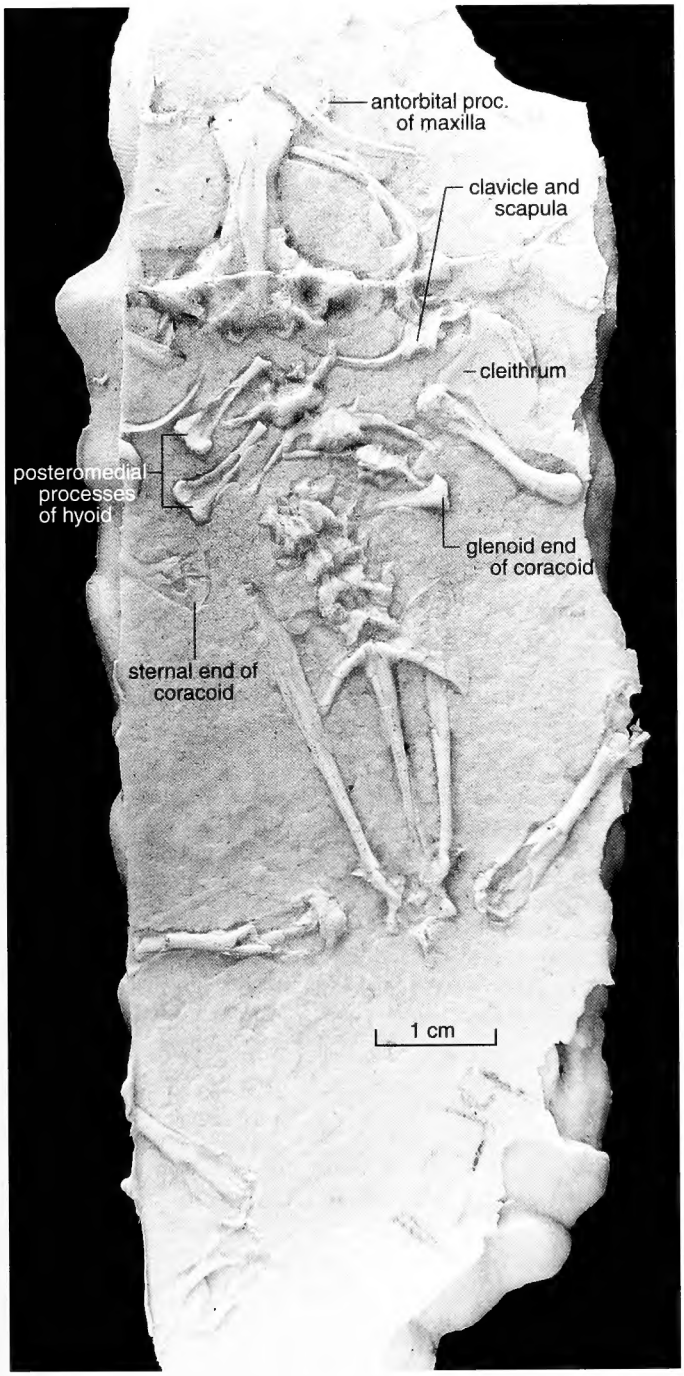


Fig. 3. Photo of a cast of *Shelania pascuali* (CPBA 12219 dusted with ammonium chloride), representing a relatively complete cranial and postcranial skeleton in dorsal view. Note in particular the right maxilla, which is located adjacent to the mandible and sphenethmoid on the right-hand side of the frog. The maxilla has been deflected 180° from its natural position; the antorbital process is clearly evident as an arcuate projection from the outer margin of the maxilla in this position.

tanelle are distinctly defined by the broad tectum anterius anteriorly (slightly posterior to the level of the planum

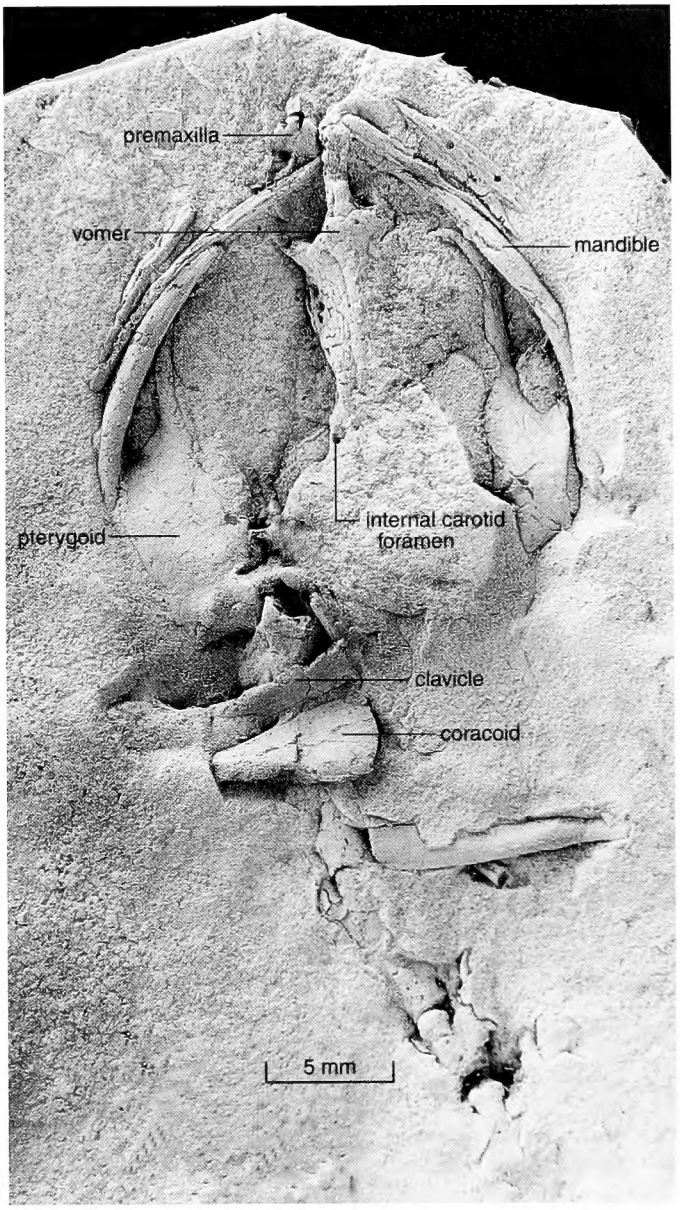


Fig. 4. Photo of a cast of the skull *Shelania pascuali* (CPBA 12224) in ventral view. The sphenethmoid, mandible, and expanded pterygoids are evident in this individual.

antorbitale) and broad taeniae tecti marginalis laterally. Judging from the proportions of the fontanelle, we think that half or more of the fontanelle lies within the sphenethmoid. The optic foramina seem to have been enclosed entirely in the sphenethmoid (CPBA 12224); the disposition of the oculomotor foramina is unknown. There is no evidence of a cartilaginous separation between the sphenethmoid and the prootics posteriorly. A pair of small foramina pierces the braincase slightly posterior and ventral to the large optic foramina (Fig. 4; CPBA 12124). These may rep-

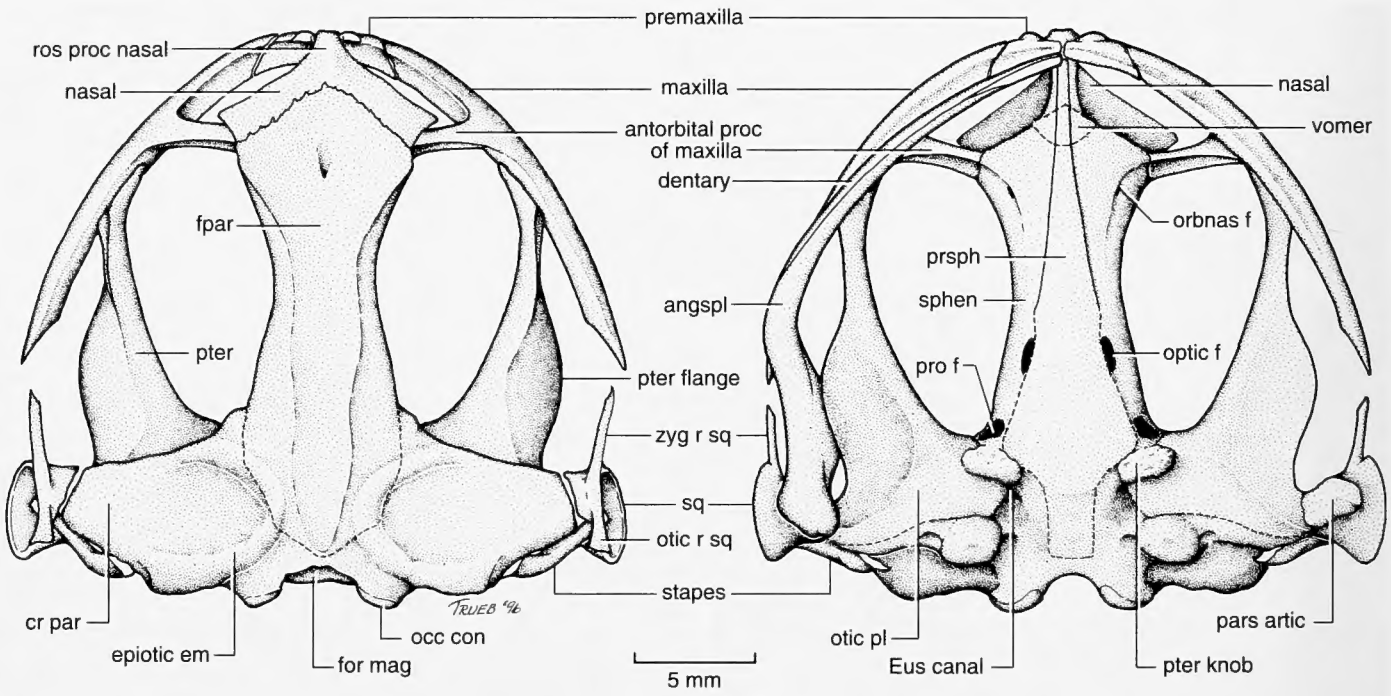


Fig. 5. Reconstruction of the skull of *Shelania pascuali* in dorsal (left) and ventral (right) views. Drawings based primarily on PVL 3989, 3991, 4082; CBPA 12219, 12224. Dashed lines represent estimations of perimeters of bones. The anteromedial end of the mandible is shown in white; the mandible lacks a mentomeckelian bone, and we assume from the configuration of the surrounding elements that Meckel's cartilage occurred in this area. Note that the shape of the parasphenoid might correspond to that of young postmetamorphic individuals. In addition, the medial ramus of the pterygoid (or otic plate) posterior to the pterygoid knob may have been less extensive than is indicated, thereby exposing more of the Eustachian canal. The prootic foramen may have been subdivided by a bony prefacial commissure to produce an internal carotid foramen anteriorly; such a structure seems to be evident in Figure 4 (CPBA 12224); it is not indicated in this illustration because the specimen illustrated in Figure 4 became available to us late in this study after the restoration had been completed. Abbreviations: angspl = angulosplenial; antorbital proc maxilla = antorbital process of the maxilla; cr par = crista parotica of the prootic; epiotic em = epiotic eminence; Eus canal = Eustachian canal; for mag = foramen magnum; fpar = frontoparietal; occ con = occipital condyle of the exoccipital; optic f = optic foramen; orbnas f = orbitonasal foramen; otic pl = otic plate of the pterygoid; otic r sq = otic ramus of the squamosal; pars artic = pars articularis of the palatoquadrate; pro f = prootic foramen; prsph = parasphenoid; pter = pterygoid; pter flange = pterygoid flange; pter knob = pterygoid knob of the prootic; ros proc nasal = rostral process of the nasal; sphen = sphenethmoid; sq = squamosal; zyg r sq = zygomatic ramus of the squamosal.

resent the internal carotid foramina, each of which would have been separated from the prootic foramen posteriorly by a bony bridge. In addition, a separate palatine foramen (for palatine ramus of the facial nerve) might have been separated from the prootic foramen by a bridge of bone that might represent a prepalatine connection.

*Prootics:* These bones form all but the posteromedial portions of the otic capsules and are synostotically fused with the exoccipitals posteromedial to them. Similarly, the anterior margins of these bones may be fused with the sphenethmoid, and form part or all of the margin of the prootic foramen. (See Sphenethmoid, above.) Owing to the condition of the specimens, we could not determine whether the prootics are fused to one another dorso- and ventromedially. In smaller specimens, including the holotype, the otic capsules are large and round and lack obvious cristae paroticae; however, in larger specimens (e.g., BAR 3722-44; Fig. 5), broad, well-developed cristae are obvious. Well-developed epiotic eminences are obvious dorsally in all specimens. Ventrally, the prootic is characterized by a prominent pterygoid knob at the anteromedial margin of the otic capsule and a large, irregular prominence in the posteromedian part of the otic capsule, anterolateral to the occipital condyles (Fig. 5). (Smaller prominences that are similar in position in the pipid *Eoxenopoides reuningi* were thought by Estes [1977] to have served for cervical muscle attachment.) A narrow, deep Eustachian canal traverses the venter of the otic region in large specimens (e.g., PVL 3991, 3993). Most of the canal is covered by the underlying otic plate of the pterygoid, but the medial opening seems to have been located between the pterygoid knob anteriorly and the process for attachment of cervical musculature posteriorly. In smaller specimens (e.g. PVL 2186), the otic capsule is more obviously spherical in ventral view than it is in larger frogs; in these younger animals, the ventral surface of the prootic is excavated to

form a shallow Eustachian canal anterior to the hemispherical area of the inner ear.

*Exoccipitals:* These posterior neurocranial bones are fused completely to the prootics in all specimens examined, with the possible exception of the holotype in which there seems to be a visible line of suture between the two elements. In addition, the exoccipitals are not fused to one another ventromedially in the holotype. However, there is no evidence that the paired exoccipitals are not fused dorso- and ventromedially to one another in all other specimens; thus, the margin of the foramen magnum seems to be completely ossified. The occipital condyles are relatively large and distinctly separated.

*Frontoparietal:* This azygous bone lacks any indication of a median suture. The frontoparietal bears a pair of weakly sigmoid parasagittal crests that extend posteriorly over the length of the bone from its anterolateral margins; the crests unite medially near the posterior margin of the frontoparietal, thereby defining the lateral and posterior borders of a smooth dorsal skull table (Fig. 5). Supraorbital flanges and anterolateral processes are absent. Anteriorly, the frontoparietal overlies the sphenethmoid and the posterior part of the fused nasals. The pineal foramen lies in the midline of the anterior third of the bone. The characteristics of the frontoparietal in adults are clearly evident in PVL 3989, 3991, and CPBA 12219.

In young individuals (e.g., PVL 2187, MLP 62-XII-21-1), the parasagittal crests are poorly developed and the frontoparietal has a vaselike shape, being narrower anteriorly and more rounded posteriorly than in larger, older individuals (Figs. 2, 5). The shape of the frontoparietal in smaller individuals reflects the lack of expansion of the sagittate anterior end that is characteristic of this bone in larger specimens. There also is ontogenetic variation in the proportions of the skull table as defined by the parasagittal crests, with the skull table being longer and narrower in older individuals.

The frontoparietal of the holotype is clearly represented by a natural cast of its ventral surface. The anterior, triangular part is flat; Casamiquela (1961) mistakenly interpreted this part of the frontoparietal to represent the nasals. Posteriorly, a pair of elongated, elliptical convexities might correspond to the cerebral hemispheres, behind which lie more rounded convexities that mark the position of the optic lobes.

*Nasals:* Because these large, deep, arcuate bones are partially covered by the frontoparietal, only about the anterior half of the fused nasals is visible dorsally (Fig. 5). In no specimen examined (e.g., PVL 2186, 3996, 4009, CPBA 12223), including those with disarticulated skeletal elements, were the nasals found independent of one another; thus, we conclude that the bones are fused medially. Nonetheless, a medial line usually is apparent on the dorsal surface of the nasal bone; this is thought to represent the line of fusion between the paired elements. The nasal bears a short, blunt, anteromedial rostral process that is about equally as wide as long, with the length being about one-fourth to one-third the midlength of the main body of the fused bones. The posterior part of the fused nasal is a thin sheet of bone that lies between the sphenethmoid and the frontoparietal. Along the medial line of fusion, the nasal bears a ventral, longitudinal, ridge of bone that may have formed the dorsal part of the septum nasi (e.g., CPBA 12231); presumably, the ventral part of the septum was formed by an anterior extension of the sphenethmoid cartilage, as is typical of other anurans (Trueb, 1993). The posterior part of the septum nasi between the olfactory foramina was ossified.

In the holotype (Fig. 2), the fused nasals are preserved in a ventral impression, and are somewhat displaced from their natural position. The rostral process of the nasal is relatively longer and narrower in juveniles than in more mature individuals.

*Parasphenoid*: Complete parasphenoids are present as imprints in young individuals (e.g., PVL 4007A , ca. 36 mm SVL, 4086–87) in which the bone is not fused to the overlying braincase. In these specimens, the parasphenoid is lanceolate, having a truncate base posteriorly and curved sides that taper to a slender, pointed anterior process. In more mature frogs (e.g., PVL 3993, ca. 65 mm SVL), the bone is extraordinarily long, with the tip of the cultriform process lying just posterior to the premaxillae (Fig. 5). That part of the cultriform process anterior to the sphenethmoid is slender and acuminate; the process gradually widens beneath the sphenethmoid and is widest at the level of the prootic foramina at the posterior limits of the orbits. Posterior to the prootic foramina, the parasphenoid narrows and terminates in a blunt posteromedial process (e.g., CPBA 12231). There is no superficial sculpturing that would indicate insertion of the retractor bulbi muscles on the ventral surface of the parasphenoid. Although the parasphenoid seems to be fused to the braincase in the orbital region and posteriorly in large individuals, the anterior part of the cultriform process remains free (e.g., PVL 3991, ca. 98 mm SVL). The condition of the parasphenoid posterior to the optic foramina could not be assessed with certainty in larger specimens, because the braincase and otic capsules invariably are crushed in these individuals.

*Vomers:* The only evidence of these ventral palatal bones is the presence of a poorly defined, rhomboidal impression of bone at the anteromedial margin of the sphenethmoid; the vomer(s) seem to have been superficial to the parasphenoid (e.g., PVL 3991, CPBA 12224; Fig. 5). The vomers might have been either azygous or paired,

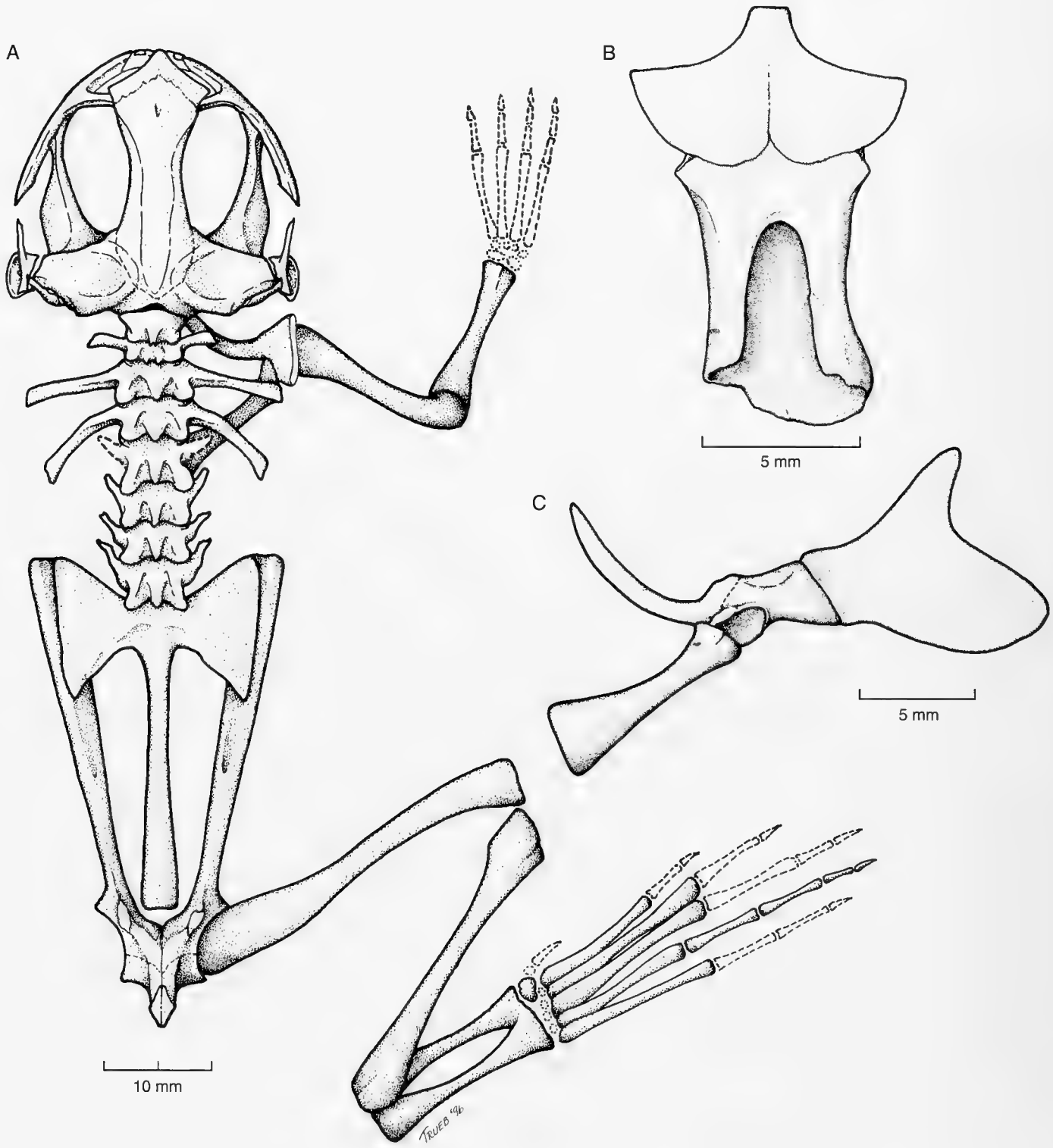


Fig. 6. *Shelania pascuali*. A. Partial reconstruction of the skeleton in dorsal view based on a variety of specimens (e.g., PVL 3989, 3990–91, 4002A, 4082; CBPA 12219, 12224). Right half of pectoral girdle (excluding suprascapula) shown. B. Isolated nasal and sphenethmoid complex in dorsal aspect (CBPA 12213). Note the trace of a suture medially on the azygous nasal and the well-developed frontoparietal foramen in the sphenethmoid. C. Ventral view of the left half of the pectoral girdle, with the cleithrum of suprascapular blade deflected into the ventral plane. Restoration based on PVL 3993–94, 4085; CBPA 12231.

and may have been fused to the parasphenoid medially and the sphenethmoid laterally.

*Premaxillae:* Because the premaxillae are either crushed or missing in most specimens, it is difficult to describe them. The premaxilla is edentate and bears a wide pars palatina that seems to have had an oblique articulation with the pars palatina of the adjacent maxilla (Fig. 5); there is no evidence of a distinct palatine process. The alary processes are well developed. Their vertical axes are approximately straight—i.e., not laterally divergent from the midline in frontal aspect (CPBA 12224). The base of each process is constricted and the distal (i.e., dorsal) margin is unnotched.

*Maxillae:* These elements are robust and long; in their natural position, the free, acuminate posterior ends lie well posterior to the midlength of the orbit (Fig. 5). The anterior end of the maxilla is acuminate; the margin of the pars palatina seems to have formed an oblique articulation with the premaxilla medially, and the low, slender pars facialis may have overlapped the premaxilla. The maxilla, like the premaxilla, is edentate; the ventral surface is concave and, thus, lacks any indication of a pars dentalis (PVL 3996, 4009; CPBA 12219).

At the anterior margin of the orbit, the maxilla bears a long medial process in the region of the planum antorbitale (PVL 3988–89, 4009, 4085; MLP 61-XII-20-1; CPBA 12219; Fig. 5); herein, this process is termed the antorbital process of the maxilla. The base of the antorbital process seems to be formed by an elaboration of the inner surfaces of the partes facialis and palatina. The anterodorsal surface is shallowly convex and the posteroventral surface concave. The position of the process suggests that it may have invested the planum antorbitale, thereby forming a structural support element between the maxillary arcade and the sphenethmoid. This antorbital process consistently appears in all specimens in which the maxilla is preserved, and is evident in the holotype and MLP 62-XII-22-1, which are among the six first known specimens described by Casamiquela (1960; 1961; 1965).

A distinct pars facialis (apparently lacking a preorbital process) and pars palatina are apparent only on the part of the maxilla anterior to the antorbital process. Posterior to the process in the orbital region, the maxilla is solid and triangular in cross section.

*Quadratojugals:* These posterior elements of the maxillary arcade are absent; thus, the maxillary arcade is incomplete.

*Pterygoids:* These massive elements lack a distinctly triradiate structure (Fig. 5). The anterior ramus is long and robust. It bears an exceedingly broad, ventrolaterally oriented flange anterior to the otic capsules (e.g., BAR 3722-44; PVL 3993; CPBA 12224); the flange diminishes in width in the midregion of the orbit. The slender anterior part of the ramus extends anterolaterally toward the maxilla in the anterior orbital region. Its expanded, footlike terminal portion lies medially adjacent to medial surface of the maxilla posterior to the antorbital process of this bone. In dorsal aspect, a canal is evident along the lateral margin of the anterior ramus (e.g., PVL 3989, 4009, 4082); presumably, this canal accommodated the cartilaginous pterygoid process of the palatoquadrate cartilage in the living animal.

The posterior and medial rami of the pterygoid are expanded to form a broad otic plate that underlies the otic capsules and forms the bony floor to the Eustachian canal (e.g., CPBA 12231; MPEF-PV 1150, 1151; Fig. 5). The posterior process is short and blunt, and presumably terminates at the pars articularis of the palatoquadrate cartilage. The medial process seems to terminate laterally adjacent to the prominent pseudobasal process. The medial and posterior processes are difficult to distinguish owing to their respective contributions to the otic plate. The posterior margin of the otic plate cannot be discerned with certainty because the otic regions of all specimens are crushed.

*Squamosals:* These bones are relatively well preserved in specimens PVL 4009, 4010B, and 4082. The ventral portion of the squamosal is conch shaped and partially surrounds the stapes (Fig. 5); this structure probably was produced by synostotic fusion of the squamosal and the tympanic annulus, as it is in living pipids (Trueb and Cannatella, 1986). The posterodorsal margin of the squamosal ring is incomplete; short processes of the squamosal on each side of this gap support the stapes. A narrow, well-developed zygomatic process projects anteriorly toward the maxilla, and a short, blunt otic process projects posteriorly.

*Stapes:* The stapes (= columella) is slightly bent and rodlike (PVL 3996, 4082; Fig. 5). The long, styliform pars media plectri is thicker proximally than it is distally, and seems to lack discrete, protuberant processes for the articulation with the squamosal. Proximally, the pars interna plectri forms a broad, well-defined footplate that fits into the anterior part of the fenestra ovalis. The presence of a pars externa plectri and an operculum could not be determined.

*Mandible:* The lower jaw is recurved posteriorly, and the articulation of the jaw with the skull lies anterior to the level of the fenestra ovalis (Fig. 5). The mandible is composed of angulosplenials and dentaries, and lacks mentomeckelian bones. The angulosplenial is robust and long, investing as much as 80–85% of the inner surface of the mandible; posteriorly, it bears a well-developed, laminar coronoid process for the insertion of the adductor muscles. The edentulous dentary extends posteriorly from the mandibular symphysis more than half the length of the mandible along its lateral surface.

*Hyoid apparatus:* The posteromedial processes of the hyoid have been identified in a few specimens (Fig. 3; CPBA 12219; PVL 3990). The anterior end of this long bone is narrow, but the posterior end is widely expanded.

### Axial Skeleton

*Presacral vertebrae:* Eight opisthocoelous presacral vertebrae are present (PVL 4009, 4010B; MLP 62-XII-22-1; CPBA 9855; Fig. 6A). We have seen no evidence of fusions between presacral centra. The vertebral centra are oval in cross section; probably this indicates that they were epichordal in development. In at least one large individual (PVL 3991, ca. 95 mm SVL), the boundary between the neural arches of Presacrals I and II is difficult to trace; this suggests that the dorsal parts of these two presacrals might be partially fused. Presacral I, the atlas, is robust and bears a pair of well-developed cotyles that are separated medially by a distinct notch. Presacral II is markedly shorter than the atlas. The neural arches of all presacral vertebrae are imbricate and bear thick irregular longitudinal crests, more or less centered on the lateral surfaces of the neural arches (PVL 3989A, 3991; CPBA 12219). In young individuals (e.g., PVL 2187), the neural arches are almost smooth, with small, posteriorly projecting spinous processes, and a narrow, longitudinal ridge on the midline. The articular surfaces of the pre- and postzygapophyses are simple (PVL 3990, 3991), lacking ridges and grooves.

Presacral Vertebrae II–VIII bear transverse processes (Fig. 6A). The processes of Presacral II are relatively short, directed slightly anterolaterally, and slightly expanded distally (PVL 4082). The processes of Presacral III are long, slender, straight, and oriented at a slight posterolateral angle; the total width of the vertebra, from the tip of the left transverse process to that of the right, exceeds that of the sacrum and those of all other vertebrae. The processes of Presacral IV are slender, curved, and oriented posterolaterally; the overall width of this vertebra is slightly less than that of Presacral III and about the same as that of the sacrum. In most specimens (e.g., PVL 4082; CPBA 12219), the transverse processes of Presacrals III and IV seem to have an unusual shape. The base of each of these processes is about the same width as the distal end, but the shaft of each of the processes seems to narrow slightly distal to the vertebral base; owing to this configuration, these transverse processes seem to be slightly expanded distally in most specimens we observed. In CPBA 12231, there are well-preserved, isolated anterior presacral vertebrae complete with transverse processes that are not crushed. This specimen reveals that principal surfaces of the proximal and distal ends of the transverse processes lie in the horizontal body plane, whereas the widest portion of the shaft of the process lies approximately in the transverse plane. Compression of this structure probably is responsible for the peculiar appearance of the transverse processes in most of the specimens we examined. There is no evidence, even in the smallest individuals, of the presence of free ribs or of ankylosus of ribs to the transverse processes. Each of Presacral Vertebrae V–VIII bears a pair of short transverse processes that are oriented in an acute anterolateral direction. These processes are thickest proximally, and seem to increase in length posteriorly, with those of Presacral V being the shortest and those of Presacral VIII, the longest.

*Sacrum:* The sacrum is formed by the Vertebra IX, to which the urostyle is fused. The sacral diapophyses are dilated and nearly symmetrical, with the angle between the leading edge of the diapophysis and the midline of the column being about 53° and that between the posterior edge of the diapophysis and the midline about 47° (Fig. 6A). The leading edge of the diapophysis is smooth, whereas the posterior margin is slightly irregular. The width across the sacral vertebrae is slightly wider at the anterolateral corners of the sacral diapophyses than at the posterolateral corners. The sacrum consists of only a single vertebra in almost all specimens that we have examined; we have observed no accessory nerve foramina that would evidence incorporation of additional vertebrae. However, an asymmetrical (i.e., on one side only) small flange at the anterior end of the urostyle contacts the posterior edge of the sacral diapophyses in a few specimens (e.g., PVL 4085). Also, the anterior portion of the dorsal surface of the urostyle may be expanded to form a flange that is fused to the posterior margins of the sacral diapophyses (BAR 3722-44); this suggests the occasional participation of one postsacral vertebra in the sacrum formation.

*Urostyle:* The urostyle or coccyx is fused to the sacrum. Its proximal width at the union of the bone with the sacrum is about equal to its width at the distal terminus; the midlength is markedly more slender. This peculiar shape results from dorsoventral compression of the urostyle during fossilization that flattens the posterior end of the bone to produce a blunt, club-shaped terminus (Fig. 6A).

In the smallest specimens (holotype and PVL 2188), the urostyle is not formed fully. In these ventral impressions, at least half of the rodlike hypochord is preserved, and the anterior tip lies on the ventral surface of the sacral centra in the midline. It is not possible to determine whether the structures are fused or not. In *Xenopus laevis*, the urostyle has been observed to form by ossification of the hypochord and fusion of the anterior hypochord with neural arches of postsacral vertebrae dorsal to it (Trueb and Hanken, 1992). If the urostyle forms in a similar manner in *Shelania pascuali*, then we might speculate that in these smallest individuals, fusion was incomplete and that the ossified hypochord might have been shifted anteriorly beneath the sacrum after death.

### Appendicular Skeleton

*Pectoral girdle:* Based on the morphology, and relative positions of the clavicles and coracoids, the pectoral girdle seems to have been arciferal; however, impressions of the cartilaginous portions are not preserved. The clavicles are moderately curved with a concave anterior margin (Fig. 6C). The orientation of the long axis of the clavicle and leading edge of the girdle cannot be determined with certainty, but based on specimens in which the clavicles are articulated with the scapula (PVL 3988; CPBA 12219), we estimate that the leading angle between the long axis of the clavicle and a longitudinal line projected through the glenoid fossa would have approximated 45–60°. The clavicle is slender; the anteromedial end is acuminate, whereas the posterolateral end is slightly expanded and positioned on the pars acromialis of the scapula. In smaller individuals (e.g., PVL 2186, 3993, 3994, 4009; CPBA 12231), the clavicles are separated from the scapulae, indicating that the two bones were not fused. In larger specimens in which the clavicles are preserved in articulation with the scapula (e.g., PVL 3989, 3988; CPBA 12219; all in dorsal view), a suture is visible between the bones.

The coracoids are robust (PVL 4009, 3994; Fig. 6C). Both ends of the bone are distinctly expanded, with the sternal end being the larger. The expansion of the sternal end of the coracoid is clearly asymmetrical in larger individuals (e.g., CPBA 12219; MJHG 2.3-72; PVL 3991), suggesting that growth has occurred differentially along the leading, rather than the posterior, edge of the bone. The total width of the expansion is about two and one-half times that of the shaft of the coracoid at the midlength of the bone. The total width of the expansion of the glenoid end of the coracoid is about twice that of the shaft at the midlength of the bone. The coracoid forms the ventromedial part of the glenoid fossa, but seems to have been narrowly separated from the clavicle by procoracoid cartilage. We estimate that the posterior angle between the long axis of the coracoid and a longitudinal line projected through the glenoid fossa would have approximated 60°.

The scapula is robust, thick, and about twice as long as wide. The anterior and posterior margins of the dorsal (or medial) surface of the bone are moderately concave (e.g., PVL 3994; CPBA 12231; Fig. 6C). The ventral (or lateral) surface of the scapula is constricted adjacent to the partes acromialis and glenoidalis, such that the bone is much narrower on its ventral surface than on its dorsal surface, and has a "bow" shape when viewed from the ventral aspect. The scapula lacks a distinct medial notch separating the partes acromialis and glenoidalis. The pars acromialis bears a ventral projection that forms the anteroventral margin of the glenoid cavity.

The cleithrum is relatively large; medially, at the level of the scapula-suprascapular joint, it surrounds the suprascapular cartilage, and laterally it is forms two robust prongs that extend on the outer (i.e., dorsal) surface of the suprascapula (PVL 4082; CPBA 12219; MPEF 1150; Fig. 6C). The anterior prong invests the leading edge of the suprascapula, whereas the posterior prong, a large and broad blade, seems to have extended to the posterior rim of the suprascapula, because a groove is evident along the posterior margin of the suprascapula on the inner (i.e., ventral) side.

*Forelimb:* The humerus (Fig. 6A) has a well-developed deltoid crest (= crista ventralis of Gaupp [1896]). At approximately the level of the proximal third of the bone, there is another crest lateral to the deltoid crest; this is not the crista medialis, which in *Rana* is present on the opposite side of the humerus. This additional crest extends distally, and a relatively deep canal is formed between it and the deltoid crest; possibly this canal housed the tendon of the *M. coracoradialis*. The presence of a conspicuous, spherical humeral ball (= eminentia capitata of Gaupp [1896]) is clear from impressions of this bone in ventral (PVL 4085), medial, and lateral aspects (e.g., PVL 3991). This sphere is centered on the midline of the shaft of the humerus; thus, the distal part of this bone is relatively symmetrical in shape, because the ball is not displaced to the left or right. The humeral ball is relatively large with respect to the distal width of the bone; dorsally, the olecranon scar is approximately triangular. In smaller individuals (e.g., PVL 2196, 2188), the ends of the humerus are truncate, indicating that these portions of the bone were unossified.

The radioulna has no distinguishing characteristics. In the smallest specimens, the olecranon process is absent. In no specimen is an articulate manus preserved; thus, we were unable to identify and assess the number of carpals present or determine the phalangeal formula. Metacarpal IV is the shortest of the four metacarpals, all of which are long. The terminal phalanges are pointed.

*Pelvic girdle:* The ilial shafts are long; the anterior half of each is dorsoventrally compressed, whereas the posterior half is rodlike with a slight lateral compression (PVL 3991, 3994, 4085; Fig. 6A). Posteriorly, there is an extended interiliac symphysis on the midline. The dorsal prominence is well developed with a wide base that extends posteriorly to the border between ilium and ischium. The supraacetabular portion of the ilium and ischium is well developed, but its shape and dimensions could not be determined. The pubis is ossified in larger specimens (e.g., PVL 3991; CPBA 12224). The acetabulum is dumbbell shaped, with most of its border being formed by the ilium. The preacetabular area lacks lateral exposure, with the surface

of the preacetabulum facing anteriorly. The preacetabular angle is obtuse.

*Hind limb:* The femur is shallowly sigmoid shaped and has slightly expanded ends, as does the tibiofibula (PVL 3993; Fig. 6A). The sulcus separating the tibial and fibular regions at the proximal and distal ends of the tibiofibula is obvious in smaller individuals (e.g., PVL 2186). The tibiale and fibulare are fused distally only in the largest specimens (e.g., PVL 3991; CPBA 12219). At least three distal tarsals are present. The largest element preserved in natural position occurs between the bases of Metatarsals II and III (PVL 3990). Two smaller bones located medial to the large distal tarsal probably also represent tarsal elements (PVL 3990). The sizes of the metatarsals in increasing order of length are: I-IV-II-V-III; the longest metatarsal is equal in length to, or longer than, the tibiofibulare. The phalanges are long, and the terminal phalanges are pointed. No pes is sufficiently complete to allow determination the phalangeal formula.

## ANALYSIS OF CHARACTERS

The 51 characters and their character states analyzed in this study are described below. Cranial characters (1–34) are presented first, followed by axial features (35–43), pectoral-girdle characters (44–49) and pelvic-girdle features (50–51). The data matrix is presented in the Appendix.

**1. Skull shape.**—In *Xenopus*, *"Xenopus" romeri*, *Silurana*, *Palaeobatrachus*, *Rhinophrynus*, *Shelania*, *Eoxenopoides*, *Saltenia*, and the outgroups, the skull is rounded and domed in lateral profile (State 0; Figs. 7, 8). In the hymenochirines and *Pipa*, the skull is wedge shaped (State 1; Fig. 7), as noted by Cannatella and Trueb (1988). The preservation of *Saltenia* and *Chelomophrynus* prevents scoring this character in these taxa.

0: Skull rounded in lateral profile.

1: Skull wedge-shaped in lateral profile.

**2. Orbital region of braincase.**—In *Pelobates*, *Rhinophrynus*, and most other anurans, the anterior braincase is formed by sphenethmoid cartilage that is replaced by bone (Trueb, 1993). This cartilage is contiguous anteriorly with the septum nasi that separates the nasal capsules from one another medially and synchondrotically united laterally with the planum antorbitale, which forms a vertical wall separating the nasal capsule from the orbit posteriorly. The anterodorsal sphenethmoid cartilage is the tectum anterius; the posterior margin of the tectum forms the anterior border of the frontoparietal fontanelle in larval and adult frogs. In the region of the frontoparietal fontanelle, the braincase is represented by an incomplete girdle of cartilage or bone that forms the ventral and lateral walls of the neurocranium (Fig. 7); the dorsolateral margins of the braincase and the lateral margins of the frontoparietal fontanelle are formed by a narrow shelf of sphenethmoid cartilage or bone, the taenia tecti marginalis. Although the sphenethmoid cartilage is variably replaced by bone in different taxa, the configuration of this anterior braincase element is distinctive and easily recognized, and is typical of palaeobatrachids (Špinar, 1972: pl. 27; Vergnaud-Grazzini and Hoffstetter, 1972) and *Shelania* (State 0; Fig. 9). In *"Xenopus" romeri*, there is a clear, but exceedingly narrow, transverse bridge of sphenethmoidal bone forming the anterior margin of the frontoparietal fontanelle. Although it seems likely that *Chelomophrynus* has a typical anuran sphenethmoid, we could not confirm this from Henrici's (1991) description.

In *Xenopus laevis*, Trueb and Hanken (1992) demonstrated that the orbital region of the braincase develops in a strikingly different way than in other anurans for which there are descriptions. A frontoparietal fontanelle is present in the larval chondrocranium, but it lacks a distinct anterior margin (Trueb and Hanken, 1992:fig.1), apparently owing to the depression of the braincase in this region. Between larval Stages 59 and 60 (of Nieuwkoop and Faber, 1956), the ethmoidal cartilage that forms the lateral walls of the braincase in the orbital region disappears and the sphenethmoid ossifies as two thin, sheetlike bones in connective tissue to form the lateral walls of the braincase; eventually (Stage 66 + 1 mo), the sphenethmoid ossifications unite to one another ventromedially above the parasphenoid to which they fuse. As a result of this peculiar mode of formation, "sphenethmoid" cartilage in adult *Xenopus laevis* is limited to the septum nasi and the planae antorbitalae.

We have examined cleared-and-stained specimens, as well as serial cross sections of the crania of adult *Xenopus laevis*, *X. muelleri*, *Silurana tropicalis*, *Pipa carvalhoi*, *P. parva*, *P. pipa*, and *Hymenochirus curtipes*. Each of these taxa lacks any trace of cartilage in the orbital region and any indication of a frontoparietal fontanelle dorsally; moreover, the braincase walls in the orbital region are solid, lacking the vacuities typical of bone formed by replacement (Fig. 10). The orbital region of the braincase in adult specimens of these taxa seems to be composed of a girdle of dermal bone formed by the parasphenoid, sphenethmoid (as defined by Trueb and Hanken, 1992), and frontoparietal. The parasphenoid and sphenethmoid always are fused to one another, and the frontoparietal is variably fused depending on the region and the taxon. For example, at the level of the optic foramen in *Xenopus muelleri* (Fig. 10), there is a barely perceptible separation (in transverse sections) between the frontoparietal and the sphenethmoid along the

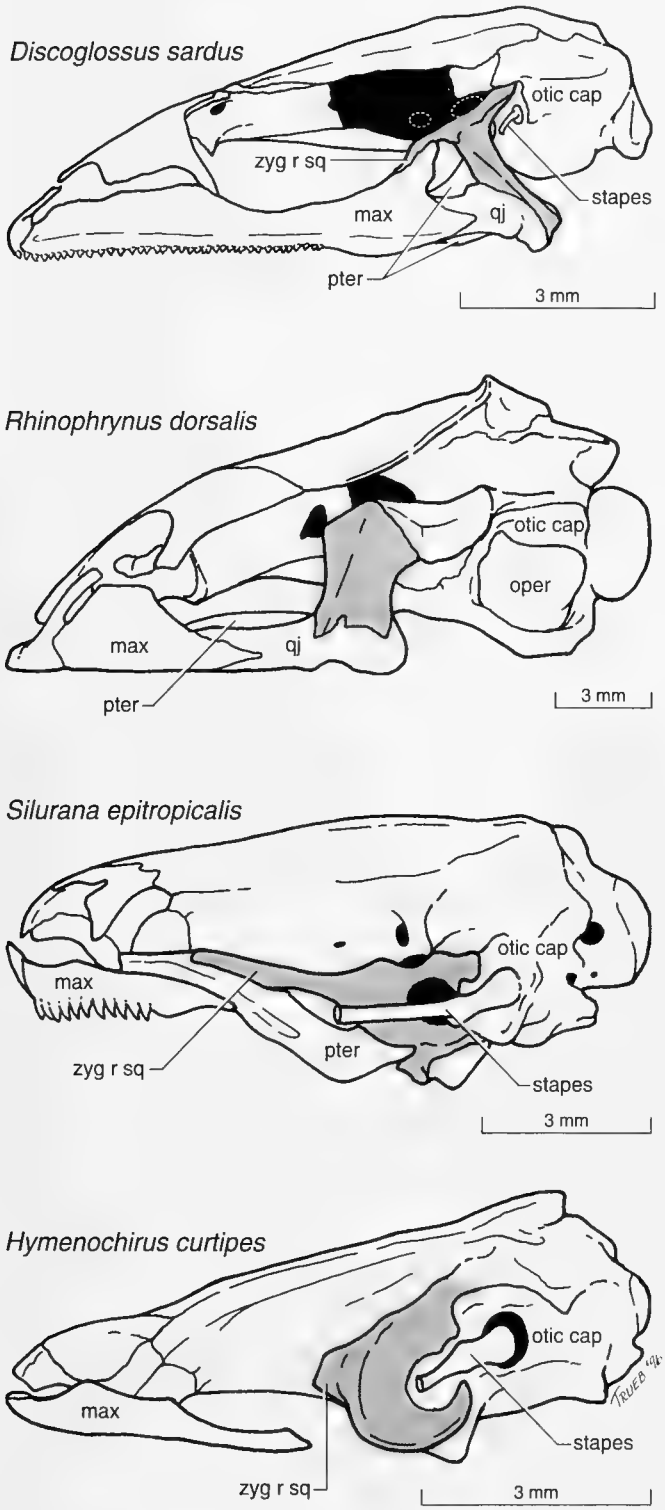


Fig. 7. Lateral views of the skulls of examples of outgroup and ingroup taxa to illustration variation in the structure of the squamosal (shaded gray) and the stapes: *Discoglossus sardus* (KU 129239, male); *Rhinophrynus dorsalis* (KU 84886, female); *Silurana epitropicalis* (KU 195660, female); and *Hymenochirus curtipes* (KU 204127, female). Approximate positions of optic and prootic foramina in cartilage in *Discoglossus* are indicated by dashed white lines. Abbreviations: max = maxilla; oper = operculum; otic cap = otic capsule; pter = pterygoid; qj = quadratojugal; zyg r sq = zygomatic ramus of the squamosal.

lateral wall of the braincase; the two bones are tightly bound to one another with dense connective tissue. In other pipoid taxa such as hymenochirines, *Pipa*, and *Silurana*, the frontoparietal seems to be synostotically united with ventral parts of the braincase in the orbital region (Fig. 10). This peculiar morphology results in a complete and unified braincase that lacks distinct sutures and a frontoparietal fontanelle in the adults.

From these observations, we conclude that the orbital region of the braincase in living pipids (State 1) differs fundamentally in its formation and adult configuration from that of all other anurans (State 0) for which osteological data are known; it should be noted that we could not determine the condition of this region of the cranium in *Eoxenopoides* because Estes (1977) did not describe the sphenethmoid in dorsal aspect, and in all the peels available to us, this region is covered by the frontoparietal.

0: Orbital region of braincase formed by cartilage replacement bone in Recent anurans, with frontoparietal fontanelle present in adults.

1: Orbital region of braincase formed by dermal elements in Recent anurans and lacking frontoparietal fontanelle in adults.

**3. Olfactory nerve foramina.**—The posterior wall of each nasal capsule is ossified and pierced by a foramen for the olfactory nerve; the nerves (and their foramina) are separated medially by a well-ossified medial septum (State 0) in *Discoglossus*, *Pelobates*, *Rhinophrynus*, "*Xenopus*" *romeri*, *Palaeobatrachus*, *Pipa*, hymenochirines, *Saltenia*, and *Shelania*. We assume that this also is the condition in *Eoxenopoides*, because Estes (1977) noted the presence of olfactory tracts lined with bone. Similarly, the foramina seem to have been bony in *Chelomophrynus* owing to the extensive ossification in the ventral ethmoidal region (Henrici, 1991:fig. 16). However, in *Xenopus* and *Silurana*, the posterior wall and septum nasi remain mostly cartilaginous (State 1).

0: Margin of olfactory nerves foramina bound in bone.

1: Margin of olfactory nerves foramina cartilaginous.

**4. Antorbital plane of skull.**—In *Hymenochirus* and *Eoxenopoides*, the posterolateral wall of each olfactory capsule (and anterior margin of the orbit) is formed by a fully ossified planum antorbitale, which extends from the sphenethmoid to the region of the maxilla laterally (State 1). In all the other taxa considered, the planum antorbitale

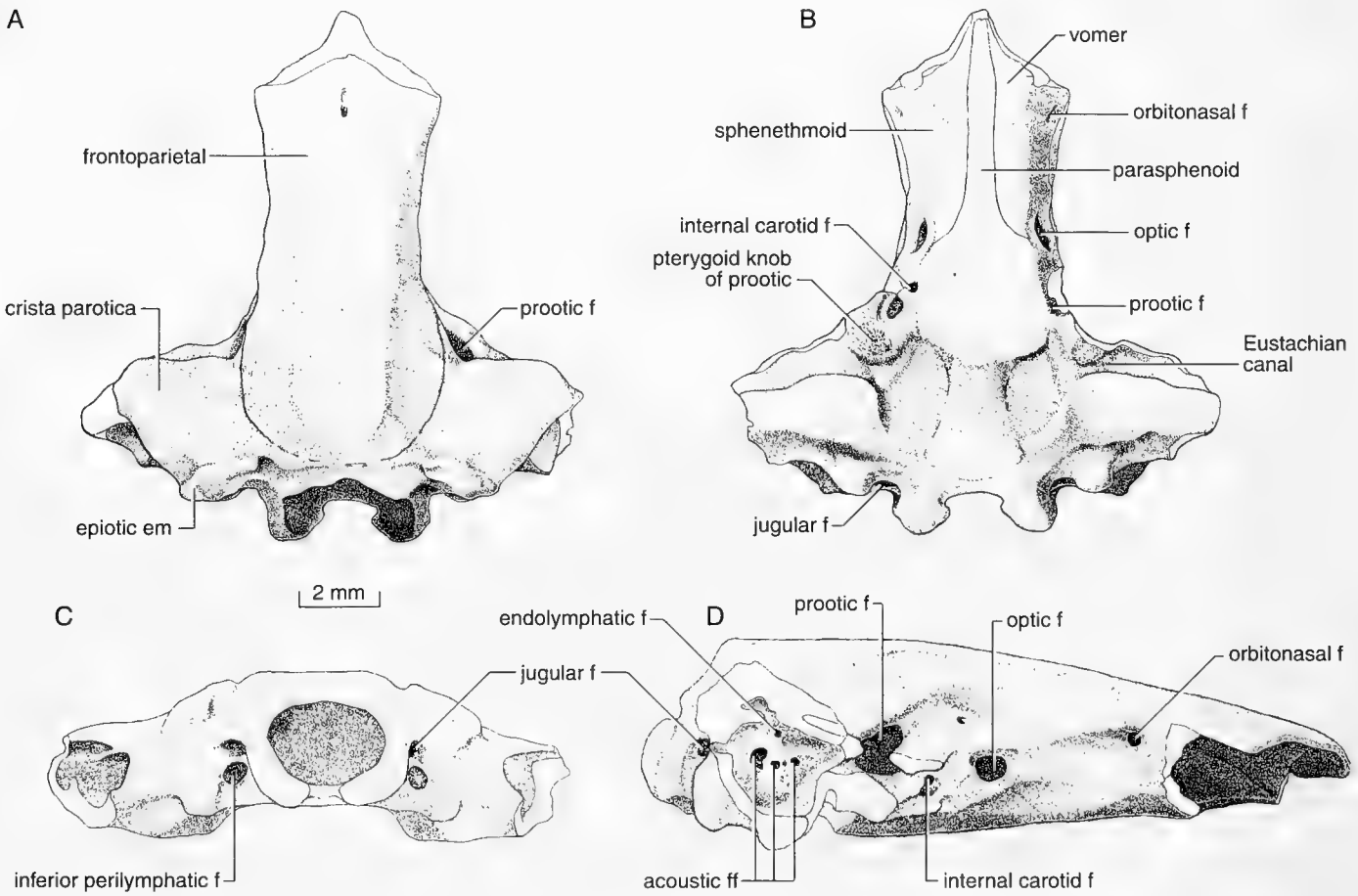


Fig. 8. *"Xenopus" romeri*, skull. Dorsal (A), ventral (B), and posterior (C) views of the holotype (DGM 568). Lateral view (D) of skull (DGM 569). All drawings from Estes (1975a, b). Abbreviations: em = eminence; f = foramen; ff = foramina.

is partially ossified medially, or bears mineral deposits (State 0). The condition in *Saltenia* could not be determined.

0: Planum antorbitale ossified (or mineralized) only partially in medial region.

1: Planum antorbitale fully ossified between sphenethmoid and maxilla.

**5. Ventrolateral configuration of braincase in orbital region.**—Viewed in ventral aspect (or transverse section), the floor of the braincase (sphenethmoid + parasphenoid) is broadly curved or dorsolaterally sloped toward the roof of the cranium in *Discoglossus, Pelobates, Rhinophrynus, Shelania, Saltenia, Silurana, Xenopus*, and *"Xenopus" romeri* (State 0; Fig. 10). However, in *Palaeobatrachus, Eoxenopoides, Pipa*, and hymenochirines, there is a distinct angle that is sometimes elaborated into a ventrolateral keel in this region (State 1). The condition of the ventrolateral region of the braincase in *Chelomophrynus* could not be determined with certainty.

0: Braincase sloping or broadly curved ventrolaterally.

1: Braincase distinctly angled, with or without a keel, ventrolaterally.

**6. Optic foramen.**—The margin of the optic foramen may be completely cartilaginous (*Discoglossus*), bony anteriorly and cartilaginous (*Pelobates* and *Palaeobatrachus*) or membranous posteriorly (*Rhinophrynus* and *Chelomophrynus*) (State 0), or formed completely by and within the sphenethmoid in the remaining taxa (State 1).

0: Margin of optic foramen incompletely ossified.

1: Margin of optic foramen complete in sphenethmoid.

**7. Eustachian canal.**—Although a few anurans lack Eustachian tubes (e.g., *Rhinophrynus*), most possess a short tube on each side of the head that opens from the middle ear into the buccal cavity at the posterior corner of the roof of the mouth (e.g., *Discoglossus, Pelobates*). The ventral surfaces of the otic capsules of these anurans lack a transverse furrow or Eustachian canal to accommodate the Eustachian tube (State 0). In *Xenopus, "Xenopus" romeri, Silurana, Pipa*, and hymenochirines, the Eustachian tubes are elongated

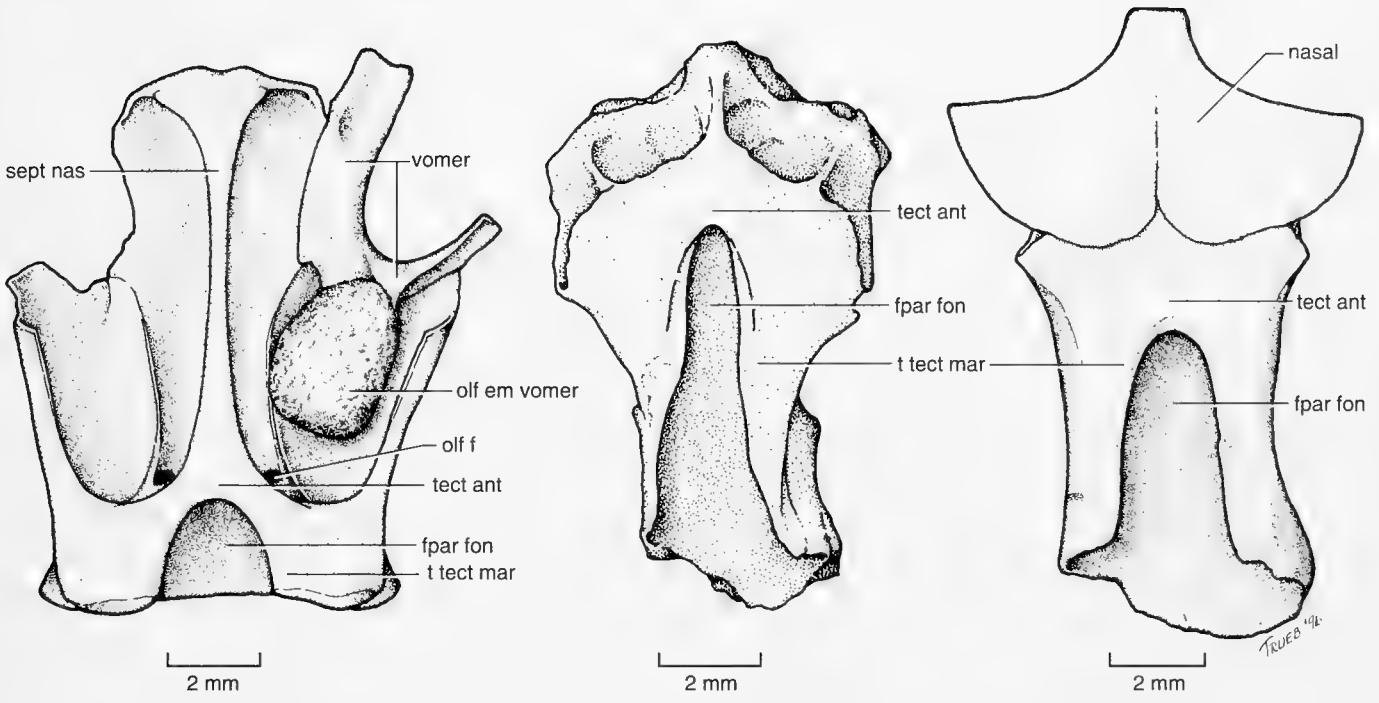


Fig. 9. Sphenethmoids and some associated bones of three pipoid frogs (*Rhinophrynus dorsalis*, KU 84885; *Palaeobatrachus* sp., unnumbered cast from Richard Estes' private collection; *Shelania pascuali*, CBPA 12213) in dorsal aspect. Note the presence of well-defined frontoparietal fontanelles in each species. The anterior border of the fontanelle is the tectum anterius; the lateral borders are formed by the taeniae tecti marginalis. Abbreviations: fpar fon = frontoparietal fontanelle; olf em vomer = olfactory eminence of vomer; olf f = olfactory foramen; sept nas = septum nasi; t tect mar = taenia tecti marginalis; tect ant = tectum anterius.

medially and open into the pharynx via a single, median aperture in the roof of the mouth (Cannatella and Trueb, 1988). These taxa bear a distinct transverse furrow, the Eustachian canal, in the venter of the prootic portion of the otic capsule to accommodate the Eustachian tube (State 1; Fig. 8). Distinct Eustachian canals are present in *Eoxenopoides*, "*Xenopus*" *romeri*, *Saltenia*, and *Shelania;* thus, we assume that they also had one medial opening for the Eustachian tubes. In the several casts of *Palaeobatrachus* examined (*Palaeobatrachus* sp.: KUVP 124976A, B; 124971A, B; 124972A, B; *P. novotny:* KUVP 124909; *P. diluvianus:* KUVP 124939), Eustachian canals are absent; this condition was confirmed by J.-C. Rage (pers. comm. to Báez, 1996), who examined isolated otic capsules of palaeobatrachids preserved in three dimensions from the Tertiary of Europe. The prootics of *Chelomophrynus* also lack Eustachian canals (Henrici, 1991).

0: Eustachian canal absent in prootic.
1: Eustachian canal present in prootic.

**8. Inferior perilymphatic foramen.**—The inner ear in anurans contains perilymphatic and endolymphatic fluid systems, each of which is contained within distinct sets of membranes housed in a series of intracapsular and extra- and intracranial spaces. The membranous intracapsular and intracranial sacs of the perilymphatic system are connected with one another via perilymphatic ducts that pass through perilymphatic foramina in the posteromedial wall of the otic capsule. In most anurans, one perilymphatic duct passes from the perilymphatic sac of the inner ear through the inferior perilymphatic foramen in the floor of the posteromedial wall of the otic capsule to the exterior (State 0; Fig. 8). A true inferior perilymphatic foramen opening extracranially from the otic capsule is absent in *Pipa* and hymenochirines (State 1), whereas it is present in the posteromedial wall of the otic capsules in *Palaeobatrachus* (Vergnaud-Grazzini and Hoffstetter, 1972), *Chelomophrynus* (Henrici, 1991), *Xenopus*, *Silurana*, "*Xenopus*" *romeri*, and *Shelania*. The condition in *Eoxenopoides* and *Saltenia* is unknown.

0: Inferior perilymphatic foramen present.
1: Inferior perilymphatic foramen absent.

**9. Superior perilymphatic foramen.**—In most anurans, a perilymphatic duct passes through the superior perilymphatic foramen from the inner ear to an intracranial space (State 0). In *Xenopus*, "*Xenopus*" *romeri*, and *Silurana*, a separate superior perilymphatic foramen is absent (Paterson,

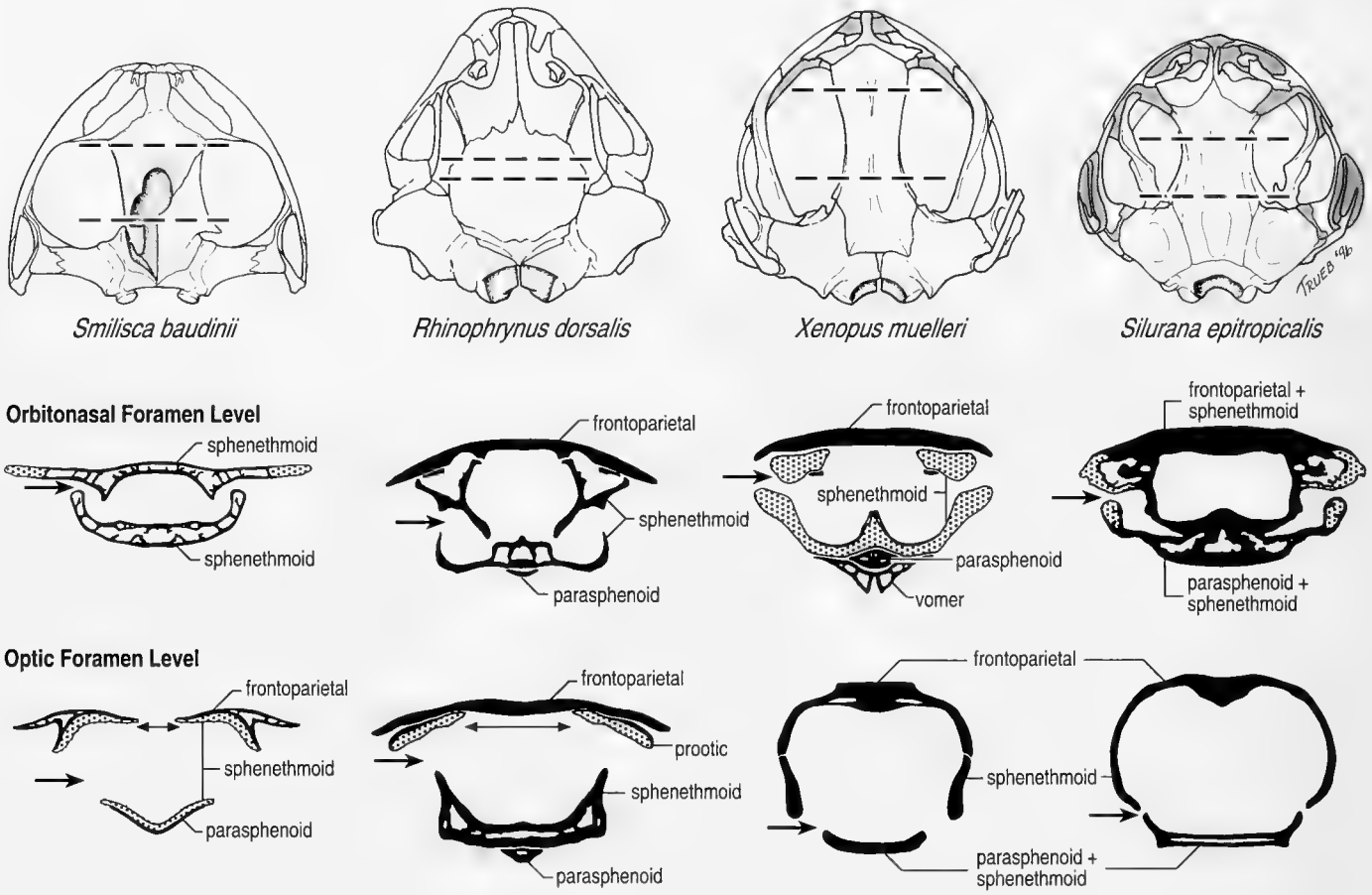


Fig. 10. Diagrams of the skulls and transverse sections through the regions of the orbitonasal and optic foramina of four anurans illustrating the similarities and differences in the structure of the sphenethmoid and its relationship with adjacent bones, the shape of the ventral braincase, and the position of the optic foramina. The hylid frog *Smilisca baudinii* (KU 89924) is used to represent the usual condition in anurans, whereas *Rhinophrynus dorsalis* (KU 186799), *Xenopus muelleri* (KU 196041), and *Silurana epitropicalis* (KU 216330) illustrate various derived conditions typical of pipoid anurans. Dashed lines through the skulls indicate the levels of the sections depicted below each skull. In the orbitonasal region, an arrow shows the position of the orbitonasal foramen. In the optic region, the arrow shows the position of the optic foramen. The double-headed arrow indicates the extent of the frontoparietal foramen in the skull roof; note its absence in *Xenopus* and *Silurana*. In the transverse sections, bone is indicated by black and the stippled pattern indicates cartilage. Cartilage in the skulls of *Xenopus* and *Silurana* is shown in gray.

1960; State 1; Fig. 8). Discrete superior perilymphatic foramina are present in *Palaeobatrachus* (Vergnaud-Grazzini and Hoffstetter, 1972) and *Chelomophrynus* (Henrici, 1991); their presence could not be assessed in the remaining fossils considered.

0: Superior perilymphatic foramen present.
1: Superior perilymphatic foramen absent.

**10. Jaw articulation, position.**—In most anurans, the pars articularis of the palatoquadrate is located lateral or slightly posterolateral to the otic capsule (State 0; Fig. 11). In hymenochirines, *Rhinophrynus, Saltenia,* and the basal *Pipa* (*P. carvalhoi, P. myersi,* and *P. parva*), the pars articularis is anterolateral to the otic capsule (State 1; Figs. 11, 12). The condition of this character is unknown in *Chelomophrynus* and *"Xenopus" romeri.*

0: Pars articularis lateral or posterolateral to otic capsule.
1: Pars articularis anterolateral to otic capsule.

**11. Frontoparietal fusion.**—The frontoparietal is a paired or azygous bone that covers the braincase dorsally. Most anurans, including *Discoglossus,* have paired frontoparietals (State 0; Fig. 11). Adult rhinophrynids, *Pelobates, Palaeobatrachus, Shelania, Saltenia, Eoxenopoides, "Xenopus" romeri,* and all living pipids possess azygous frontoparietals (State 1; Figs. 8, 11, 12) that tend to overlap the nasals anteriorly and roof the entire neurocranium.

0: Paired frontoparietals.
1: Azygous frontoparietal.

**12. Frontoparietal, anterior extent.**—The anterior margin of the frontoparietal usually is separated from the na-

sals (e.g., *Discoglossus*), although in some taxa such as *Pelobates*, and some hymenochirines, the anterior margin is partially or wholly in contact with the posterior margins of the nasals (State 0; Figs. 11, 12). In *Rhinophrynus*, *Xenopus*, *Silurana*, *Pipa*, *Saltenia*, and *Shelania*, and possibly some hymenochirines (*Pseudhymenochirus*) the frontoparietal covers the underlying sphenethmoid and overlaps the posteromedial part(s) of the nasal(s) (State 1; Figs. 11, 12). This latter condition is present in *"Xenopus" romeri;* on reexamination of the holotype, we noted that broken pieces of the posterior portion of the nasals lie between the dorsal surface of the sphenethmoid and ventral surface of the frontoparietal. In *Palaeobatrachus*, the nasals are extremely narrow and it seems unlikely that they were covered by the frontoparietal (Špinar, 1972). The condition of this character is unknown in *Chelomophrynus*.

0: Anterior part of frontoparietal does not overlap the posterior part of nasals.
1: Anterior part of frontoparietal overlaps the posterior part(s) of nasal(s).

**13. Nasals.**—The nasals usually are paired bones that roof the olfactory capsule (e.g., *Discoglossus*, *Pelobates*, rhinophrynids, *Palaeobatrachus*, *Saltenia*, *Silurana*, *Pipa*, *Eoxenopoides*, *"Xenopus" romeri*, and hymenochirines) (State 0; Figs. 11, 12). In postmetamorphic *Shelania* and most *Xenopus*, these bones are fused to one another medially (State 1; Figs. 11, 12); however, paired nasals have been reported in *X. longipes* by Loumont and Kobel (1991).

0: Paired nasals.
1: Azygous nasal.

**14. Septomaxilla.**—The septomaxillae provide support to the internal cartilages and cava of the olfactory capsule. In *Discoglossus*, *Pelobates*, *Rhinophrynus*, and *Palaeobatrachus*, the bones are complex and triradiate (State 0; Fig. 11), and resemble the septomaxillae of most other anurans. In contrast, the septomaxillae of the Recent pipids are much larger structures that are arcuate in dorsal aspect (State 1; Fig. 12). The septomaxillae of *Chelomophrynus*, *Shelania*, *Saltenia*, *Eoxenopoides*, and *"Xenopus" romeri* are unknown.

0: Small, complex, triradiate septomaxilla.
1: Large, arcuate septomaxilla.

**15. Vomers.**—The vomers are large, paired bones that underlie the nasal capsules and support the margins of the choanae in *Discoglossus*, *Pelobates*, rhinophrynids, and *Palaeobatrachus* (Fig. 11). In *Saltenia* (Báez, pers. obs), *Shelania*, *"Xenopus" romeri*, and *Eoxenopoides*, the fused vomers invest the parasphenoid ventrally (Fig. 11). In most *Xenopus*, the vomers are azygous and fused to the parasphenoid; however, we observed paired vomers in *X. largeni* (KU 206863) and their presence has been noted in other species of *Xenopus* (Báez and Rage, **in press**). Presence of vomers is considered to be State 0, whereas their absence in *Silurana*, *Pipa*, and the hymenochirines is State 1 (Fig. 12).

0: Vomers present.
1: Vomers absent.

**16. Vomer, anterior process.**—Anurans having well-developed vomers, such as *Discoglossus*, *Pelobates*, rhinophrynids, and *Palaeobatrachus*, possess an anterior process on the bone that extends anteriorly or anterolaterally toward the maxillary arcade (State 0; Fig. 11). An anterior process is absent in taxa having median vomers and, obviously, those that lack vomers altogether (State 1; Figs. 11, 12).

0: Anterior process of vomer present.
1: Anterior process of vomer absent.

**17. Premaxilla, alary process.**—All anurans have an alary process (pars dorsalis of some authors) on the premaxilla, against which the prenasal cartilages of the nasal capsule abut posteriorly. In *Discoglossus*, *Pelobates*, *Palaeobatrachus*, and *Shelania*, these processes are moderately high, narrow, and uniform in width (State 0; Fig. 13). The alary processes of *Xenopus*, *Silurana*, and *Eoxenopoides* are low and wider dorsally than at their bases (State 1; Fig. 13). Those of *Pipa* and hymenochirines are so poorly developed as to be scarcely evident (State 2; Fig. 13). In *Chelomophrynus*, the alary process of the premaxilla is small and triangular (Henrici, 1991); the condition in *Saltenia* and *"Xenopus" romeri* could not be ascertained.

0: Alary process of premaxilla notably higher than wide, not expanded dorsolaterally.
1: Alary process of premaxilla about as wide as high, expanded dorsolaterally.
2: Alary process of premaxilla lower than wide, scarcely evident.

**18. Maxilla, contact of pars facialis with alary process of premaxilla.**—In most anurans, the pars facialis of the maxilla does not broadly overlap the lateral part of the premaxilla and touch the alary process of that bone (State 0; Fig. 13). In *Palaeobatrachus*, *Saltenia*, *Shelania*, *Xenopus*, *Silurana*, *Pipa*, and hymenochirines, the maxilla is extraordinarily long anteriorly, and reaches or overlaps the lateral margin of the alary process of the premaxilla (State 1; Fig. 13). The condition is unknown in *Chelomophrynus* and *"Xenopus" romeri*.

0: Maxilla not extending to alary process of premaxilla.
1: Maxilla extending to, or overlapping, lateral margin of alary process of premaxilla.

**19. Maxilla, antorbital process.**—The maxillae in *Saltenia* and *Shelania* have a conspicuous, thick process that

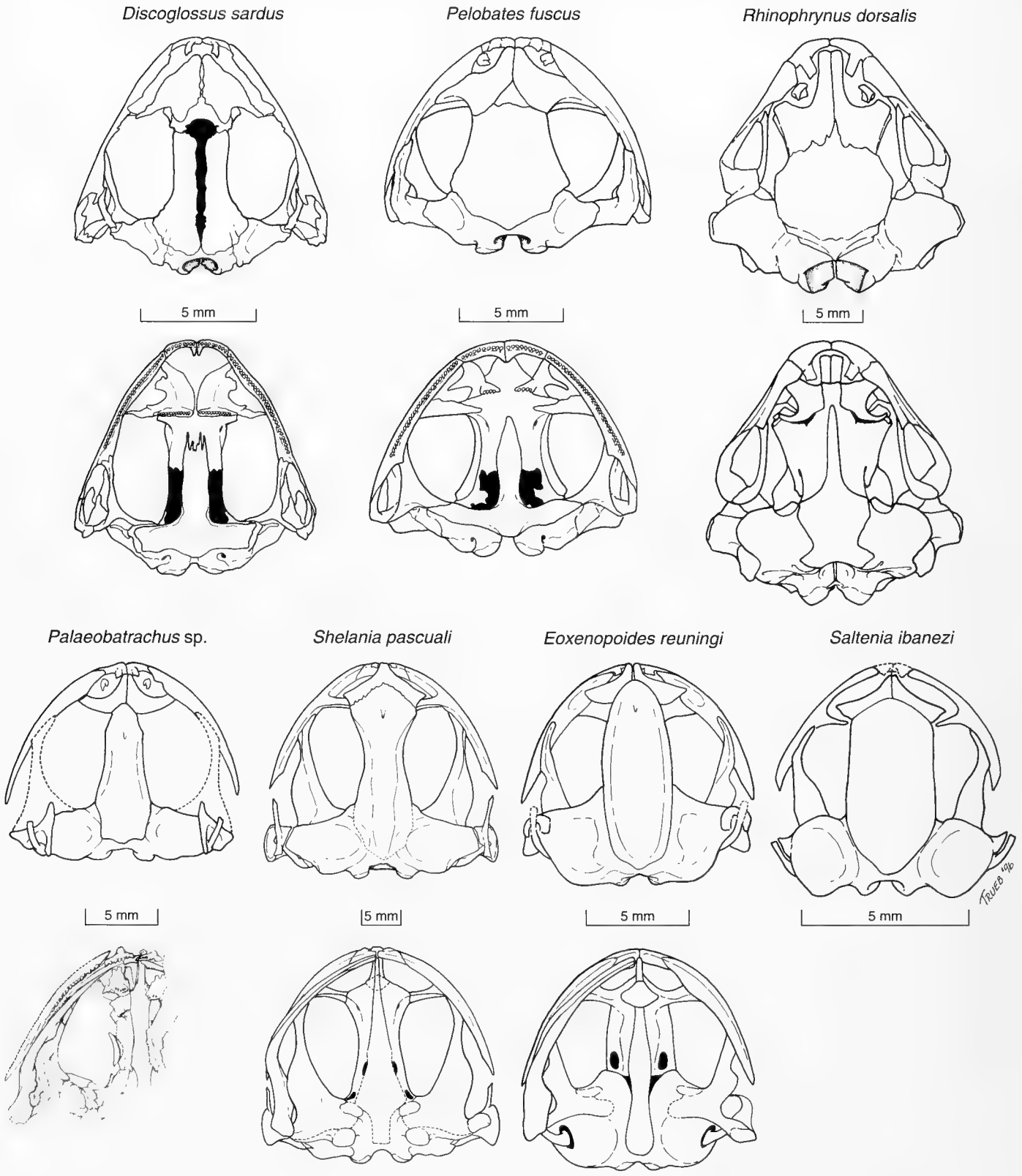
Discoglossus sardus
Pelobates fuscus
Rhinophrynus dorsalis
5 mm
5 mm
5 mm
Palaeobatrachus sp.
Shelania pascuali
Eoxenopoides reuningi
Saltenia ibanezi
5 mm
5 mm
5 mm
5 mm

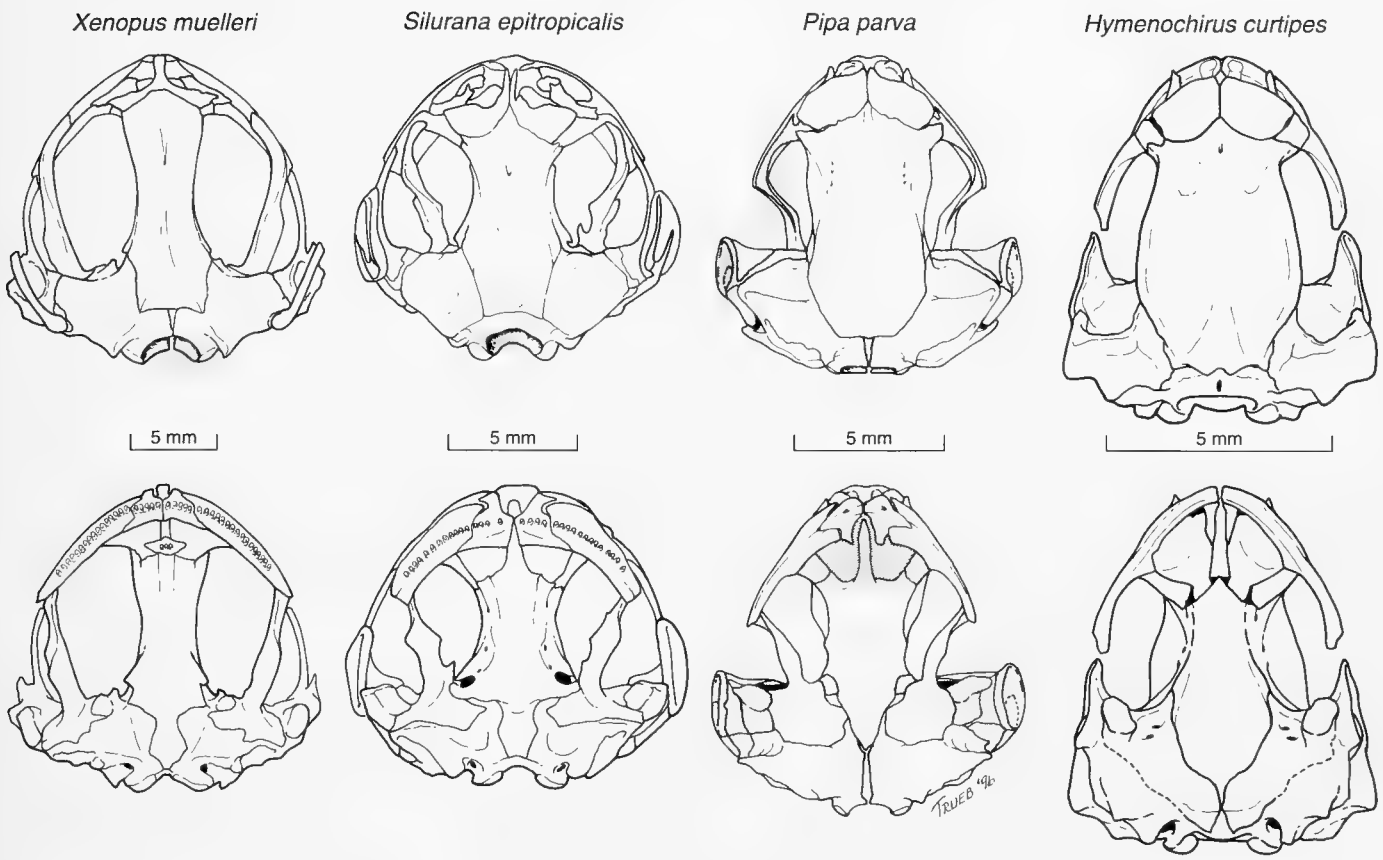


Fig. 12. Skulls in dorsal (upper of each pair) and ventral (lower of each pair) views of examples of living pipid frogs. *Xenopus muelleri* (KU 196043, female) and *Silurana epitropicalis* (KU 195660, female) based on Cannatella and Trueb (1988:fig. 2B). *Pipa parva* (USNM 115775, female) and *Hymenochirus curtipes* (KU 204127, female) based on Cannatella and Trueb (1988:fig. 3). Stippled pattern in *Pipa* indicates cartilage, whereas dashed line in *Hymenochirus* represents probably margin of pterygoid. Black areas represent foramina or other openings in the skulls.

arises from the medial margin of the pars facialis of the maxilla and extends medially toward the braincase in association with the planum antorbitale (State 1; Fig. 11). In *Discoglossus* and pelobatids (including *Pelobates*), the inner surface of the maxilla bears a process, called a palatine process in pelobatoids by Roček (1981); this process is directed anteromedially and arises in the angle between the pars facialis and pars palatina. Because of the vastly different configuration of the maxilla in pipids relative to these other taxa, it is not clear whether the antorbital processes of *Shelania* and *Saltenia* are homologous to the palatine processes of *Discoglossus* and pelobatoids. In all other taxa, the maxilla lacks such process (State 0; Figs. 11, 12). The maxilla of "*Xenopus*" *romeri* is unknown.

0: Maxilla lacking antorbital process.
1: Maxilla having antorbital process.

**20. Maxilla, configuration in orbital region.**—In *Discoglossus*, *Pelobates*, and rhinophrynids, the configuration of the maxilla in cross section is tripartite, consisting of a low pars facialis dorsally and laterally, a pars dentalis ventrally, and a shelflike pars palatina medially (State 0; Fig. 14). In *Palaeobatrachus*, the maxilla has at least a distinct pars facialis and pars palatina (Vergnaud-Grazzini and Młynarski, 1969; Vergnaud-Grazzini and Hoffstetter, 1972). The maxillae of *Eoxenopoides*, *Xenopus*, *Silurana*, *Shelania*, *Pipa*, and hymenochirines lack distinct partes in the orbital region (State 1; Fig. 14). The condition in *Saltenia* can not be determined owing to poor preservation, and the maxilla of "*Xenopus*" *romeri* is unknown.

Fig. 11. Skulls in dorsal (upper of each pair) and ventral (lower of each pair) views of extant exemplars of outgroup taxa (*Discoglossus sardus*, KU 129239, male; *Pelobates fuscus*, KU 129240, female) and ingroup taxa (*Rhinophrynus dorsalis*, KU 84886, female). The representation of the dorsum of *Palaeobatrachus* is adapted from Špinar (1972:text-fig. 4); the partial ventral view is *Palaeobatrachus* sp. (KUVP 124976A). *Shelania pascuali* based on restoration prepared for Figure 6. *Eoxenopoides reuningi* adapted from Estes (1977:fig. 2). *Saltenia ibanezi* redrawn from Báez (1981:fig. 2); a ventral reconstruction of the skull of *Saltenia* is not available. Black areas indicate foramina or fenestrae, and dashed lines represent estimations of margins of bones.

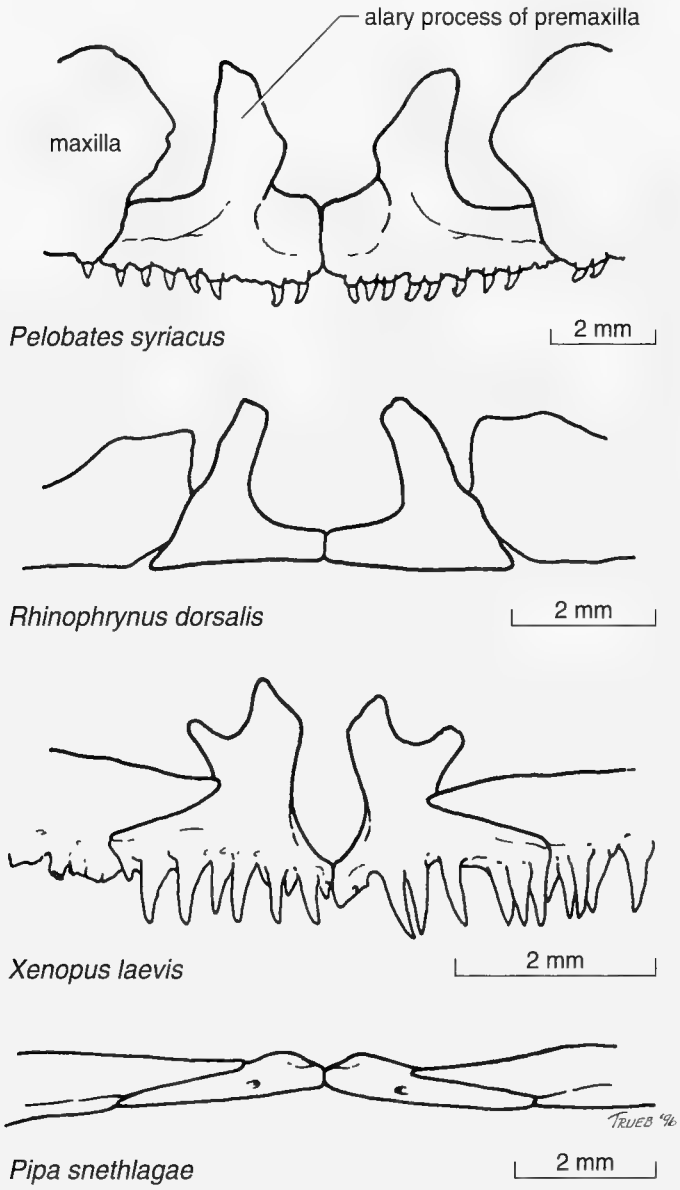


Fig. 13. Frontal views of premaxillae and anterior ends of maxillae in *Pelobates syriacus* (KU 146856, female), *Rhinophrynus dorsalis* (KU 84886, female), *Xenopus laevis* (KU 195934, female), and *Pipa snethlagae* (MCZ 85572).

0: Maxilla tripartite in section, possessing partes dentalis, facialis, and palatina.
1: Maxilla lacking distinct partes.

**21. Quadratojugal.**—The quadratojugal is the posterior member of the maxillary arcade in anurans. It is present and maxillary arcade is complete in *Discoglossus, Pelobates,* and rhinophrynids (State 0; Fig. 11), whereas it is absent and the maxillary arcade is incomplete in *Palaeobatrachus, Saltenia, Eoxenopoides, Shelania, Xenopus, Silurana, Pipa,* and hymenochirines (State 1; Figs. 11, 12). The quadrato-jugal has not been identified in *Chelomophrynus;* therefore, the condition in this taxon is uncertain. In *"Xenopus" romeri,* the maxillary arcade is not preserved.

0: Quadratojugal present and maxillary arcade complete.
1: Quadratojugal absent and maxillary arcade incomplete.

**22. Prootic, pterygoid knob.**—The anteromedial margin of the ventral surface of the otic capsule usually is smooth, lacking any distinct protuberances (State 0; Fig. 11). Pyles (1988:150; fig. 24) noted the presence of a "peculiar modification of the prootic [that] abuts the anteromedial corner of the expanded medial pterygoid ramus" in *Xenopus laevis* and *X. clivii.* We have observed this knoblike protuberance to be present also in *Palaeobatrachus, "Xenopus" romeri, Silurana, Saltenia,* and *Shelania* (State 1; Figs. 8, 11, 12).

0: Prootic lacking ventral, anteromedial knoblike protuberance.
1: Prootic possessing ventral, anteromedial knoblike protuberance.

**23. Pterygoid, relation of anterior ramus to maxilla.**—The anterior ramus of the pterygoid extends anterolaterally beneath the orbit from the otic region toward the maxilla. In most anurans (e.g., *Discoglossus, Pelobates, Rhinophrynus, Palaeobatrachus, Saltenia,* and *Shelania*), the end of the anterior ramus lies medially adjacent to the maxilla (State 0; Fig. 11). In all living pipids, except hymenochirines which lack an anterior pterygoid ramus, and *Eoxenopoides,* the terminus of this ramus overlies the dorsal surface of the maxilla (State 1; Figs. 11, 12). The pterygoid is not preserved in *"Xenopus" romeri.*

0: Anterior ramus of pterygoid lateral to maxilla.
1: Anterior ramus of pterygoid dorsal to maxilla.

**24. Pterygoid, configuration of anterior portion of anterior ramus.**—The anterior ramus, or ramus maxillaris, of the pterygoid bears a canal or groove to accommodate the pterygoid process of the palatoquadrate cartilage in most anurans. This groove extends along the lateral margin of the distal (i.e., anterior), narrow portion of this ramus (State 0) in *Discoglossus, Pelobates, Palaeobatrachus, Pipa, Eoxenopoides,* and *Shelania.* Although *Rhinophrynus* lacks a well-defined canal, the pterygoid process of the palatoquadrate is associated with the lateral margin of the bone (Trueb and Cannatella, 1982); thus, this condition is interpreted as State 0. In *Xenopus* and *Silurana,* the distal portion of this branch is laminar and oriented parallel to the sagittal plane of the skull; the pterygoid process of the palatoquadrate is associated with the ventral margin of

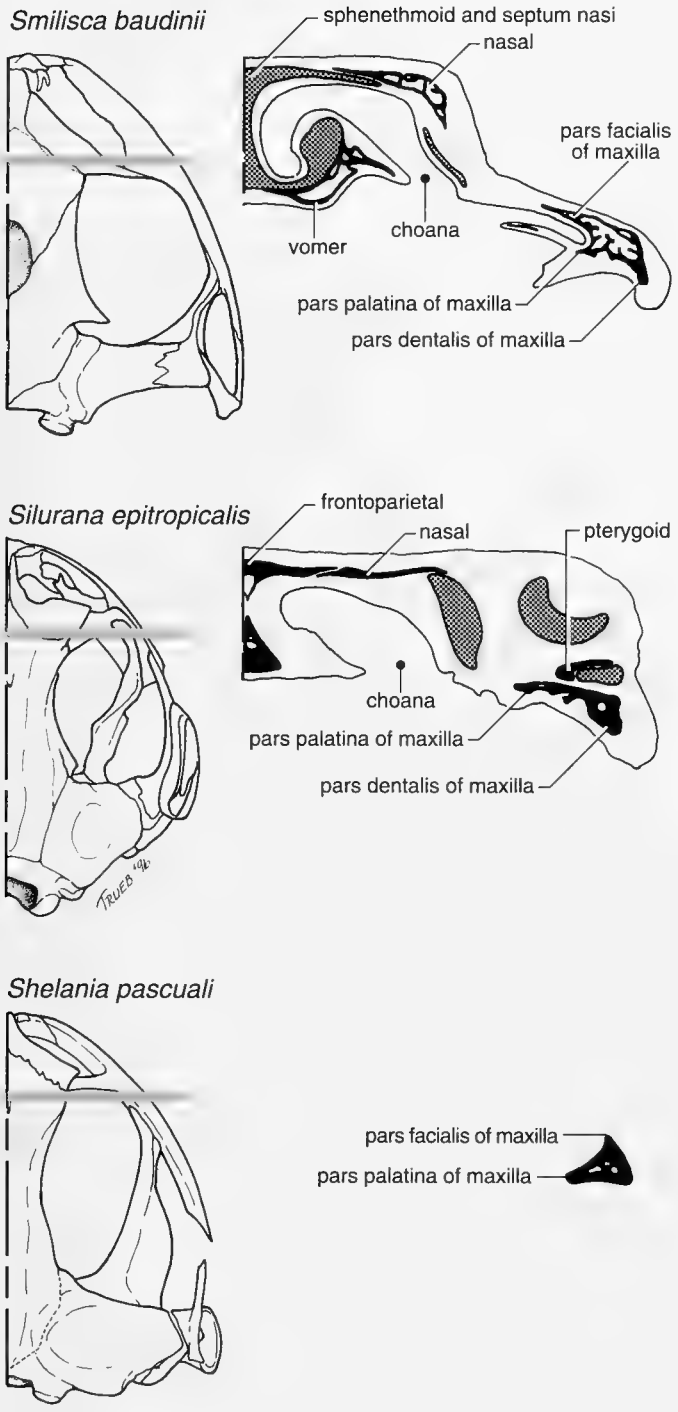


Fig. 14. Schematic drawings of the right side of the skull in *Smilisca baudinii*, *Silurana epitropicalis* (KU 195660), and *Shelania pascuali*. The gray bar intersects each skull at the approximate level of the section (*Smilisca*, KU 89924; *Silurana tropicalis*, KU 216330) illustrated to the right. The stipple pattern indicates cartilage, whereas bone is shown in black. The section of the maxilla shown for *Shelania* is a visualization that is not based on a section.

the pterygoid (State 1; Fig. 14). In hymenochirines, the anterior ramus of the pterygoid is absent. The condition in *Saltenia* could not be determined owing to the poor preservation of all available specimens, and the pterygoid of *"Xenopus" romeri* is unknown.

0: Anterior portion of anterior ramus rodlike with or without a lateral groove to accommodate the pterygoid process of the palatoquadrate.
1: Anterior portion of anterior ramus laminar and oriented parallel to sagittal plane; pterygoid process of palatoquadrate associated with ventral margin of anterior ramus.

**25. Pterygoid, anterior ramus position.**—The anterior ramus of the pterygoid arises lateral to the anteromedial corner of the otic capsule in *Pelobates*, *Discoglossus*, *Palaeobatrachus*, and *Rhinophrynus* (State 0; Fig. 11). In *Eoxenopoides*, and *Saltenia*, basal *Pipa*, *Xenopus*, *Silurana*, and *Shelania*, the anterior ramus arises near the anteromedial corner of the otic capsule (State 1; Figs. 11, 12). Living hymenochirines lack the anterior ramus of the pterygoid. The pterygoid of *Chelomophrynus* has not been positively identified (Henrici, 1991) and the pterygoid of *"Xenopus" romeri* is unknown.

0: Anterior ramus of pterygoid arises well laterally with respect to the anteromedial corner of otic capsule.
1: Anterior ramus of pterygoid arises near the anteromedial corner of otic capsule.

**26. Pterygoid, relation of medial ramus to otic capsule.**—Typically, the pterygoid is a triradiate structure in anurans; the medial ramus usually abuts or overlaps the anteroventral ledge of the otic capsule (e.g., *Discoglossus*, *Pelobates;* State 0; Fig. 11). In *Palaeobatrachus*, the medial ramus is slightly expanded to invest the anterolateral region of the otic capsule (State 1; Fig. 11). The medial ramus, in combination with the posterior ramus, is variably expanded to form an otic plate (Trueb and Cannatella, 1986) that underlies the otic capsule in living pipids, *Shelania*, *Eoxenopoides*, and *Saltenia* (State 2; Figs. 11, 12). The condition is unknown in *Chelomophrynus* and *"Xenopus" romeri*.

0: Medial ramus of pterygoid not expanded, articulating with anteroventral ledge of otic capsule.
1: Medial ramus of pterygoid expanded to invest anterolateral region of otic capsule.
2: Medial ramus of pterygoid expanded to form otic plate.

**27. Pterygoid, medial ramus shape.**—In *Xenopus*, *Silurana*, and *Shelania*, the medial margin of the medial ramus, or otic plate, of the pterygoid has a round indentation that separates a small, pointed anterior process from

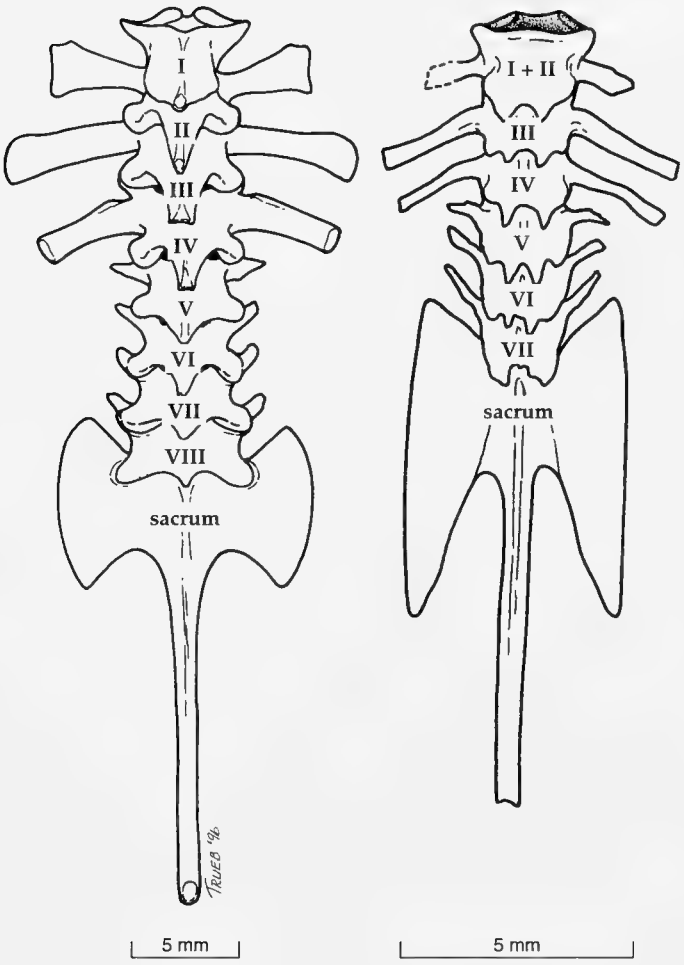


Fig. 15. Vertebral columns of a representative pelobatoid, *Scaphiopus couchii* (left; KU 73385), and *Hymenochirus curtipes* (right, KU 204131) in dorsal view. Broken line indicates reconstruction.

a laminar posterior process that underlies part of the Eustachian canal (State 1; Figs. 11, 12). Such an indentation is absent in *Discoglossus, Pelobates, Palaeobatrachus, Pipa,* and hymenochirines (State 0; Figs. 11, 12). In *Eoxenopoides*, a bifurcated medial ramus was described by Estes (1977); however, we were not able to confirm this condition. A medial ramus is absent in *Rhinophrynus,* and the pterygoid of *Chelomophrynus* has not been identified (Henrici, 1991). The pterygoid of *"Xenopus" romeri* is unknown.

0: Medial margin of medial ramus or otic plate of pterygoid lacking round indentation.
1: Medial margin of medial ramus, or otic plate, of pterygoid having round indentation.

**28. Parasphenoid, fusion with braincase.**—The dermal parasphenoid underlies the ethmoidal and prootic portions of the braincase. In *Discoglossus, Pelobates,* rhino-phrynids, and palaeobatrachids, as in most other anurans, the parasphenoid is not united synostotically with the overlying sphenethmoid(s), prootics, or exoccipitals (State 0; Fig. 11). However, in adult *Shelania, Saltenia, Eoxenopoides, "Xenopus" romeri,* and the living pipids, the parasphenoid is partially or totally fused with the braincase above it (State 1; Figs. 8, 11, 12).

0: Parasphenoid not fused with overlying braincase.
1: Parasphenoid fused partially or completely with overlying braincase.

**29. Parasphenoid, anterior terminus.**—In anurans such as *Discoglossus, Pelobates,* rhinophrynids, and hymenochirine pipids, the anterior end of the cultriform process of the parasphenoid lies in the anterior part of the orbit at the level of the region of the planum antorbitale (State 0; Figs. 11, 12). *Palaeobatrachus, Shelania, Saltenia, Eoxenopoides,* and pipids other than hymenochirines have extraordinarily long cultriform processes that terminate just posterior to the premaxillae (State 1; Figs. 11, 12). Although in all known specimens of *"Xenopus" romeri* the most anterior terminus of the cultriform process is broken, we interpret that a long parasphenoid was present.

0: Anterior tip of parasphenoid not reaching maxillary arcade.
1: Anterior tip of parasphenoid reaching maxillary arcade.

**30. Parasphenoid alae.**—Typically (e.g., *Discoglossus, Pelobates*), the parasphenoid is a T-shaped element that underlies the neurocranium, with the leg of the T (the cultriform process) beneath the braincase and the head of the T forming alae that extend beneath the otic capsule on each side of the cranium (State 0; Fig. 11). In rhinophrynids, *Palaeobatrachus, Saltenia, Eoxenopoides, "Xenopus" romeri,* and the living pipids, the parasphenoid lacks posterior alae (State 1; Figs. 8, 11, 12). We assume that *Shelania* also lacked alae, but the condition of the parasphenoid posterior to the optic foramina could not be assessed.

0: Parasphenoid T-shaped, with subotic alae.
1: Parasphenoid lacking subotic alae.

**31. Parasphenoid, posteromedial margin.**—In most anurans, the posterior margin of the parasphenoid lies near the margin of the foramen magnum between the posterior regions of the otic capsules (e.g., *Discoglossus, Pelobates, Rhinophrynus, Shelania, Eoxenopoides, Saltenia, Xenopus, "Xenopus" romeri,* and *Silurana*) (State 0; Figs. 8, 11, 12). In *Pipa* and the hymenochirines, the posterior terminus of the parasphenoid lies approximately at the midlevel of the otic capsules far anterior to the margin of the foramen magnum (State 1).

0: Posteromedial process of parasphenoid terminating on or near margin of foramen magnum at or near posterior limits of otic capsules.

1: Posterior margin of parasphenoid terminating anterior to foramen magnum between otic capsules.

**32. Squamosal, relationship with stapes.**—The squamosal of most anurans is a T-shaped bone in lateral profile (Fig. 7). The leg of the T invests the lateral surface of the palatoquadrate cartilage. Two rami form the head of the T; the posterior otic ramus is associated with the crista parotica of the prootic, whereas the anterior zygomatic ramus extends toward the maxilla. If present, the stapes extends dorsally and laterally or anterolaterally from the fenestra ovalis to emerge between the otic and ventral rami. The stapes is weakly supported distally by a tenuous connection of the pars externa plectri to the tympanic annulus in those anurans (e.g., *Discoglossus, Pelobates*) that possess a complete ear (State 0; Figs. 7, 10). Rhinophrynids lack a stapes. *Palaeobatrachus* possesses a posterior process at the bottom of the ventral ramus of the squamosal (Špinar, 1972); the latter, in combination with the curved otic ramus, probably supported the large stapes (State 1; Fig. 11). In *Shelania, Saltenia, Eoxenopoides,* and pipids, the ventral ramus of the squamosal is associated with a conch-shaped bone that, in living pipids, is derived from ossification of the tympanic annulus and synostosis between this element and the squamosal (Trueb and Cannatella, 1986; Trueb and Hanken, 1992). The modified tympano-squamosal bone (like the tympanic annulus in other anurans) is incomplete posterodorsally. There is a process on the dorsal margin of the gap and one on the ventral margin of the gap that are associated with the stapes that passes between them (State 2; Figs. 7, 10, 11). The squamosal is not preserved in *"Xenopus" romeri.*

0: Squamosal lacking processes associated with the stapes.
1: Squamosal with ventral process and modified otic ramus surrounding the stapes.
2: Squamosal modified into conch-shaped tympanosquamosal bone.

**33. Squamosal, zygomatic ramus.**—In most anurans (e.g., *Discoglossus, Pelobates, Palaeobatrachus, Xenopus, Silurana,* and *Shelania*), the zygomatic ramus is obvious and well developed (State 0; Figs. 7, 10, 11), whereas in rhinophrynids, *Pipa, Saltenia, Eoxenopoides,* and hymenochirines, the zygomatic ramus is absent or present but exceedingly short (State 1; Figs. 7, 10, 11). The squamosal in *"Xenopus" romeri* is unknown

0: Zygomatic ramus of squamosal present and well developed.
1: Zygomatic ramus of squamosal absent or scarcely evident.

**34. Angulosplenial, coronoid process.**—*Discoglossus, Pelobates, Palaeobatrachus,* and rhinophrynids, like most other anurans, possesses a coronoid process along the posteromedial margin of the mandible; the process is broad-based and subtriangular in configuration (State 0). In *Shelania, Eoxenopoides, Saltenia,* and the living pipids, the coronoid process forms a broad laminar plate that is rounded marginally and rectangular (State 1; Trueb, 1996:fig. 19.5). The mandible in *"Xenopus" romeri* is not preserved.

0: Coronoid process of angulosplenial not expanded.
1: Coronoid process of angulosplenial broad-based and expanded into flat blade.

**35. Vertebral centra, shape.**—The several schemes that have been devised during the past 75 years to describe and categorize differences in the development, shapes, and associations of anuran vertebral centra were summarized most recently by Duellman and Trueb (1994:332–333). Regrettably, there is no resolution among these schemes that facilitates the use of available ontogenetic data and the condition of the vertebrae in adult anurans in phylogenetic analyses. Thus, we limit our application of characters of the centrum to its shape in adults—i.e., whether they are approximately round in cross section versus being distinctly depressed and ovoid in cross section—with the full realization that apparent similarities may be the result of different developmental mechanisms that, as yet, are not well understood or fully investigated. The vertebral centra of *Discoglossus, Pelobates,* and rhinophrynids are round in cross section (State 0; Fig. 15), whereas those of the remaining taxa are depressed (State 1; Fig. 15).

0: Cylindrical.
1: Depressed.

**36. Vertebral centra, articulations.**—Of the several intervertebral articular conditions known to exist in anurans (Duellman and Trueb, 1994), we consider here only three. *Discoglossus, Saltenia, "Xenopus" romeri, Shelania, Eoxenopoides,* and the living pipids possess opisthocoelous vertebral centra (State 1). In rhinophrynids, the intervertebral disc adheres to the anterior end of the centrum, but can be dislodged from it easily. Moreover, the centra retain vestiges of the notochord (Cannatella, pers. comm.). For these reasons, their vertebral articulation is coded as notochordal (State 0). The vertebral centra of pelobatids have a variety of configurations, but in *Pelobates,* there is an intervertebral disc that in adults is synostotically united with the anteriorly adjacent centrum to form a procoelous vertebra (State 2); adult palaeobatrachids possess procoelous centra. Although it is possible that the procoelous condition in adult palaeobatrachids is achieved in the same way as it is in *Pelobates,* there is no information in the literature describing the vertebral centra of young palaeobatrachids to support this speculation; thus, we designate the condition in palaeobatrachids as State 2.

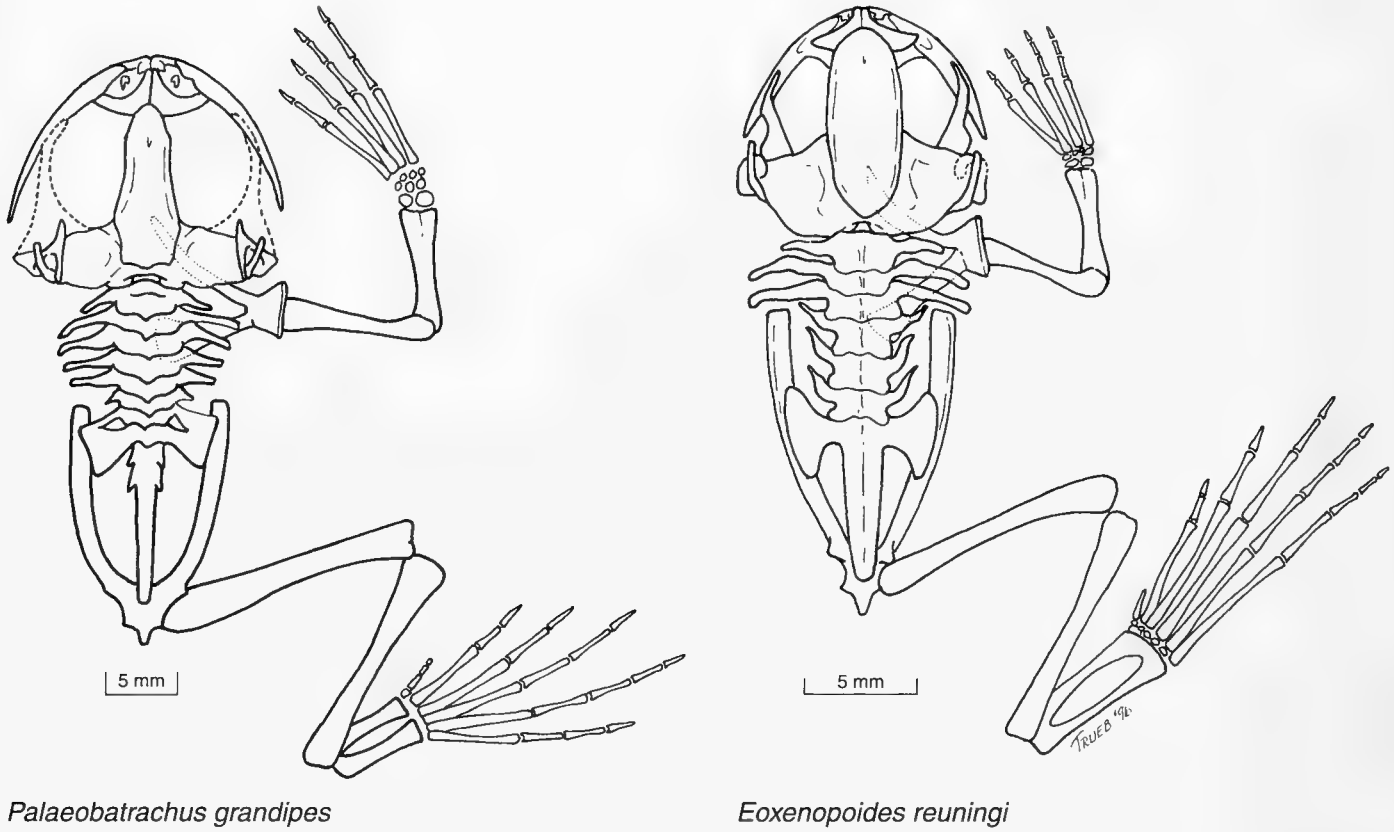


Fig. 16. Reconstructions of the skeletons in dorsal view of *Palaeobatrachus grandipes* (based on Špinar, 1972:text-fig. 4) and *Eoxenopoides reuningi* (adapted from Estes, 1977:fig. 2).

0: Notochordal.
1: Opisthocoelous.
2: Procoelous.

**37. Presacral vertebrae, total number of vertebrae and nature of posterior presacrals.**—The number of presacral vertebrae in anurans varies from five to 10 (e.g., 10 in the Early Jurassic *Vieraella herbstii*, and occasionally in the extant *Ascaphus truei;* Báez and Basso, 1996), with reductions having occurred by fusion of Presacrals I and II, and incorporation of presacral vertebrae into the sacrum posteriorly. In most anurans, there are eight identifiable presacral vertebrae, of which the posterior four usually bear transverse processes that are shorter and/or more slender than those on the anterior presacrals (State 0; Fig. 15). In *Eoxenopoides* and hymenochirine pipids, there is a total of seven presacral vertebrae, of which only the posterior three bear short transverse processes (State 1; Fig. 15). *Palaeobatrachus* has eight presacrals, although the trans-

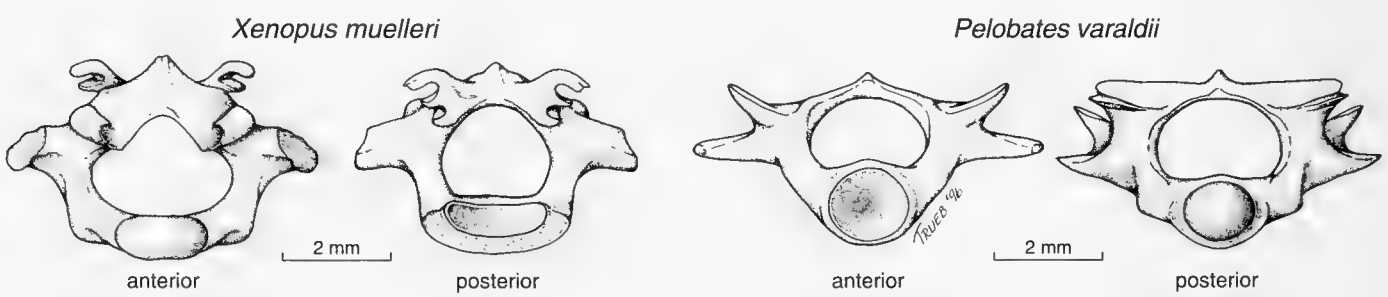


Fig. 17. Presacral vertebrae of *Xenopus muelleri* (MCZ 51689) and *Pelobates varaldii* (MCZ 31970). Note the differences in the shapes of the centra and the configurations of the pre- and postzygapophyses.

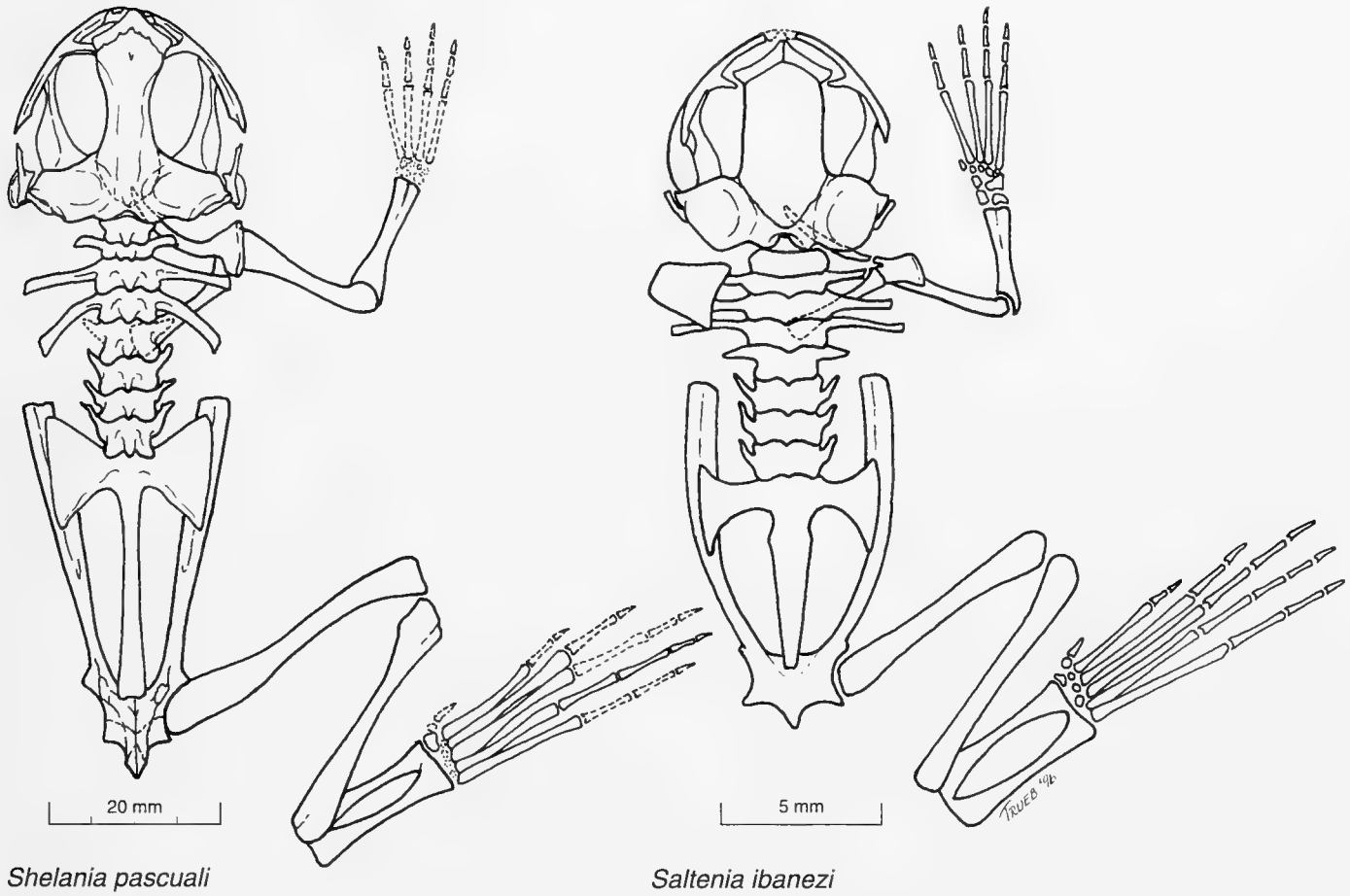


Fig. 18. Reconstructions of the skeletons in dorsal view of *Shelania pascuali* and *Saltenia ibanezi* (redrawn from Báez, 1981:fig. 2).

verse processes of the eighth and seventh vertebrae may be partially or totally fused to the sacral diapophyses. The total number of presacral vertebrae in *"Xenopus" romeri* is uncertain because an articulated vertebral column has not been preserved. Three morphologically distinct presacral vertebrae, corresponding to vertebrae posterior to Presacral IV, are known; thus, at least seven presacrals, of which Presacrals I and II are fused, were present.

0: Eight presacral vertebrae with the four vertebrae anterior to the sacrum bearing short transverse processes.
1: Seven presacral vertebrae with only three vertebrae anterior to the sacrum bearing short transverse processes.

**38. Vertebrae, pre- and postzygapophyses.**—Most anurans possess vertebrae having simple, flat articulations between the pre- and postzygapophyses (State 0; Fig. 17). In some living pipids, the articular surfaces develop sulci and ridges to form an elaborate, intervertebral locking mechanism (Vergnaud-Grazzini, 1966). In adult living *Xenopus* and *Silurana*, the prezygapophysis covers the lateral margin of the postzygapophysis (State 1; Fig. 17). In hymenochirines, the articular surfaces lack sulci and ridges, and the postzygapophysis wraps ventrally around the prezygapophysis (State 2).

0: Pre- and postzygapophyses with simple, flat articular surfaces.
1: Prezygapophysis covering lateral margin of postzygapophysis; articular surfaces bearing sulci and ridges.
2: Postzygapophysis covering lateral margin of prezygapophysis; articular surfaces simple.

**39. Presacral vertebrae neural spines.**—Usually, the neural arches of the vertebrae bear a single, posteriorly directed spinous process that overlaps the succeeding vertebra (State 0; Fig. 15). In *Pipa* and *Hymenochirus*, the neural arches are expanded posteriorly in the parasagittal regions, to form paired processes (State 1; Fig. 15).

0: Single sagittal spinous process.
1: Parasagittal spinous processes.

**40. Presacral Vertebra VIII.**—In most anurans (e.g., *Discoglossus, Pelobates,* rhinophrynids, *Shelania,* and *Saltenia*), Presacral Vertebra VIII is not involved in formation of the sacrum (State 0; Figs. 15, 18). However, this vertebra forms the sacrum in *Eoxenopoides* and hymenochirines (State 1; Figs. 15, 16). In *Palaeobatrachus,* the eighth vertebra is always partially or completely fused to the sacrum, to form the so-called synsacrum with the variable participation of Vertebra VII (Fig. 16; Špinar, 1972). The condition in *"Xenopus" romeri* is unknown, because the total number of presacral vertebrae is uncertain.

0: Eighth vertebra does not participate in sacrum formation.
1. Eighth vertebra is involved in sacrum formation.

**41. Vertebra IX.**—In *Discoglossus, Pelobates, Rhinophrynus, Chelomophrynus, Shelania, Saltenia, Palaeobatrachus, Xenopus, "Xenopus" romeri, Silurana,* and *Pipa* the ninth vertebra is involved in the sacrum formation (State 0; Figs. 16, 18). In Eoxenopoides, the sacrum is formed by the eighth vertebra only; thus, Vertebra IX does not participate in sacrum formation (State 1; Figs. 15, 16). In hymenochirines, the sacrum is formed mainly by Vertebra VIII, but a posterior vertebra (IX) also is incorporated into the sacrum. The condition in *"Xenopus" romeri* is unknown.

0: Vertebra IX involved in sacrum formation.
1: Sacrum formed by one or more vertebrae, one of which is Vertebra VIII.

**42. Vertebra X.**—In *Discoglossus, Pelobates, Shelania, Saltenia, Eoxenopoides, Palaeobatrachus,* and hymenochirines, Vertebra X usually is not involved in sacrum formation (State 0; Fig. 16). Although the sacrum is formed mainly by Vertebra IX in *Xenopus, Silurana,* and *Pipa,* a posterior vertebra (X) contributes to the sacrum (State 1; Trueb, 1996:fig. 19.7). In *"Xenopus" romeri,* the sacrum is formed by one vertebra (either VIII or IX owing to the unlikelihood that this taxon possessed 9 presacrals); thus, Vertebra X is not involved in the formation of the sacrum.

0: Vertebra X does not participate in sacrum formation.
1: Sacrum formed by more than one vertebra, one of which is Vertebra X.

**43. Fusion of urostyle and sacrum.**—In *Discoglossus, Pelobates,* rhinophrynids, and palaeobatrachids, the sacrum is not fused to the urostyle (State 0; Figs. 15, 16). (However, this feature is known to vary in some species of *Pelobates.* For example, Rodríguez Talavera [1990] noted that of 64 vertebral columns of *P. cultripes* that she examined, 17.2% had the sacrum fused to the urostyle, whereas in the rest of the sample, there was a monocondylar articulation between the two bones.) In *Saltenia, Shelania, "Xenopus" romeri, Eoxenopoides,* and the living pipids, the sacrum and urostyle are fused (State 1; Figs. 16, 18).

0: Sacrum and urostyle articulating, not fused.
1: Sacrum fused to urostyle.

**44. Fusion of clavicle and scapula.**—In most anurans (e.g., *Discoglossus, Pelobates, Shelania, Saltenia,* rhinophrynids, and palaeobatrachids), the clavicle articulates with, and is not fused to, the adjacent scapula (State 0; Trueb, 1996:fig. 19.10). The clavicles of *Xenopus, Silurana, "Xenopus" romeri,* and hymenochirine pipids are fused to the scapula (State 1; Trueb, 1996:fig. 19.10). The condition is uncertain in *Eoxenopoides.*

0: Clavicle and scapula articulating, not fused.
1: Clavicle and scapula fused.

**45. Clavicle, medial expansion.**—The clavicles of most anurans, including *Discoglossus, Pelobates,* rhinophrynids, palaeobatrachids, *Shelania, Saltenia, Eoxenopoides,* and *Pipa,* are slender or acuminate medially (State 0; Trueb, 1996:fig. 19.10), whereas those of *Xenopus* and *Silurana* are expanded (State 1; Trueb, 1996:fig. 19.10). In *"Xenopus" romeri,* the anterior portion of the clavicle is unknown.

0: Medial end of clavicle slender.
1: Medial end of clavicle expanded and wider than lateral end.

**46. Scapula, length.**—The greatest length of the scapula is short in *Discoglossus, "Xenopus" romeri, Silurana,* and *Xenopus* relative to the scapulae of the other taxa that we examined. In the former taxa, the diameter of the glenoid fossa comprises half or more of the total length of the scapula (State 1; Trueb, 1996:fig. 19.10). In all of the remaining taxa, the scapula proportionally is long, and the diameter of the glenoid fossa comprises half or usually much less than half the total length of the scapular shaft (State 0; Trueb, 1996:fig. 19.10).

0: Diameter of glenoid fossa less than half total length of scapula.
1: Diameter of glenoid fossa half or more than half of total length of scapula.

**47. Coracoid, relative widths of sternal and glenoid ends.**—The coracoid is expanded medially at its sternal end and laterally at its glenoid end. In *Discoglossus, Pelobates, Silurana, Xenopus, Eoxenopoides, Saltenia,* and *Shelania,* the expansion of the sternal end is about equal to, or only slightly greater than, that of the glenoid end (State 0; Trueb, 1996:fig. 19.10). The coracoids of hymenochirines, rhinophrynids, *Pipa,* and *Palaeo-batrachus* are distinguished by having greatly expanded sternal ends, which are more than twice as wide as the glenoid expansion (State 1; Cannatella and Trueb, 1988:fig. 4). The condition in *"Xenopus" romeri* is unknown.

0: Sternal expansion of coracoid equal to, or only slightly greater than, glenoid expansion.
1: Sternal expansion of coracoid more than twice that of glenoid expansion.

**48. Coracoid, expansion of sternal end relative to length of bone.**—In anurans such as *Discoglossus, Eoxenopoides, Xenopus, Silurana, Saltenia,* and *Shelania,* the expansion of the sternal ends of the coracoids comprises less than half the length of the long axis of the bones (State 0; Trueb, 1996:fig. 19.10). Rhinophrynids, *Pelobates,* and *Palaeobatrachus* are distinguished by having coracoids in which the expansion of the sternal ends is equal to about half the overall length of the bone (State 1; Trueb, 1996:fig. 19.10). In hymenochirines and *Pipa,* the sternal expansion of the coracoids is nearly equal to the length of the bone (State 2; Cannatella and Trueb, 1988:fig. 4). The coracoid is not preserved in *"Xenopus" romeri.*

0: Sternal expansion of coracoid less than half length of bone.
1: Sternal expansion equal to approximately half length of bone.
2: Sternal expansion nearly equal to length of the bone.

**49. Ilium, supra-acetabular configuration.**—The posterodorsal end of the ilium forms the supra-acetabular part of the pelvis. In *Discoglossus, Pelobates,* rhinophrynids, *Palaeobatrachus, Saltenia,* and *Eoxenopoides,* this region is laterally compressed and relatively narrow in dorsal view; in lateral aspect, the supra-acetabular ilium is expanded dorsally in a bladelike configuration (State 0; Trueb, 1996:fig. 19.8). *Shelania, "Xenopus" romeri,* and the living pipids lack any dorsal expansion of the supra-acetabular ilium in lateral aspect; this area is broadly expanded in dorsal aspect (State 1; Trueb, 1996:fig. 19.8).

0: Supra-acetabular ilium laterally compressed in dorsal view, and expanded and bladelike in lateral view.
1: Supra-acetabular ilium wide in dorsal aspect and lacking dorsal expansion in lateral aspect.

**50. Ilium, interilial preacetabular expansion.**—In ventral view, the preacetabular ilium is relatively narrow in width in *Discoglossus, Pelobates,* and rhinophrynids (State 0). As a result, the interilial configuration is V-shaped with the ilial shafts converging on one another at a distinct angle (e.g., *Rhinophrynus;* Trueb, 1996:fig. 19.8) or forming a narrowly rounded base (e.g., *Pelobates*). In contrast, the interilial region is broadly expanded in the remaining taxa examined (State 1; Figs. 16, 18), such that the internal profile of the ilia is a broad-based U-shape.

0: Ventral preacetabular ilium narrow.
1: Ventral preacetabular ilium wide.

**51. Pubis.**—In most anurans (e.g., *Discoglossus, Pelobates,* rhinophrynids), the pubis remains cartilaginous in adults, although the cartilage may be mineralized (State 0; Trueb, 1996:fig. 19.8). However, in *Palaeobatrachus, Shelania, Eoxenopoides,* and the living pipids, the pubis is reduced and ossified in most taxa (State 1; Trueb, 1996:fig. 19.8). The condition in *"Xenopus" romeri* is unknown.

0: Well-developed, cartilaginous pubis with or without mineral deposits.
1: Pubis poorly developed and usually ossified.

## RESULTS

The measures of support associated with the phylogenetic arrangements hypothesized are, as follow: total tree length; consistency index, both including (CI) and excluding (CI*) uninformative characters; homoplasy index, both including (HI) and excluding (HI*) uninformative characters; and rescaled consistency index (RC). The exact search yielded three equally most-parsimonious trees (M-PTs 1–3), each of which is 84 steps long and has a CI of 0.690 (CI* = 0.675), HI of 0.321 (HI* = 0.329) and a RC of 0.550. All M-PTs (Figs. 19–21) show Rhinophrynidae (*Rhinophrynus* + *Chelomophrynus*) and *Palaeobatrachus* as successive sister groups of a large clade that includes all other terminal taxa of the ingroup, with Rhinophrynidae being the most basal. The trees supported the sister-group relationship of *"Xenopus" romeri* and a clade comprised by *Xenopus* and *Silurana,* and the monophyly of Pipinae (hymenochirines + *Pipa*), with the fossil *Eoxenopoides* placed as its sister taxon. The topological variants differ in the position of *Shelania* and *Saltenia.* In M-PT 1 (Fig. 20), *Saltenia* and *Shelania* are successive sister taxa of a clade that includes living pipids, in addition to *"Xenopus" romeri* and *Eoxenopoides,* whereas in M-PT 2, there are two sister clades—one composed of *Shelania* and [*"Xenopus" romeri* + [*Xenopus* + *Silurana*]], and the other of *Saltenia* and [*Eoxenopoides* + [hymenochirines + *Pipa*]]. Figure 21 depicts M-PT 3.

In the strict consensus tree (Fig. 19) that is used to summarize areas of congruence among the equally most-parsimonious trees, there is a polytomy that indicates unresolved relationships involving the following taxa: (1) *Saltenia;* (2) *Shelania;* (3) [*Eoxenopoides* + [hymenochirines + *Pipa*]]; and (4) [*"Xenopus" romeri* + [*Silurana* + *Xenopus*]]. Bremer values (Bremer, 1988; 1994) indicate strong support for the clades composed of (1) *Palaeo-batrachus* and the remaining ingroup taxa, (2) ingroup taxa, (3) pipines, and (4) xenopines. The three most weakly supported clades (value = 1) are (1) rhinophrynids + *Palaeobatrachus* + ingroup taxa, (2) xenopines + *"Xenopus" romeri,* and (3) *Eoxenopoides* + pipines.

In order to evaluate the impact of missing data in producing these results, different analyses were performed adding and deleting the fossil taxa for which we had in-

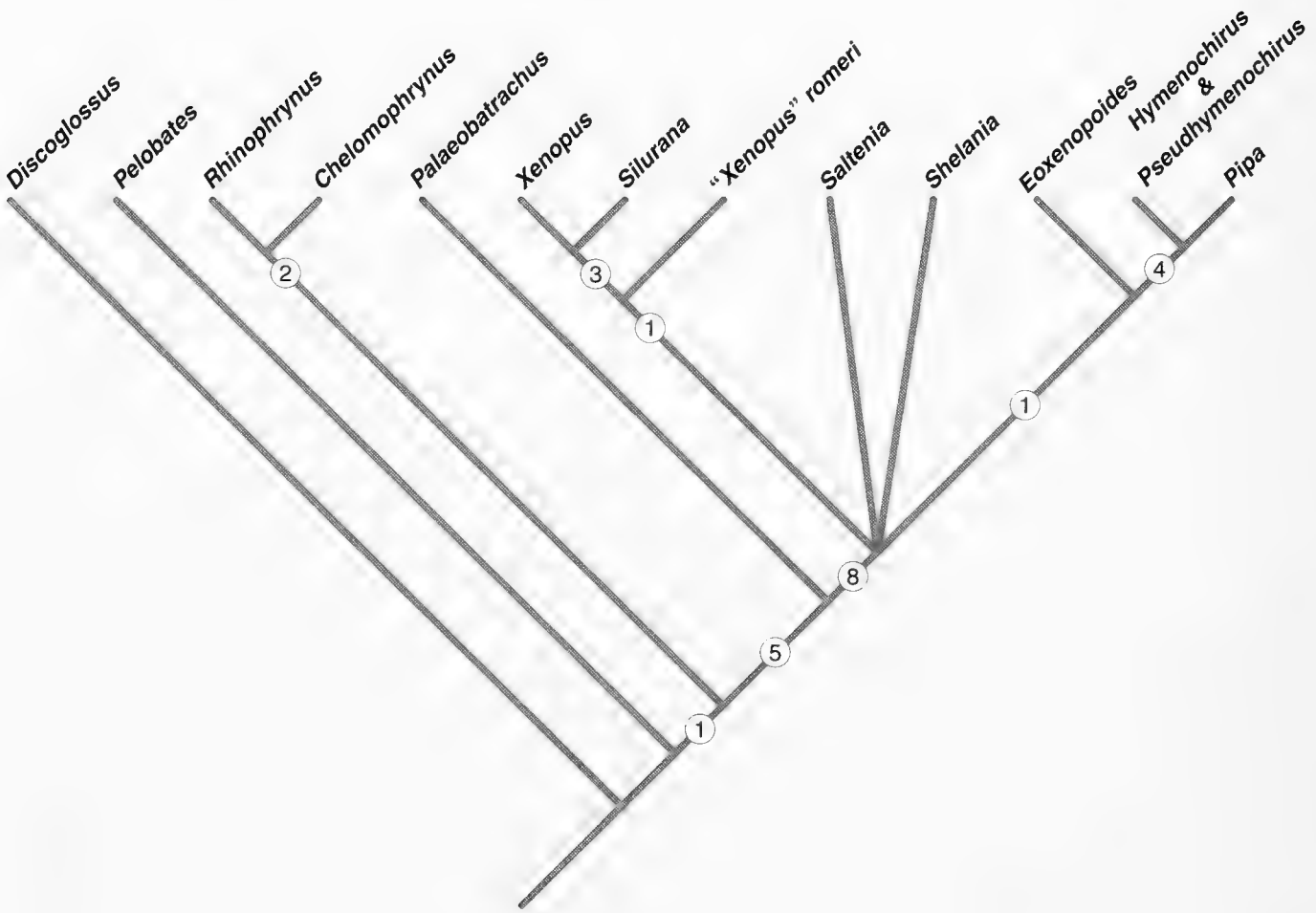


Fig. 19. Strict consensus of the three most-parsimonious trees obtained in the parsimony analysis. Bremer values for clades are indicated by circled numbers.

complete data. Parsimony analysis of the data matrix deleting all fossil taxa resulted in one tree of 63 steps (CI* = 0.821, HI* = 0.182, RC = 0.745). Addition of *Shelania* (Characters 9 and 14 unknown; 4% of missing entries) produces two minimum-length trees (67 steps) in which this fossil taxon has alternate positions relative to the unambiguous relationships of the terminal extant taxa. In one tree, *Shelania* is the sister taxon to the clade [[*Xenopus* + *Silurana*] + [*Pipa* + hymenochirines]]. In the alternate arrangement, [*Pipa* + hymenochirines] is the sister clade to [*Shelania* + [*Xenopus* + *Silurana*]]. When *Palaeobatrachus* (all characters scored) is included, the same two trees are obtained, although the length of each increases seven steps. *"Xenopus" romeri* is the fossil taxon for which we have the least complete data set (about 43% of the characters uncoded). Deletion of this taxon from the analysis of the complete matrix (i.e., the matrix including all other fossil and Recent taxa) produced two trees (83 steps) that are topologically identical to M-PTs 1 and 3 (Figs. 20, 21). However, deletion of *Saltenia* (with only 20% of the characters uncoded) resulted in a single tree (81 steps) in which *Shelania* has the same sister-group relationship with the remaining taxa as in M-PT 1. These results suggest that the number of equally parsimonious trees generated in this analysis is not simply related to the relative amount of missing data, but also results from the combination of character states known to be present in some fossil taxa.

Successive searches were performed using PAUP's a posteriori–character weighting algorithm. Characters were reweighted according to their consistency indices and rescaled consistency indexes, and on both the best-fit and mean-fit options. In each case, this procedure yielded one tree topologically identical with one of the original set of most-parsimonious trees (i.e., shortest under equal weights)—M-PT 3 (Fig. 21). The "preferred" tree has a CI* of 0.859, an HI* of 0.142, and a RC of 0.811 after successive weighting. Synapomorphies that support the nodes in M-PT 3 are listed below. The character states described specify

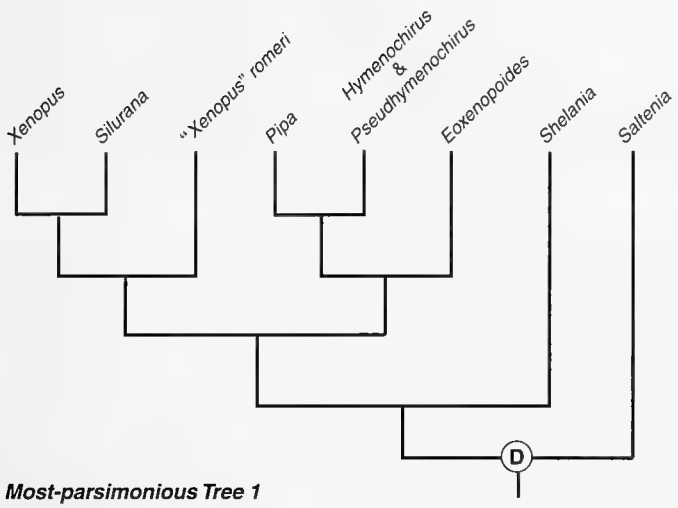


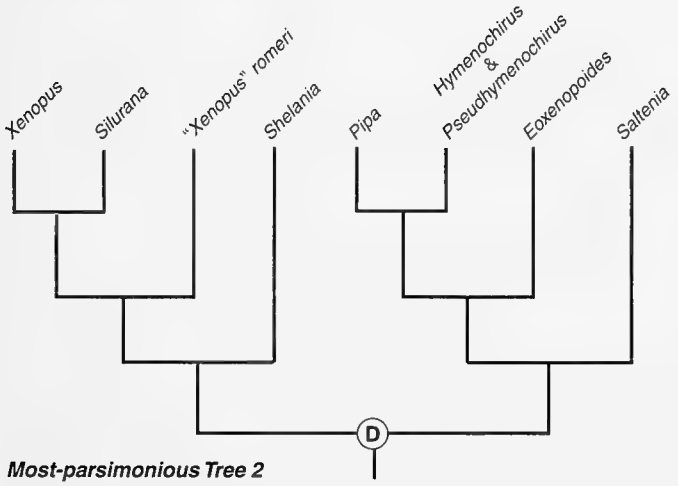


Fig. 20. Most-parsimonious Trees (M-PTs) 1 and 2 obtained in the parsimony analysis; arrangement of other taxa as in Figures 19 and 21. Labeled node "D" corresponds to the same node in M-PT 3 (Fig. 21).

the apomorphic condition, and the numbers in brackets refer to the identity of the characters. Only unambiguous characters are considered, unless stated otherwise. The internal nodes, the synapomorphies that support internal nodes, and autapomorphies of terminal taxa exclusively in this tree are denoted with an asterisk, whereas those common to all three M-PTs are unmarked.

**Node A (Pipoidea).**—The monophyly of the ingroup (Rhinophrynidae + the remaining ingroup taxa) is supported by one unique, shared-derived character (30)—possession of a parasphenoid that lacks subotic alae. We consider possession of an azygous frontoparietal (11) to be an additional synapomorphy at this node; azygous frontoparietals in some pelobatoids (e.g., *Pelobates*) possibly evolved independently.

**Node B (Rhinophrynidae).**—The clade [*Rhinophrynus* + *Chelomophrynus*] is supported by one homoplastic character—the possession of a squamosal that lacks a zygomatic ramus or possesses a ramus so poorly developed as to scarcely be evident (33); however, this feature is convergent within Pipidae. In addition, the presence of notochordal vertebrae (36) occurs only in rhinophrynids among the taxa included in the analysis.

***Rhinophrynus.***—This genus lacks any autapomorphies based on the characters included in this analysis.

***Chelomophrynus.***—This fossil taxon has a single autapomorphy (17), possession of a premaxilla with an alary process that is lower than wide and scarcely evident. This feature is homoplastic with regard to the same condition in living pipines.

**Node C (unnamed).**—The monophyly of *Palaeobatrachus* and the remaining ingroup taxa is supported by a suite of seven characters of which five are unique. The anterior end of the maxilla extends to, or overlaps, the lateral process of alary process of the premaxilla (18), and owing to the lack of a quadratojugal, the maxillary arcade is incomplete (21). The vertebral centra are depressed (35). The pelvic girdle is characterized by having a broad, U-shaped interilial profile in ventral aspect (50) and a poorly developed pubis that is ossified (51). The remaining two characters are reversed within the ingroup. The prootic possesses a pterygoid knob (22; absent in [*Eoxenopoides* + pipines]), and the cultriform process of the parasphenoid extends anteriorly to the level of the maxillary arcade except in hymenochirines (29).

***Palaeobatrachus.***—This taxon possesses two derived character states that evolved convergently within Pipidae. With respect to the floor of the braincase, the lateral walls are distinctly angled (5)—a feature that also unites *Eoxenopoides* and pipines at Node H. Character 40, involvement of the eighth vertebra in the formation of a sacrum, is homoplastic with regard to its occurrence in *Eoxenopoides* and hymenochirines.

**Node D (Pipidae).**—The monophyly of Pipidae, as used herein, is supported by nine unique, shared-derived characters. These include possession of an optic foramen with a complete bony margin formed by the sphenethmoid (6), and possession of an Eustachian canal (7) in the ventral surface of the floor of the otic capsule. The anterior ramus of the pterygoid arises near the anteromedial corner of the otic capsule (25). The vomer lacks an anterior process if the bone is present (16). The parasphenoid is fused at least partially with the overlying braincase (28). In the orbital region, the maxilla lacks distinct partes (20*). The mandible bears a broad-based, bladelike coronoid process along its posteromedial margin (34), and the sacrum and urostyle are fused (43). The sternal end of the coracoid is not widely expanded (48; State 0).

**Node E* (unnamed).**—Two unique synapomorphies occur at this node. The anterior ramus of pterygoids are

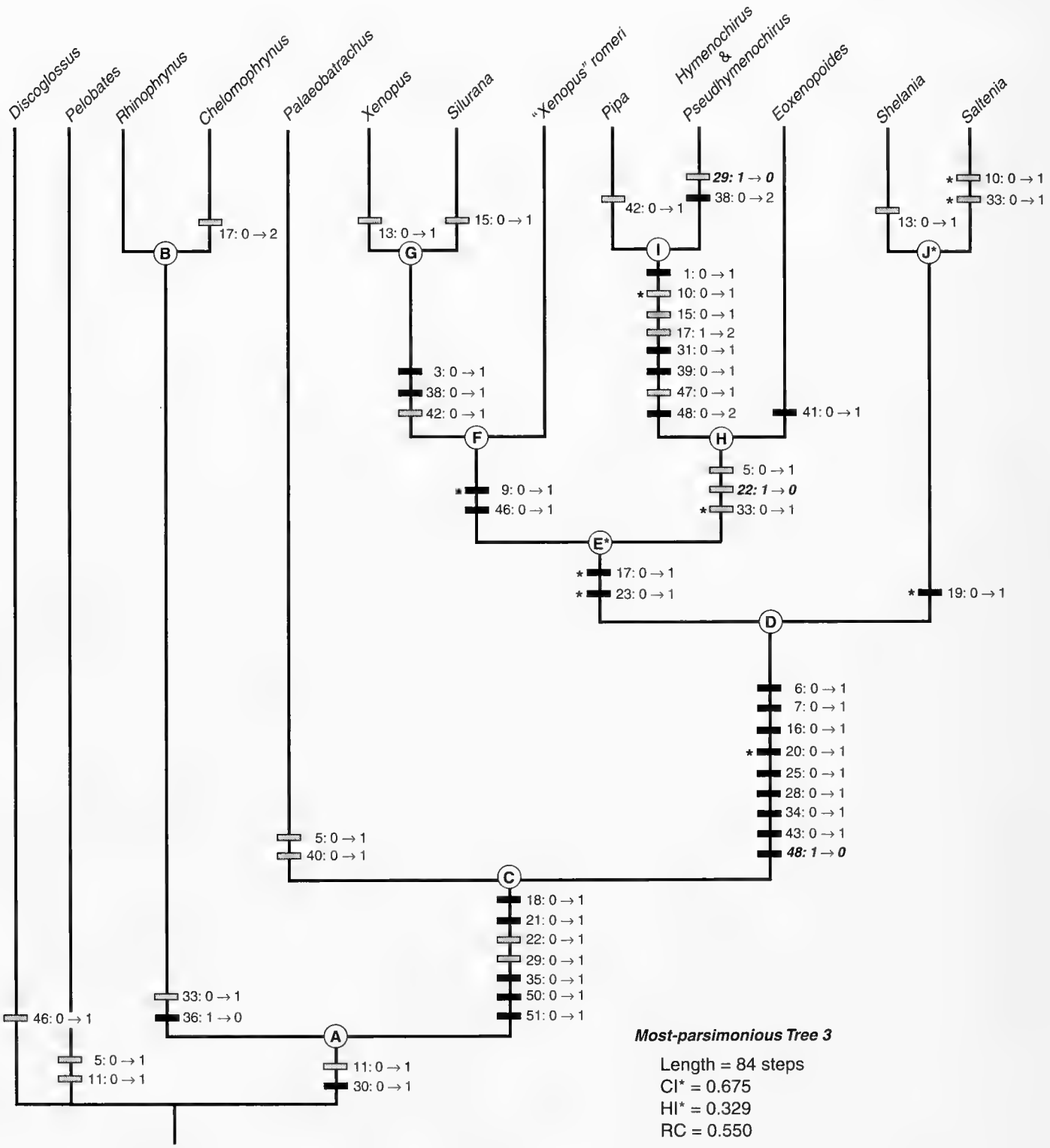


Fig. 21. Most-parsimonious Tree (M-PT) 3. Black bars represent unique transformations; gray bars are replications; characters noted in bold-faced italics are reversals. All transformations are unambiguous and occur on the same branch in all M-PTs, except those marked with an asterisk, which are unambiguous transformations on this tree only. Nodes are labeled with letters.

dorsal with respect to the maxilla (23*) and the premaxillae bear alary processes that are expanded dorsolaterally (17*; State 1).

**Node F (unnamed).**—The monophyly of [*"Xenopus" romeri* + [*Xenopus* + *Silurana*]] is supported by one shared-derived feature of the pectoral girdle—the scapula is extremely reduced in size (46); a similar condition seems to have been evolved independently in *Discoglossus*. In addition, this clade lacks a superior perilymphatic foramen (9*).

**Node G (Xenopodinae).**—The monophyly of [*Xenopus* + *Silurana*] is supported by five synapomorphies. Four characters are unique, shared-derived features. The margins of olfactory foramina are cartilaginous (3). The articular surfaces of the vertebral pre- and postzygapophyses bear sulci and ridges (38), with the prezygapophysis covering the lateral margin of the postzygapophysis. The formation of the sacrum by more than one vertebra, one of which is Vertebra X (42), is homoplastic with respect to *Pipa*. In addition, the anterior process of the pterygoid is laminar (24). The medial end of the clavicle is more expanded than the lateral end (45). These two latter characters, however, are ambiguous, as the states present in the sister taxon of xenopodines, *"Xenopus" romeri*, are unknown. This causes different possible interpretations of the evolution of characters depending on the optimization options; one or both corresponding derived conditions might be unambiguous synapomorphies at Node G or F.

***Xenopus.***—This genus is supported by a single autapomorphy—presence of an azygous nasal (13), which is convergent with regard to *Shelania*.

***Silurana.***—This taxon possesses a single autapomorphy—absence of a vomer (15), which is convergent with regard to pipines (Node I).

**Node H (unnamed).**—Three homoplastic synapomorphies unite *Eoxenopoides* to pipines. The lateral walls of the braincase are distinctly angled (5)—a feature convergent with the condition in *Palaeobatrachus*. The lack of a pterygoid knob on the prootic is a reversal of Character 22 from Node C [*Palaeobatrachus* + Pipidae]. The absence or poor development of the zygomatic ramus of the squamosal (33*) is homoplastic with regard to *Saltenia* and Node B, Rhinophrynidae.

**Node I (Pipinae).**—The clade [*Pipa* + hymenochirines (*Hymenochirus* + *Pseudhymenochirus*)] is supported by eight synapomorphies, of which four are unique, whereas four are homoplastic. Among the unique features are the wedge-shaped skull (1), anterior position of the posterior margin of the parasphenoid (31), possession of vertebrae with parasagittal spinous processes (39), and possession of short coracoids that are broadly expanded at their sternal ends (48; State 2). The anterolateral position of the jaw articulation (10*) is convergent with respect to *Rhinophrynus* (Node B; condition unknown in *Chelomophrynus*), and the lack of a vomer (15) evolved independently in *Silurana*. The sternal expansion of the coracoid (47) also occurs in rhinophrynids and *Palaeobatrachus*. The poorly developed alary process of the premaxilla (17; State 2) is convergent with the similar condition in *Chelomophrynus*.

***Pipa.***—This taxon possesses only one autapomorphy. The sacrum is formed by more than one vertebra, one of which is Vertebra X (42); this condition is convergent at Node G.

**Hymenochirini.**—Two synapomorphies provide support for the monophyly of the hymenochirines [*Pseudhymenochirus* + *Hymenochirus*]. These taxa possess unique, complex intervertebral articulations in which the postzygapophysis covers the lateral margin of the posteriorly adjacent prezygapophysis (38; State 2). The short parasphenoid (29) is a possible reversal.

***Eoxenopoides.***—This fossil genus is diagnosed a single, unique, shared-derived feature—Character 41, in which the sacrum is composed only of Vertebra VIII.

**Node J* (unnamed).**—One unique, shared-derived character unites *Shelania* and *Saltenia*. Both taxa possess an antorbital process on the maxilla (19*).

***Shelania.***—This fossil taxon lacks any unique autapomorphies. It possesses an azygous nasal (13)—a derived condition that also occurs in *Xenopus*.

***Saltenia.***—*Saltenia* possesses two homoplastic autapomorphies. The zygomatic ramus of the squamosal is poorly developed (33*)—a feature that also occurs in rhinophrynids (Node B) and [*Eoxenopoides* + pipines] (Node H). In addition, the jaw articulation is located anteriorly (10*), as it is in pipines (Node I) and *Rhinophrynus*.

## DISCUSSION

### TAXONOMIC CONSIDERATIONS

The inclusion of fossils in phylogenetic analyses and their role in understanding the evolutionary history of a group of extant organisms have been debated vigorously during the last 20 years (e.g., Patterson, 1981; Donoghue et al., 1989; Wilson, 1992). Among living taxa in which large morphological hiatuses exist, information from fossil taxa may elucidate or alter patterns of homologies that have been hypothesized solely from neontological data. Thus, the discovery of several relatively complete specimens of adult *Shelania* offered the opportunity to assess its relationships, and test explicit hypotheses of character evolu-

tion among pipoid frogs (e.g., Báez, 1981; Cannatella and Trueb, 1988a, b). However, the data and results presented here should be considered as preliminary in the sense that they provide a basic framework to which other characters and taxa may be added. It has been suggested that the addition of relatively complete (i.e., with high percentage of scorable characters) fossil taxa that are temporally close to the ancestor may provide greater resolution of the ancestral condition of a given character (Huelsenbeck, 1991). The Early Cretaceous pipoids from Israel, *Thoraciliacus* and *Cordicephalus* (Nevo, 1968), quite likely represent examples of such taxa, but they must be redescribed before they can be incorporated in an analysis.

The addition of several described taxa of fossil pipoids posed some problems. For example, owing to dissimilarities of preservation (both in quality and quantity), different sets of characters were scored for different taxa. No a priori reason could be invoked, however, to exclude any of these fossil taxa from our analysis.

In general, the resolution of the interrelationships among extant pipoid taxa was not affected by the inclusion of fossil taxa. The suggested sister-group relationship of the African hymenochirines and South American *Pipa* (Báez, 1981; Cannatella and Trueb, 1988a, b) is well supported by seven unambiguous synapomorphies. In most iterations of PAUP, *Eoxenopoides* groups with pipines. The node is supported by at least three synapomorphies, but two features are replications (sensu Swofford and Maddison, 1992) and the third is a reversal. *Palaeobatrachus* consistently appears as the sister taxon of pipids, as proposed by Estes and Reig (1973) and Cannatella and de Sá (1993).

In this analysis, *Silurana* and *Xenopus* appear as sister taxa (a possibility suggested by Cannatella and de Sá [1993]); thus, the closer relationship of *Silurana* to the pipines hypothesized by Cannatella and Trueb (1988b) is not substantiated. *Silurana* could be included in the genus *Xenopus*. Because "*Xenopus*" *romeri* consistently clusters with the xenopines as their plesiomorphic sister taxon, it also might be referred to the genus *Xenopus*. However, this action would obscure the significant number of primitive characters that are present in this fossil species (e.g., extensively ossified olfactory capsules, and lack of complex articulations between vertebrae) and absent in living xenopines. The phylogenetic position of "*Xenopus*" *romeri* precludes its inclusion in *Silurana*, because this action would render *Silurana* paraphyletic. At this time, we refrain from creating a new genus for "*Xenopus*" *romeri* because future analyses that include other, as yet undescribed, fossil taxa may support an alternate position for *Shelania*—perhaps as the sister taxon to "*Xenopus*" *romeri*, or to "*Xenopus*" *romeri* + the extant xenopines (Fig. 20, M-PT 2).

We are cautious about the proposed sister-group relationship of *Saltenia* and *Shelania*, and the basal position of these taxa to the remaining pipids. The clade is supported by only one synapomorphy—possession of a conspicuous antorbital process on the maxilla—a feature that we know is possessed by at least two other undescribed fossil pipid taxa (Báez, 1996; pers. obs.).

## CHARACTERS

It is gratifying to observe that the inclusion of fossil taxa alters and supplements some previous hypotheses of character evolution in the pipoids. There is evidence of several features that could have had independent origins from different ancestral species. This is the case of the formation of the orbital region of the braincase in dermal bone in living xenopodines and pipines, and the involvement of additional postsacral vertebrae in a multivertebral sacrum in xenopodines, hymenochirines, and *Pipa*. The loss of the vomer seems to have occurred independently in *Silurana* and pipines, as suggested by Báez and Rage (**in press**). Possession of a braincase having distinctly angled lateral walls occurs in palaeobatrachids, as well as in [*Eoxenopoides* + pipines]. Similarly, incorporation of the eighth vertebra into the sacrum has occurred in *Palaeobatrachus*, hymenochirines, and *Eoxenopoides*.

Within the context of our phylogenetic hypothesis, information about the evolutionary order and associations of several characters emerges. Thus, some derived characters that previously were thought to diagnose pipids seem to be synapomorphies of more inclusive clades. Moderate expansion of the pterygoid (*Palaeobatrachus*) may have preceded the appearance of a complete otic plate in association with an Eustachian canal in the pipids. An anterior elongation of the maxilla to overlap the premaxilla, absence of a quadratojugal, development of a pterygoid knob on the prootic, extension of the cultriform process of the parasphenoid to the maxillary arcade, and a ventral expansion of the iliac symphysis occur in *Palaeobatrachus* and the Pipidae; these features might have been present in their common ancestor. In both palaeobatrachids and pipids, the squamosals are modified to provide support for the long, anterolaterally curved stapes of these taxa; however, this is accomplished by two distinctly different structural modifications. Thus, the squamosal of *Palaeobatrachus* resembles that of most other anurans in being basically T-shaped. However, the ventral ramus of the bone bears a posterior-posterodorsally oriented spur that seems to have provided support for the stapes, whereas support in pipids is provided by the unique conch-shaped tympano-squa-

mosal bone. The origin of the anterior ramus of the pterygoid near the anterolateral corner of the otic capsule, rather than well lateral to this structure, seems to have arisen in the common ancestor of pipids. Whereas the anteromedial origin of the pterygoid anterior ramus might be associated with an anterior shift of the jaw articulation (and shortening of the maxillary arcade) with respect to the otic capsules in pipids, the distributions of these characters on the tree suggest that these traits have not evolved jointly.

Some characters have proven to be patently troublesome and demand further investigation before we can hope to understand their historical pattern of change. The most obvious of these is the structure and nature of the articulations of the vertebral centra in all anurans. Numerous authors have discussed issues of vertebral characters and evolution (e.g., Kluge and Farris, 1969; Trueb, 1973; Cannatella, 1985), but we still seek resolution. Less attention has been directed to the diversity of structures that seem to brace the maxilla against the neurocranium in the anterior region of the orbit. Cannatella (1985) noted that many "basal" anurans (archaeobatrachians) lack a palatine. Trueb and Cloutier (1991) hypothesized that Lissamphibia lacks the palatine, and Trueb (1993) proposed that the slender bone underlying the planum antorbitale in neobatrachians was a neopalatine. Although archaeobatrachians lack a palatine and neopalatine, nearly all taxa possess bony reinforcement of the planum antorbitale. In some (e.g., hymenochirines and *Eoxenopoides*), the planum is ossified. In others (e.g., *Hymenochirus*), the pars palatina of the maxilla is modified as a support structure. In *Discoglossus* and at least some pelobatoids, a "palatine" process has been described as arising from the lingual surface of the facial process of the maxilla and extending beneath the planum toward the neurocranium (Roček, 1981). And in *Shelania* and *Saltenia*, the maxilla bears a distinct and robust medial process that clearly seems to support the maxilla, but it seems structurally (and presumably developmentally) different from apparently analogous structures in other taxa. The structure, function, and developmental origin of these various elements need to be investigated carefully among extant anurans before we can resolve their evolutionary status.

The morphological traits of living pipid frogs identified as presumably adaptive for an aquatic life style were described and discussed most recently by Trueb (1996) and include depression of the head and body, the inability to move the limbs under the body, shortening of the trunk, and loss of axial flexibility. The ear apparatus seems to be modified for hearing under water. The derived suspensory apparatus presumably is associated with feeding in water without a tongue—an evolutionary novelty that had the consequence of allowing modification of the hyoid into a unique vocal apparatus. In addition, the rostral area of the skull is altered significantly from the usual anuran morphology The changes include overall shortening of the olfactory region, depression of the premaxillae and lateral reinforcement of these bones by the maxillae, elongation of the parasphenoid, and modification of the nasals and septomaxillae into structures unique among anurans. The functional consequences of these changes are not clear because the internal anatomy of the nasal region has neither been investigated rigorously or comparatively, nor is much known about feeding and the physiology of chemosensation in these taxa (but see Elepfandt [1996] and Yager [1996]). However, because reference to phylogeny provides an historical context for evolutionary ecological explanations, information from fossil representatives has provided evidence that some, but not all, of these dramatic changes occurred early in the history of pipoid frogs. For example, palaeobatrachids are characterized by depressed skulls with short rostral regions and expanded pterygoids, yet they retained septomaxillae and vomers not unlike those of most other extant anurans. More marked modifications appeared as a suite of characters in the common ancestor of the lineages represented today by the pipids. Within this group, the fossil taxa reveal substantial morphological diversity, particularly in the structure of the iliosacral region, the proportions of the limbs with respect to the body, and the length of individual limb segments; this variation can be interpreted to document different evolutionary trends that are not observed among their extant relatives.

## LITERATURE CITED

Arguijo, M., and E. J. Romero. 1981. Análisis bio-estratigráfico de formaciones portadoras de tafofloras terciarias. Actas VIII Congreso Geológico Argentino. IV:691–717.

Aragón, E., and E. J. Romero. 1984. Geología, paleo-ambientes, y paleobotánica de yacimientos terciarios del occidente de Río Negro, Neuquén y Chubut, Argentina. Actas IX Congreso Geológico Argentino. IV:475–507.

Archangelsky, S. 1974. Sobre la edad de la tafoflora de la Laguna del Hunco, provincia de Chubut. Ameghiniana. 7:413–417.

Báez, A. M. 1976. El significado paleogeográfico y paleoecológico de los pípidos (Amphibia, Anura) fósiles de América del Sur. Actas VI Congreso Geológico Argentino. 1:333–340.

Báez, A. M. 1981. Redescription and relationships of *Saltenia ibanezi*, a Late Cretaceous pipid frog from northwestern Argentina. Ameghiniana. 3–4:127–154.

Báez, A. M. 1991. Anuros en el Eógeno de los alrededores del Lago Nahuel Huapí, Neuquén meridional. Ame-ghiniana. 28:403.

Báez, A. M. 1996. The fossil record of the Pipidae. Pp. 329–347 *in* Tinsley,

ety of London. Oxford: Clarendon Press. xx + 440 pp.

Báez, A. M., and N. Basso. 1996. The earliest known frogs of the Jurassic of South America: review and cladistic appraisal of their relationships. Pp. 131–158 *in* Arratia, G. (ed.), *Contributions of Southern South America to Vertebrate Paleontology*. Münchner Geowissenschaftliche Abhandlungen, Reihe A. Geologie und Paläontologie. 30. München.

Báez, A. M. and J. O. Calvo. 1989. Nuevo anuro pipoideo del Cretácico medio del noroeste de Patagonia, Argentina. Ameghiniana. 26:238.

Báez, A. M., and Z. B. Gasparini, de. 1977. Orígenes y evolución de los anfibios y reptiles del Cenozoico del América del Sur. Acta Geológica Lilloana. 14:140–232.

Báez, A. M., and Z. B. Gasparini, de. 1979. The South American herpetofauna: an evaluation of the fossil record. Pp. 29–54 *in* Duellman, W. E. (ed.), The South American herpetofauna: its origin, evolution and dispersal. Monograph. Museum of Natural History, University of Kansas. 7, 478 pp.

Báez, A. M., and J.-C. Rage. **In press.** Pipid frogs from the Upper Cretaceous of In Beceten, Niger. Palaeontology **000:000–000**.

Báez, A. M., M. C. Samaloa, and E. J. Romero. 1991. Nuevos hallazgos de microfloras y anuros paleógenos en el noroeste de Patagoina: implicancias paleoambientales y paleobiogeográficas. Ameghiniana. 27:83–94.

Baldauf, R. J. 1958. A procedure for the staining and sectioning of the heads of adult anurans. Texas Journal of Science. 10:448–451.

Berggren, W. A., D. V. Kent, M. P. Aubry, and J. Hardenbol. 1995. A revised Cenozoic geochronology and chrono-stratigraphy. Pp. 129–212 *in* Berggren, W. A., d. V. Kent, M.-P. Aubry, and J. Hardenbol (eds.), *Geochronology Time Scales and Global Stratigraphic Correlation*. Society of Sedimentary Geology. Special Publication 54.

Berry, E. W. 1925. A Miocene flora from Patagonia. Johns Hopkins University Studies in Geology. 6:183–252.

Berry, E. W. 1938. Tertiary flora from the Río Pichileufu, Argentina. Geological Society of America. Special Papers 12.

Bremer, K. 1988. The limits of amino acid sequence data in angiosperm phylogenetic reconstruction. Evolution. 42:795–803.

Bremer, K. 1994. Branch support and tree stability. Cladistics. 10:295–304.

Buffetaut, E., and J.-C. Rage. 1993. Fossil amphibians and reptiles and the Africa–South America connection. Pp. 87–99 *in* George, W., and R. Lavocat (eds.), *The Africa–South America Connection*. Oxford: Clarendon Press. 166 pp.

Cannatella, D. C. 1985. *A Phylogeny of Primitive Frogs (Archaeobatrachians)*. Doctoral dissertation. Lawrence: The University of Kansas. 404 pp.

Cannatella, D. C., and R. O. de Sá. 1993. *Xenopus laevis* as a model organism. Systematic Biology. 42: 476–507.

Cannatella, D. C., and L. Trueb. 1988a. Evolution of pipoid frogs: Intergeneric relationships of the aquatic frog family Pipidae (Anura). Zoological Journal of the Linnean Society. 94:1–38.

Cannatella, D. C., and L. Trueb. 1988b. Evolution of pipoid frogs: morphology and phylogenetic relationships of *Pseudhymenochirus*. Journal of Herpetology. 22(4):439–456.

Casamiquela, R. M. 1960. Datos preliminares sobre un pipoideo fósil de Patagonia. Actas y Trabajos del Primer Congreso Sudamericano de Zoología. pp. 17–22.

Casamiquela, R. M. 1961. Un pipoideo fósil de Patagonia. Revista del Museo de La Plata. Sección Paleontología. (Nueva Serie) 4(22):71–123.

Casamiquela, R. M. 1965. Nuevos ejemplares de *Shelania pascuali* (Anura, Pipoidea) del Eoterciario de la Patagonia. Ameghiniana. 4:41–51.

de Sá, R. O., and D. Hillis. 1990. Phylogenetic relationships of the pipid frogs *Xenopus* and *Silurana*. An integration of ribosomal DNA and morphology. Molecular Biology and Evolution. 7: 365–376.

Dingerkus, G., and L. D. Uhler. 1977. Enzyme clearing of Alcian blue stained whole small vertebrates for demonstration of cartilage. Stain Technology. 52(4):229–232.

Dolgopol de Sáez, M. 1941. Noticias sobre peces fósiles argentinos. Siluroideos terciarios de Chubut. Notas Museo de La Plata. (Paleontología) 6:451–457.

Donoghue, M. J., J. A. Doyle, J. Gauthier, A. G. Kluge, and T. Rowe. The importance of fossils in phylogeny reconstruction. Annual Review of Ecology and Systematics. 20:431–460.

Duellman, W. E., and L. Trueb. 1994. *Biology of Amphibians*. Baltimore: Johns Hopkins University Press. xvii + 670 pp.

Elepfandt, A. 1996. Sensory perception and the lateral line system in the clawed frog, *Xenopus*. Pp. 97–120 *in* Tinsley, R. C., and H. R. Kobel (eds.), *The Biology of Xenopus*. Zoological Society of London. Oxford: Clarendon Press. xx + 440 pp.

Eriksson, T., and N. Wikström. 1995. AutoDecay. Version 3.0. Botaniska Institutionen, Stockholm University. Stockholm.

Estes, R. 1975a. *Xenopus* from the Palaeocene of Brazil and its zoogeographic importance. Nature. 254:48–50.

Estes, R. 1975b. Fossil *Xenopus* from the Paleocene of South America and the zoogeography of pipid frogs. Herpetologica. 31:263–278.

Estes, R. 1977. Relationships of the South African fossil frog *Eoxenopoides reuningi* (Anura, Pipidae). Annals of the South African Museum. 73:49–80.

Estes, R., and O. A. Reig. 1973. The early fossil record of frogs: a review of the evidence. Pp. 11–63 *in* VIAL, J. (ed), *Evolutionary Biology of the Anurans: Contemporary Research on Major Problems*. Columbia: University of Missouri Press. vii + 470 pp.

Evans, S., A. R. Milner, and C. Werner. 1996. Sirenid salamanders and a gymnophionan amphibian from the Cretaceous of the Sudan. Palaeontology. 39:77–95.

Feruglio, E. 1949. *Descripción Geológica de la Patagonia*. Vol. 2. Ministerio de Industria y Comercio de la Nación, Dirección General de Yacimientos Petrolíferos Fiscales. Buenos Aires: Imprenta Coni. 349 pp.

Ford, L. S., and D. C. Cannatella. 1993. The major clades of frogs. Herpetological Monographs. 7:94–117. 162 pp.

Frenguelli, J. 1940. Viaje a las zonas central y andina de Patagonia septentrional. Revista del Museo de La Plata. (Nueva Serie) 1939:53–76.

Gasparini, Z., and A. M. Báez. 1975. Aportes al conoci-miento de la herpetofauna terciaria de la Argentina. Actas I Congreso Argentino de Paleontología y Bioestratigrafía. 1:377–415.

Gaupp, E. 1896. *Anatomie des Frosches. Abt. 1. Lehre vom Skelet und vom Muskelsystem*. Braunschweig: Druck und Verlag von Friedrich Vieweg und Sohn. xiii + 229 pp.

Haughton, S. 1931. On a collection of fossil frogs at Banke. Transactions of the Royal Society of South Africa. 18:233–249.

Hecht, M. K. 1963. A reevaluation of the early history of the frogs. Part II. Systematic Zoology. 12 (1):20–35.

Henrici, A. C. 1991. *Chelomophrynus bayi* (Amphibia, Anura, Rhinophrynidae), a new genus and species from the middle Eocene of Wyoming:ontogeny and relationships. Annals of the Carnegie Museum. 60 (2):97–144.

Huelsenbeck, J. P. 1991. When are fossils better than extant taxa in phylogenetic analysis? Systematic Zoology. 40: 458–469.

Kluge, A. G., and J. S. Farris. 1969. Quantitative phyletics and the evolution of anurans. Systematic Zoology. 18:1–32.

Lathrop, A. 1997. Taxonomic review of the megophryid frogs (Anura: Pelobatoidea). Asiatic Herpetological Research. 7:68–79.

Loumont, C. and H. R. Kobel. 1991. *Xenopus longipes* sp. nov., a new polyploid pipid from western Cameroon. Revue Suisse de Zoologie 98:731–738.

Maddison, W. P., and D. R. Maddison. 1992. MacClade. Analysis of Phylogeny and Character Evolution. Version 3.0. Sutherland, Massachu-

setts: Sinauer Associates.

Mazzoni, M., and E. Aragón. 1985. El complejo piroclástico-volcánico de la Formación Huitrera (Paleoceno–Eoceno) en el área del Río Chubut Medio, República Argentina. IV Congreso Geológico Chileno. 3:275–279.

Mazzoni, M., K. Kawashita, S. Harrison, and E. Aragón. 1991. Edades radimétricas eocenas. Borde occidental del Macizo Norpatagónico. Revista de la Asociación Geológica Argentina. 46:150–158.

Nevo, E. 1968. Pipid frogs from the Early Cretaceous of Israel and pipid evolution. Bulletin of the Museum of Comparative Zoology, Harvard University. 136:255–318.

Nieuwkoop, P. D., and J. Faber. 1956. *Normal Table of Xenopus laevis (Daudin). A Systematical and Chronological Survey of the Development from the Fertilized Egg till the End of Metamorphosis.* Amsterdam: North-Holland Publ. Co.

Pascual, R., and E. Ortiz Jaureguizar. 1990. Evolving climates and mammalian faunas in Cenozoic South America. Journal of Human Evolution. 19: 23–60.

Pascual, R., E. Ortiz Jaureguizar, and J. L. Prado. 1996. Land mammals: paradigm for Cenozoic South American geobiotic evolution. Pp. 265–319 *in* Arratia, G. (ed.), *Contributions of Southern South America to Vertebrate Paleontology.* Münchner Geowissenschaftliche Abhandlungen, Reihe A. Geologie und Paläontologie. 30. München.

Paterson, N. F. 1960. The inner ear of some members of the Pipidae. Proceedings of the Zoological Society of London. 134:509–546.

Patterson, C. 1981. Significance of fossils in determining evolutionary relationships. Annual Review of Ecology and Systematics. 12:195–223.

Petersen, C. S. 1946. Estudios geológicos en la región del Río Chubut Medio. Boletín de la Dirección General de Minería y Geología. 59. Buenos Aires.

Pianitzki, A. 1936. Estudio de la región del Río Genoa y del Río Chubut. Boletín de Informaciones Petroleras 137. Buenos Aires.

Proserpio, C. 1978. Descripción de la Hoja 42d, Gastre, Provincia del Chubut. Servicio Geológico Nacional 159. Buenos Aires.

Pyles, R. A. 1988. *Morphology and Mechanics of the Jaws of Anuran Amphibians.* Doctoral dissertation. Lawrence: The University of Kansas. xvi + 445 pp.

Rapela, C. W., L. A. Spalletti, J. C. Merodio, and E. Aragón. 1984. El vulcanismo paleoceno-eoceno de la Provincia Volcánica Andino-Patagónica. IX Congreso Geológico Argentino. Relatorio, Geología, y Recursos Naturales de la Provincia de Río Negro. pp. 189–213. 784 pp.

Rapela, C. W., L. A. Spalletti, J. C. Merodio, and E. Aragón. 1988. Temporal evolution and spatial variation of early Tertiary vulcanism in the Patagonian Andes (40°S–30°S). Journal of South American Earth Sciences. 1:75–88.

Reig, O. A. 1959. Primeros datos descriptivos sobre los anuros del Eocretáceo de la provincia de Salta (Rep. Argentina). Ameghiniana. 1:3–8.

Roček, Z. 1981 "1980." Cranial anatomy of frogs of the family Pelobatidae Stannius, 1856, with outlines of their phylogeny and systematics. Acta Universitatis Caro-linae–Biologica. 3:1–164.

Rodríguez Talavera, M.-R. 1990. *Evolución de Pelobátidos y Pelodítidos (Amphibia, Anura): Morfología y Desarrollo del Sistema Esquelético.* Colección Tesis Doctorales, No. 188/90:Universidad Complutense de Madrid, Facultad de Ciencias Biológicas, Departamento de Biología Animal I. 282 pp.

Romero, E. J. 1978. Paleoecología y paleofitogeografía de las Tafofloras del Cenofítico de Argentina y áreas vecinas. Ameghiniana. 15:209–227.

Scholtz, A. 1985. The palynology of the upper lacustrine sediments of the Arnot pipe, Banke, Namaqualand. Annals of the South African Museum. 95:1–109.

Smith, R. M. H. 1988. Palaeoenvironmental reconstruction of a Cretaceous crater-lake deposit in Bushman-land, South Africa. Pp. 27–41 *in* Heine, K. (ed.), *Palaeoecology of Africa and the Surrounding Islands. Vol. 19.* Rotterdam: A. A. Balkema.

Špinar, Z. 1972. *Tertiary Frogs from Central Europe.* The Hague: W. Junk. 286 pp.

Swofford, D. L. 1991. PAUP. Phylogenetic Analysis Using Parsimony. PAUP 3.1 User's Manual. Privately published.

Swofford, D. L., and W. P. Maddison. 1992. Parsimony, character-state reconstructions, and evolutionary inferences. Pp. 186–223 *in* Mayden, R. L. (ed.), *Systematics, Historical Ecology, and North American Freshwater Fishes.* Stanford, California: Stanford University Press. xxvi + 962 pp.

Trueb, L. 1973. Bones, frogs, and evolution. Pp. 65–132 *in* Vial, J. (ed.), *Evolutionary Biology of the Anurans: Contemporary Research on Major Problems.* Columbia: University Missouri Press. vii + 470 pp.

Trueb, L. 1993. Patterns of cranial diversity among the Lissamphibia. Pp. 255–343 *in* Hanken, J., and B. K. Hall (eds.), *The Skull. Volume 2. Patterns of Structural and Systematic Diversity.* Chicago: The University of Chicago Press. xiii +566 pp.

Trueb, L. 1996. Historical constraints and morphological novelties in the evolution of the skeletal system of pipid frogs (Anura: Pipidae). Pp. 349–377 *in* Tinsley, R. C., and H. R. Kobel (eds.), *The Biology of* Xenopus. The Zoological Society of London. Oxford: Clarendon Press. xx + 440 pp.

Trueb, L., and D. C. Cannatella. 1982. The cranial osteology and hyolaryngeal apparatus of *Rhinophrynus dorsalis* (Anura: Rhinophrynidae) with comparisons to Recent pipid frogs. Journal of Morphology. 171:11–40.

Trueb, L., and D. C. Cannatella. 1986. Systematics, morphology, and phylogeny of the genus *Pipa* (Anura, Pipidae). Herpetologica. 42: 412–449.

Trueb, L., and R. Cloutier. A phylogenetic investigation of the inter- and intrarelationships of the Lissamphibia (Amphibia: Temnospondyli). Pp. 223–313 *in* Schultze, H.-P., and L. Trueb (eds.), *Origins of the Higher Groups of Tetrapods: Controversy and Consensus.* Comstock Publishing Associates. Ithaca and London: Cornell University Press. xii + 724 pp.

Trueb, L., and J. Hanken. 1992. Skeletal development in *Xenopus laevis* (Anura: Pipidae). Journal of Morphology. 214:1–41.

Vergnaud-Grazzini, C. 1966. Les amphibiens du Miocène de Beni-Mellal. Notes du Service Géologique du Maroc. 27:43–69.

Vergnaud-Grazzini, C., and R. Hoffstetter. 1972. Présence de Palaeobatrachidae (Anura) dans des gisements tertiaires français. Caractérisation, distribution et affinités de la famille. Palaeovertebrata. 5:157–177.

Vergnaud-Grazzini, C., and M. Młynarski. 1969. Position systématique du genre *Pliobatrachus* Fejérváry 1917. Comtes Rendus des Sceances de l'Académie des Sciences. 268:2399–2402.

Volkheimer, W., and J. Lage. 1981. Descripción de la Hoja 42c, Cerro Mirador, provincia del Chubut. Servicio Geológico Nacional. Boletin 181. Buenos Aires.

Van Dijk, D. E. 1995. African fossil Lissamphibia. Palaeontologia Africana. 32:39–43.

Wilson, M. V. H. 1992. Importance for phylogeny of single and multiple stem-group fossil species with examples from freshwater fishes. Systematic Biology. 41(4):462–470.

Yager, D. D. 1996. Sound production and acoustic communication in Xenopus borealis. Pp. 121–141 in Tinsley, R. C., and H. R. Kobel (eds.), The Biology of Xenopus. Zoological Society of London. Oxford: Clarendon Press. xx + 440 pp.

## APPENDIX

Data matrix of osteological character states designated as 0, 1, and 2; ? = unknown; N = character not applicable. The characters ? and N were coded as ? in the analyzed matrix.

Characters 1–18

| Taxon | 1 | 2 | 3 | 4 | 5 | 6 | 7 | 8 | 9 | 10 | 11 | 12 | 13 | 14 | 15 | 16 | 17 | 18 |
|---|---|---|---|---|---|---|---|---|---|---|---|---|---|---|---|---|---|---|
| *Discoglossus* | 0 | 0 | 0 | 0 | 0 | 0 | 0 | 0 | 0 | 0 | 0 | 0 | 0 | 0 | 0 | 0 | 0 | 0 |
| *Pelobates* | 0 | 0 | 0 | 0 | 0 | 0 | 0 | 0 | 0 | 0 | 1 | 0 | 0 | 0 | 0 | 0 | 0 | 0 |
| *Rhinophrynus* | 0 | 0 | 0 | 0 | 0 | 0 | 0 | 0 | 0 | 1 | 1 | 1 | 0 | 0 | 0 | 0 | 0 | 0 |
| *Chelomophrynus* | 0 | ? | 0 | 0 | ? | 0 | 0 | 0 | 0 | ? | 1 | ? | 0 | ? | 0 | 0 | 2 | 0 |
| *Palaeobatrachus* | 0 | 0 | 0 | 0 | 1 | 0 | 0 | 0 | 0 | 0 | 1 | 0 | 0 | 0 | 0 | 0 | 0 | 1 |
| *Xenopus* | 0 | 1 | 1 | 0 | 0 | 1 | 1 | 0 | 1 | 0 | 1 | 1 | 1 | 1 | 0 | 1 | 1 | 1 |
| *Silurana* | 0 | 1 | 1 | 0 | 0 | 1 | 1 | 0 | 1 | 0 | 1 | 1 | 0 | 1 | 1 | N | 1 | 1 |
| *Shelania* | 0 | 0 | 0 | 0 | 0 | 1 | 1 | 0 | ? | 0 | 1 | 1 | 1 | ? | 0 | 1 | 0 | 1 |
| *Pipa* | 1 | 1 | 0 | 0 | 1 | 1 | 1 | 1 | 0 | 1 | 1 | 1 | 0 | 1 | 1 | N | 2 | 1 |
| *Eoxenopoides* | 0 | ? | 0 | 1 | 1 | 1 | 1 | ? | ? | 0 | 1 | 1 | 0 | ? | 0 | 1 | 1 | 1 |
| Hymenochirines | 1 | 1 | 0 | 1 | 1 | 1 | 1 | 1 | 0 | 1 | 1 | 0/1 | 0 | 1 | 1 | N | 2 | 1 |
| *Saltenia* | ? | 0 | 0 | ? | 0 | 1 | 1 | ? | ? | 1 | 1 | 1 | 0 | ? | 0 | 1 | ? | 1 |
| *"Xenopus" romeri* | 0 | 0 | 0 | 0 | 0 | 1 | 1 | 0 | 1 | ? | 1 | 1 | 0 | ? | 0 | 1 | ? | ? |

Characters 19–36

| Taxon | 19 | 20 | 21 | 22 | 23 | 24 | 25 | 26 | 27 | 28 | 29 | 30 | 31 | 32 | 33 | 34 | 35 | 36 |
|---|---|---|---|---|---|---|---|---|---|---|---|---|---|---|---|---|---|---|
| *Discoglossus* | 0 | 0 | 0 | 0 | 0 | 0 | 0 | 0 | 0 | 0 | 0 | 0 | 0 | 0 | 0 | 0 | 0 | 1 |
| *Pelobates* | 0 | 0 | 0 | 0 | 0 | 0 | 0 | 0 | 0 | 0 | 0 | 0 | 0 | 0 | 0 | 0 | 0 | 2 |
| *Rhinophrynus* | 0 | 0 | 0 | 0 | 0 | 0 | 0 | N | N | 0 | 0 | 1 | 0 | 0 | 1 | 0 | 0 | 0 |
| *Chelomophrynus* | 0 | 0 | 0 | 0 | ? | ? | ? | ? | ? | 0 | 0 | 1 | 0 | 0 | 1 | 0 | 0 | 0 |
| *Palaeobatrachus* | 0 | 0 | 1 | 1 | 0 | 0 | 0 | 1 | 0 | 0 | 1 | 1 | 0 | 1 | 0 | 0 | 1 | 2 |
| *Xenopus* | 0 | 1 | 1 | 1 | 1 | 1 | 1 | 2 | 1 | 1 | 1 | 1 | 0 | 2 | 0 | 1 | 1 | 1 |
| *Silurana* | 0 | 1 | 1 | 1 | 1 | 1 | 1 | 2 | 1 | 1 | 1 | 1 | 0 | 2 | 0 | 1 | 1 | 1 |
| *Shelania* | 1 | 1 | 1 | 1 | 0 | 0 | 1 | 2 | 1 | 1 | 1 | 1 | 0 | 2 | 0 | 1 | 1 | 1 |
| *Pipa* | 0 | 1 | 1 | 0 | 1 | 0 | 1 | 2 | 0 | 1 | 1 | 1 | 1 | 2 | 1 | 1 | 1 | 1 |
| *Eoxenopoides* | 0 | 1 | 1 | 0 | 1 | 0 | 1 | 2 | 0 | 1 | 1 | 1 | 0 | 2 | 1 | 1 | 1 | 1 |
| Hymenochirines | 0 | 1 | 1 | 0 | N | N | N | 2 | 0 | 1 | 0 | 1 | 1 | 2 | 1 | 1 | 1 | 1 |
| *Saltenia* | 1 | ? | 1 | 1 | 0 | ? | 1 | 2 | ? | 1 | 1 | 1 | 0 | 2 | 1 | 1 | 1 | 1 |
| *"Xenopus" romeri* | ? | ? | ? | 1 | ? | ? | ? | ? | ? | 1 | 1 | 1 | 0 | ? | ? | ? | 1 | 1 |

Characters 37–51

| Taxon | 37 | 38 | 39 | 40 | 41 | 42 | 43 | 44 | 45 | 46 | 47 | 48 | 49 | 50 | 51 |
|---|---|---|---|---|---|---|---|---|---|---|---|---|---|---|---|
| *Discoglossus* | 0 | 0 | 0 | 0 | 0 | 0 | 0 | 0 | 0 | 1 | 0 | 0 | 0 | 0 | 0 |
| *Pelobates* | 0 | 0 | 0 | 0 | 0 | 0 | 0 | 0 | 0 | 0 | 0 | 1 | 0 | 0 | 0 |
| *Rhinophrynus* | 0 | 0 | 0 | 0 | 0 | 0 | 0 | 0 | 0 | 0 | 1 | 1 | 0 | 0 | 0 |
| *Chelomophrynus* | 0 | 0 | 0 | 0 | 0 | 0 | 0 | 0 | 0 | 0 | 1 | 1 | 0 | 0 | ? |
| *Palaeobatrachus* | 0 | 0 | 0 | 1 | 0 | 0 | 0 | 0 | 0 | 0 | 1 | 1 | 0 | 1 | 1 |
| *Xenopus* | 0 | 1 | 0 | 0 | 0 | 1 | 1 | 1 | 1 | 1 | 0 | 0 | 1 | 1 | 1 |
| *Silurana* | 0 | 1 | 0 | 0 | 0 | 1 | 1 | 1 | 1 | 1 | 0 | 0 | 1 | 1 | 1 |
| *Shelania* | 0 | 0 | 0 | 0 | 0 | 0 | 1 | 0 | 0 | 0 | 0 | 0 | 1 | 1 | 1 |
| *Pipa* | 0 | 0 | 1 | 0 | 0 | 1 | 1 | 0 | 0 | 0 | 1 | 2 | 1 | 1 | 1 |
| *Eoxenopoides* | 1 | 0 | 0 | 1 | 1 | 0 | 1 | ? | 0 | 0 | 0 | 0 | 0 | 1 | 1 |
| Hymenochirines | 1 | 2 | 1 | 1 | 0 | 0 | 1 | 1 | 0 | 0 | 1 | 2 | 1 | 1 | 1 |
| *Saltenia* | 0 | 0 | 0 | 0 | 0 | 0 | 1 | 0 | 0 | 0 | 0 | 0 | 0 | 1 | ? |
| *"Xenopus" romeri* | ? | 0 | 0 | ? | ? | 0 | 1 | 1 | ? | 1 | ? | ? | 1 | 1 | ? |

## PUBLICATIONS OF THE NATURAL HISTORY MUSEUM, THE UNIVERSITY OF KANSAS

The University of Kansas Publications, Museum of Natural History, beginning with Volume 1 in 1946, was discontinued with Volume 20 in 1971. Shorter research papers formerly published in the above series were published as The University of Kansas Natural History Museum Occasional Papers until Number 180 in December 1996. The Miscellaneous Publications of The University of Kansas Natural History Museum began with Number 1 in 1946 and ended with Number 68 in February 1996. Monographs of The University of Kansas Natural History Museum were initiated in 1970 and discontinued with Number 8 in 1992. The University of Kansas Science Bulletin, beginning with Volume 1 in 1902, was discontinued with Volume 55 in 1996. The foregoing publication series are now combined in a new series entitled Scientific Papers, Natural History Museum, The University of Kansas, begun with Number 1 in 1997. Special Publications began in 1976 and continue as an outlet for longer contributions and are available by purchase only. All manuscripts are subject to critical review by intra- and extramural specialists; final acceptance is at the discretion of the editor.

The publication is printed on acid-free paper. Publications are composed using Microsoft Word® and Adobe PageMaker® on a Macintosh computer and are printed by The University of Kansas Printing Services.

Institutional libraries interested in exchanging publications may obtain the Scientific Papers, Natural History Museum, The University of Kansas, by addressing the Exchange Librarian, The University of Kansas Libraries, Lawrence, Kansas 66045-2800, USA. Available back issues of The University of Kansas Science Bulletin may be purchased from the Library Sales Section, Retrieval Services Department, The University of Kansas Libraries, Lawrence, Kansas 66045-2800, USA. Available issues of former publication series, Scientific Papers, and Special Publications of the Natural History Museum can be purchased from the Office of Publications, Natural History Museum, The University of Kansas, Lawrence, Kansas 66045-2454, USA. Purchasing information can be obtained by calling (913) 864-4450, fax (913) 864-5335, or e-mail (kunhm@ukans.edu). VISA and MasterCard accepted; include expiration date.



SERIES EDITOR: William E. Duellman

PRINTED BY
THE UNIVERSITY OF KANSAS PRINTING SERVICES
LAWRENCE, KANSAS